

Real time Segmentation of Medical Images

A Thesis Submitted to the
University of Petroleum and Energy Studies

For the Award of
Doctor of Philosophy
in

Computer Science & Engineering

By

ROOHI SILLE

Internal Supervisor(s)

Dr. Piyush Chauhan
Dr. Tanupriya Choudhury

External Supervisor

Dr. Durgansh Sharma



School of Computer Science & Engineering

University of Petroleum & Energy Studies

Dehradun-248007: Uttarakhand

Real time Segmentation of Medical Images

A Thesis Submitted to the
University of Petroleum and Energy Studies

For the Award of
Doctor of Philosophy

in

Computer Science and Engineering

By

ROOHI SILLE
(SAP ID 500042644)

Internal Supervisor(s)

Dr. Piyush Chauhan
Assistant Professor(Senior Grade)
Department of Informatics
School of Computer Science
University of Petroleum & Energy Studies

Dr. Tanupriya Choudhury
Senior Associate Professor
Department of Informatics
School of Computer Science
University of Petroleum & Energy Studies

External Supervisor

Dr. Durgansh Sharma
Associate Professor
Christ University



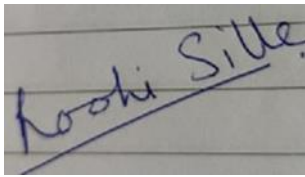
School of Computer Science

University of Petroleum & Energy Studies

Dehradun-248007:Uttarakhand

DECLARATION

I declare that the thesis entitled “Real Time Segmentation of Medical Images” has been prepared by me under the guidance of Dr. Piyush Chauhan, Assistant Professor and Dr. Tanupriya Choudhury, Senior Associate Professor, School of Computer Science, University of Petroleum and Energy Studies. No part of this thesis has formed the basis for the award of any degree or fellowship previously.

A photograph of a handwritten signature in blue ink on lined paper. The signature reads "Roohi Sille" and is underlined.

Roohi Sille

**School of Computer Science, University of Petroleum and Energy Studies, Energy Acres,
P.O. Bidholi via Prem Nagar, Dehradun, 248007, India.**

DATE : 15/2/2022



CERTIFICATE

I certify that Roohi Sille has prepared his thesis entitled “Real Time Segmentation of Medical Images”, for the award of PhD degree of the University of Petroleum & Energy Studies, under my guidance. He/she has carried out the work at the Department of School of Computer Science, University of Petroleum & Energy Studies.

Internal Supervisor

Dr. Piyush Chauhan

**School of Computer Science, University of Petroleum and Energy Studies,
Energy Acres, P.O. Bidholi via Prem Nagar, Dehradun, 248007, India.**

Internal Co-Supervisor

Dr. Tanupriya Choudhury

**School of Computer Science, University of Petroleum and Energy Studies,
Energy Acres, P.O. Bidholi via Prem Nagar, Dehradun, 248007, India.**

Date: 15/02/2022

Energy Acres Bidholi Via Prem Nagar, Dehradun - 248 007 (Uttarakhand), India T: +91 1352770137 2776053/54/91, 2776201, 9997799474 F: +91 1352776090/95
Knowledge Acres: Kandoli Via Prem Nagar, Dehradun - 248 007 (Uttarakhand), India T: +91 8171879021/2/3, 7060111775

ENGINEERING | COMPUTER SCIENCE | DESIGN | BUSINESS | LAW | HEALTH SCIENCES AND TECHNOLOGY | MODERN MEDIA | LIBERAL STUDIES



CERTIFICATE

I certify that Roohi Sille has prepared his thesis entitled “Real Time Segmentation of Medical Images”, for the award of PhD degree of the University of Petroleum & Energy Studies, under my guidance. She has carried out the work at the School of Computer Science, University of Petroleum & Energy Studies.

External Supervisor
Dr. Durgansh Sharma
Christ University, Delhi NCR
Date: 15/2/2022

Energy Acres: Bichol/Via Prem Nagar, Dehradun - 248 007 (Uttarakhand), India T: +91 1352770137, 2776053/54/91, 2776201, 9997799474 F: +91 1352776080/85
Knowledge Acres: Kandoli/Via Prem Nagar, Dehradun - 248 007 (Uttarakhand), India T: +91 8171979021/2/3, 7060111775

ENGINEERING | COMPUTER SCIENCE | DESIGN | BUSINESS | LAW | HEALTH SCIENCES AND TECHNOLOGY | MODERN MEDIA | LIBERAL STUDIES

ABSTRACT

Image segmentation is crucial in many computer vision systems. In pictures, a segmentation technique is used to identify objects and their borders. The quality of image segmentation determines the performance of image recognition systems, yet no universal algorithm has yet been discovered. Border detection in medical imaging is one of the most difficult tasks in image processing and feature categorization. Because of the importance and challenges, it is critical to build a research subject on the creation of more efficient, precise, and real-time tumour segmentation utilising MRI images using Deep Learning. It takes a long time to complete. Real-time image segmentation is still a challenge. It is important to segment the tumor's healthy tissue in order to be of therapeutic value in the treatment of brain tumours. The performance of algorithms for segmenting MRI images of brain tumours can be evaluated using dice score coefficients. If the dice score coefficient is high enough, MRI pictures of brain tumours can be segmented properly and effectively. The purpose of this study is to segment brain tumours in real time. Deep learning-based GAN are offered for real-time segmentation of brain tumours from MRI images based on the study's findings. In the suggested approach, a hierarchical dense CNN is used to segment brain tumours using MRI images. This method was demonstrated using a pre-processing stage that includes bias field inspection and intensity normalisation. The technique improved the performance of segmentation algorithms by combining qualitative indicators like dice score coefficient with quantitative features like mean square and peak signal to noise ratio. The suggested generative adversarial network model outperforms the convolutional neural network model in terms of accuracy. High accuracy and processing speed are necessary for real-time segmentation, which are both achievable with the proposed GAN model due to its high accuracy and efficiency.

ACKNOWLEDGEMENT

I bow my head humbly to pay heartfelt regards to Almighty God for giving me the strengths and blessing in completing this thesis.

There are quite a few people that have helped me in one way or another to the completion of this work. It is with great pleasure, I would like to thank all of you from very deep inside.

Foremost, I would like to express my sincere gratitude to my thesis advisors Dr. Piyush Chauhan, Dr. Tanupriya Choudhury and Dr. Durgansh Sharma, for picking me up as a student at the critical stage of my career and the continuous support of my Ph.D study and research, for his patience, motivation, enthusiasm, and immense knowledge. His guidance helped me in all the time of research and writing of this thesis.

It is absolutely difficult to succeed in the process of finding and developing an idea without the help of a specialist in the domain. I found in my advisors not only the source of wonderful ideas to develop, but also the support that a Ph.D student needs. I could not have imagined having a better advisor and mentor for my Ph.D study.

Besides my advisors, I would like to thank Chancellor Dr. S. J. Chopra, Vice chancellor and Dean SoCS Dr. Sunil Rai, and Dean R&D Dr. Devesh Kumar Avasthi at the University of Petroleum and Energy Studies for their encouragement, suggestions and valuable support for my research work.

I would like to express my special thanks to Dr. Rakhi Ruhel, Program Manager-Ph.D, University of Petroleum and Energy Studies, for his assistance during my research work.

I am grateful to the University of Petroleum and Energy Studies, for giving me an opportunity to pursue my research and for providing all facilities in School of Computer Science. I would like to thank all the Heads of School of Computer Science Departments, doctoral students for their feedback, cooperation, and of course friendship.

In addition I would like to express my gratitude to all colleagues in the university. I cannot begin to express my gratitude to my family for all of the love, support, encouragement, and prayers they have sent my way along this journey.

I am eternally indebted to my loving parents and in-laws for all the sacrifices they have made on my behalf. I would like to express my sincere gratitude to my brothers and sisters for their unconditional support throughout my PhD journey.

I would like to express sincere gratitude to my beloved husband Rajat Jaitly who believed in me and provided encouragement during challenging times. Your unconditional love and support in the moments when there was no one to answer my queries has helped me immensely.

To my daughter Rinaya Jaitly, who are the inspiration for me to complete this journey and also for the sacrifices made along the way. To all my friends Nilanjana Pradhan, Avita Katal and Dr. Ravi Tomar thank you for your support and constant encouragement.

TABLE OF CONTENT

CERTIFICATE	iv
ABSTRACT.....	iv
ACKNOWLEDGEMENT.....	viii
TABLE OF CONTENT.....	ix
LIST OF FIGURES.....	xii
LIST OF TABLES.....	xiv
CHAPTER 1: INTRODUCTION.....	1
1.1. Introduction.....	1
1.2. Brain Imaging	6
1.2.1. Imaging modalities	8
1.2.2. Magnetic resonance imaging	13
1.2.3. Magnetic Resonance Imaging Principle	13
1.3. Generative Adversarial Networks.....	17
1.4. Research Motivation	17
1.5. Research Objective	17
1.6. Research Overview	19
1.7. Thesis Organization	19
CHAPTER 2: BRAIN TUMOUR SEGMENTATION RELATED WORK.....	21
2.1 Overview.....	21
2.2 Literature Survey of Automated Medical Image Segmentation	21
2.2.1. Segmentation of Medical Images through Convolutional Neural Networks	22
2.2.2. Deep semantic segmentation of medical images	27
2.2.3. Real-Time Interactive 3-Dimensional segmentation	36

2.2.4.	Segmentation of Medical Images Using Hybridized Technique.....	41
2.2.5.	Generative adversarial network based image segmentation.....	51
2.2.6.	Fuzzy Based Medical Image Segmentation	55
2.3	Deep Learning-Based Brain Tumor Segmentation Algorithms.....	59
2.4	Problem statement.....	65
2.4.1.	Gaps in research	66
2.5	Summary	67
CHAPTER 3: PROPOSED METHODOLOGY		68
3.1	Overview.....	68
3.2	Proposed Method	68
3.2.1	Transfer Learning Algorithm.....	73
3.2.2	Dense Hierarchical CNN	74
3.2.3	Real Time GAN algorithm	77
3.3	Implications of Research Problem	79
3.4	Summary	80
CHAPTER 4: DATASETS AND EXPERIMENTS.....		81
4.1.	Overview.....	81
4.2.	Image processing benchmarks	81
4.3.	Set-Up of The BRATS Benchmark	82
4.4.	Glioma grading using Machine learning.....	82
4.5.	Multimodality Feature Acquisition.....	83
4.6.	Experiments on the BraTS 2018 Benchmark.....	83
CHAPTER 5: RESULTS AND DISCUSSION		86
5.1.	Overview.....	86

5.2.	Evaluation Measures of Brain Tumor Segmentation.....	86
5.3.	Results of Proposed Methodology	87
5.3.1.	Results of T-Net Algorithm.....	95
5.3.2.	Results of DH-CNN Algorithm.....	88
5.3.3.	Results of RT-GAN Algorithm	89
5.4.	Qualitative Results	95
5.5.	Comparative Analysis.....	97
5.6.	Statistical Analysis on Proposed Model	97
CHAPTER 6: CONCLUSION.....		104
6.1.	Overview.....	104
6.2.	Conclusion	104
6.3.	Future Scope	106
References.....		107

LIST OF FIGURES

Figure 1.1 The fourth images from left to right show the edema in green colour, enhanced tumour in yellow necrosis in red colour, and non-enhanced tumour colour in sky blue color	4
Figure 1.2 Distinct patients with Tumor (BraTS Dataset)	5
Figure 1.3 MRI shows structures such as deep nuclei, bone, white vs. gray matter by evaluating the oxygen concentration in blood haemoglobin.....	7
Figure 1.4 Outline of Research Objective and Sub-Objectives.....	18
Figure 3.1 Transfer Learning Algorithm	69
Figure 3.2 Hierarchical Dense CNN algorithm	69
Figure 3.3 Real Time Generative Adversarial Network (RT-GAN) algorithm.....	70
Figure 3.4 Proposed Methodology.....	71
Figure 3.5 Transfer Learning Architecture.....	73
Figure 3.6 Hierarchical clustering process.....	75
Figure 3.7 Hierarchical Dense CNN.....	76
Figure 4.1 Sample from BraTS 2018 datasets (a. T1, b. T1ce, c. T2 and d. FLAIR).....	84
Figure 5. 1 Discriminator summary for Tumor segmentation.....	89
Figure 5.2 Generator GAN for several layers.....	90
Figure 5.3 Combined summary for the GAN model.....	90
Figure 5.4 Parameter performance.....	91
Figure 5.5 Model Loss.....	91
Figure 5.6 Accuracy.....	92
Figure 5.7 Non-Tumor picture.....	92
Figure 5.8 Tumor Picture.....	93
Figure 5.9 Ground Truth vs Automated Segmentation.....	95
Figure 5.10 Axial Plane View.....	96

Figure 5.11 Sagittal Plane View.....	96
Figure 5.12 Coronal Plane View.....	97
Figure 5.13 Performance of Whole Tumor.....	98
Figure 5.14 Performance of Core Tumor.....	98
Figure 5.15 Performance of Active Tumor.....	99
Figure 5.16 Various Network Performance.....	99
Figure 5.17 T-Test on DSC for two proposed models.....	101
Figure 5.18 T-Test on SSIM for two proposed models.....	102
Figure 5.19 T-Test on PSNR for two proposed models.....	103

LIST OF TABLES

Table 2.1 Summary of CNN based Medical Image Segmentation	26
Table 2.2 Comparative Analysis of various CNN Frameworks	27
Table 2.3 Summary of Deep semantic segmentation techniques of medical images	33
Table 2.4 Comparative Analysis of Deep semantic segmentation frameworks	35
Table 2.5 Survey on Real-Time Interactive 3-Dimensional segmentation.....	39
Table 2.6 Comparative Analysis of Real-Time Interactive 3-Dimensional segmentation Techniques.....	40
Table 2.7 Summary of Hybridized Techniques for Medical Image Segmentation.....	48
Table 2.8 Comparative Analysis of Hybridized Techniques for Medical Image Segmentation...50	
Table 2.9 Summary of GAN based image segmentation.....	53
Table 2.10 Comparative Analysis of GAN based image segmentation techniques.....	54
Table 2.11 Summary of Fuzzy Based Medical Image Segmentation	58
Table 2.12 Comparative Analysis of Fuzzy Based Medical Image Segmentation.....	59
Table 2.13 Summary of Deep Learning-Based Brain Tumour Segmentation Algorithms.....	63
Table 2.14 Comparative Analysis of Deep Learning-Based Brain Tumour Segmentation Algorithms.....	64
Table 3.1 Hierarchical Dense CNN of Requirements.....	76
Table 4.1 Dataset Description with Division into Training, Testing and Validation Sets.....	76
Table 5.1 Tissue segmentation parameters and performance evaluation(T-Net).....	87
Table 5.2 Tissue segmentation parameters and performance evaluation (HD-CNN).....	88
Table 5.3 Analysis based on Benchmark Models	89
Table 5.4 Results using RT-GAN algorithm.....	94
Table 5.5 Comparison included with RT-GAN algorithm.....	100

Table 5.6 T-Test on DSC for two proposed models.....	101
Table 5.7 T-Test on SSIM for two proposed models.....	102
Table 5.8 T-Test on PSNR for two proposed models.....	102

CHAPTER 1

INTRODUCTION

1.1. Introduction

Segmentation of an image is the procedure of splitting a picture into various segments to transform it into a more meaningful and easy-to-analyse representation. Segmentation is a key step in the processing of images particularly in the domain of medical imaging, it is often necessary to identify or segment objects/organs/structures from their surroundings while analysing medical pictures. Researchers and practitioners have a variety of options, ranging from manual scan-by-scan tracing to fully automated segmentation. Several of them are interactive methods, which combine process automation's high accuracy, efficiency, and homogeneity with quality assurance and technical expertise gained by human supervision [1].

The quantitative analysis and image-guided interventions of the medical images have realized growth in the usage of segmentation approaches in the recent decade. Many approaches have now been explored, with some now being used in analysis systems and commercial imaging. Since segmentation of the image is generally the initial move-in information processing, a suitable, accurate, exact, and effective technique must be utilized to reduce incorrect or unacceptable findings. When selecting any segmentation approach for a certain purpose, keep in mind that not a single generally applicable segmentation approach works for all sorts of medical pictures and organs, and all segmentation techniques have their advantages and disadvantages [2].

The segmentation of a human tongue image, for example, will have an impact on sequence image processing and medical diagnosis. However, individual images have distinct qualities, and the image will be influenced by various conditions throughout the image collection process. For example, whenever a human tongue picture is captured, it will be impacted by saliva in the mouth, resulting in a large number of bright spots and zones. It is owing to the picture's complexity and image segmentation technology's dependence on certain environmental and object parameters. So yet, no universal algorithm has developed.

For the analysis of biological human body information, precise segmentation of medical photographs is essential. Computed tomography scans, magnetic resonance imaging, X-rays,

and other image modalities are used to diagnose various illnesses. Magnetic resonance imaging and computed tomography scans are frequently used for diagnostic and therapeutic purposes.

Medical imaging techniques have their advantages and disadvantages. When compared to other imaging modalities, Magnetic Resonance Image (MRI) has the following benefits: excellent resolution, the capacity to image soft tissues, and a good signal-to-noise ratio [3].

Computed Tomography (CT) scans show less soft tissue contrast than MRI images. The separation of various objects in a medical picture is aided by medical image segmentation. In a brain MRI, the following things must be segmented: grey matter, cerebrospinal fluid, cyst/tumour, and white matter. The following are three key challenges that emerge during working on automated brain MRI segmentation: Image noise has the potential to alter the image's intensity, resulting in incorrect results. The changes in single tissue classes all through images are dependent on the inhomogeneity-intensity level variations in the image [4].

Due to the limited pixel sizes of images, they are susceptible to partial volume averaging. Scanned pictures may be incompatible with one of the subclasses because if the volume terminology in clinical specimens is complicated. Electronic diagnostics are extremely crucial to assisting radiological specialists with clinical diagnosis. This enables the processing of many instances with the same degree of accuracy and in a shorter amount of time [4].

This study develops a novel interactive segmentation tool that uses segmentation techniques based on hierarchical clustering to enhance the accuracy of multi-category segmentation classification. The primary motive of this research is to boost the proficiency of the segmentation algorithm via the use of hierarchical clustering to segment intricate areas on a real-time basis. This study uses quantitative parameters like mean peak signal to noise ratio, square error, and entropy to evaluate the efficacy of the planned method, combining qualitative functionalities like sensitivity, precision, and accuracy with quantitative criteria like peak signal to noise ratio, entropy, and mean square error.

A brain tumour, also known as a cranial neoplasm, is defined by the growth of mutant cells inside the brain. The automated segment of MRI scans for neurological illnesses is preferred because to the intricacy and time-consuming nature of improved segmentation processes. The subject of autonomous tumour segmentation is rapidly developing. Living organisms are highly poisonous to brain tumours, and they frequently result in death. Early detection of brain cancers is critical for reducing mortality rates. Due to the short diagnostic time associated with automatic segmentation, cancers in MRI images can be diagnosed

immediately. Recent research has concentrated on building the most accurate and optimal automated segmentation algorithms possible, with deep learning architectures getting more involved in brain tumor segmentation [5].

Neural Networks using Convolutional Layers CNNs, stacked autoencoders SAEs, and deep belief networks are all examples of deep belief networks. DBNs are subtypes of deep learning methods used in the segmentation of brain tumors. CNN offers extremely precise findings. Therefore, it is commonly used to segment brain tumours images using MRI. There are several layers in this feed-forward neural network, including convolutional, pooling, and fully convolutional. To get a superior dice score coefficient for the segmentation process, the specifications of these layers, as well as various weights and biases, are adjusted [5].

Glioma is the most common and severe type of crucial brain tumor in youth, starting with glial cells and penetrating nearby tissues. Glial tumors, which have a high death rate in adults, are the most frequent and cancer-causing tumor kind. These cancers have a high risk of death and morbidity. Glial tumors account for more than 90% of all tumors in those over the age of 20 [6].

The segmentation procedure is more challenging in the case of glial tumors due to the tumor's heterogeneous nature, which includes necrotic (dead) and active parts. The fact that not all glial tumors have a distinct border between necrotic and active portions, and that some may not have any necrotic components, further complicates segmentation. Brain tumor structures are grouped into three regions [7]:

- The complete tumor region includes edema, necrosis non-enhancing, and enhancing structure.
- All tumor structures, excluding edema, are found in the core tumor area.
- The enhancing tumor region comprises of enhanced tumor structure.

Necrosis can be considered a lifeless element. Edema is considered as swelling induced by the tumor that can be separated in non-enhancing along with enhancing tumors. The active tumor is a subgroup of the core tumor, which is a subgroup of the overall tumor [8].

To identify these malignancies, various modalities of imaging such as MRI, positron-electron tomography (PET), CT scan with others are utilized. Moreover, there are no recognized health hazards linked with short MRI exposure. Therefore, MRI may be used to identify brain tumors in people. Manually finding abnormalities in images using MRI is a

complicated and slow process. Tumors, for example, require immediate finding and treatment, which is difficult to do with manual segmentation. For the reasons stated, automated segmentation approaches with a superior dice score coefficient are shown to be the most reliable brain tumor segment diagnostic [9].

MRI that comprises T1c weighted, T2, T1 weighted, and Fluid-attenuated inversion recovery (FLAIR), assists to spot tumor tissues and tumor influence in different tissues. There are many modalities of Magnetic resonance pictures [10] that are differentiated by contrast and brightness. These modalities are extremely susceptible and directly connected to illness because of the tissues impacted by inflammation [11].

T1 weighted imaging is the highest popular of these modalities, and it is primarily employed for analysis of the structure and separating between healthy and diseased tissues [12].

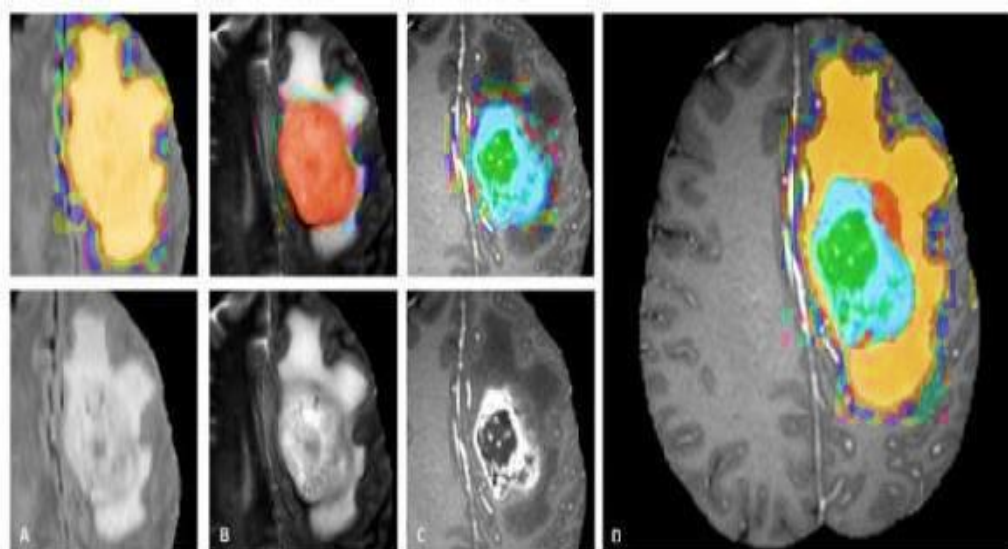


Figure 1.1 The fourth images from left to right show the edema in green color, enhanced tumor in yellow necrosis in red color, and non-enhanced tumor color in sky blue color (BraTS dataset)

T1 weighted is a novel brain tumor segmentation approach that recognizes various tumor cells in high-grade and low-grade Glioma by using a gradient as well as context-sensitive characteristics. Inside T1c mode, glioblastoma is enriched from the boundaries. T1c weighted imaging may help identify active tumors (AT) from necrotic areas. The edema region, also known as the core tumor, looks much brighter in T2 [13]. FLAIR is a method used to find the whole tumor. Images from various sequences were collected for each patient in the dataset, T1, including T2-contrasted, and FLAIR. Every one of such sequences, as previously indicated, takes advantage of the various features of the tissues, resulting in the contrast among the

pictures. For best segment process outcomes, the contrast qualities of all visual modalities take use of varied features of the tissues recovered. The Whole Tumour (WT) is evident inside the sequence Flair. The T2 sequence shows the Core tumor structure, whereas Figure 1.1 shows the ET (enhancing tumor) structure. Therefore, MR images are needed from many sequences to accurately identify and describe the intra-tumor structure [13][14].

Handcrafted features are manually obtained in prior segmentation methods, resulting in a greater degree of complexity. Deep learning has reduced the challenge of manually collecting features since segmentation methods based on deep learning use features extracted straight from the input with a growing hierarchy.

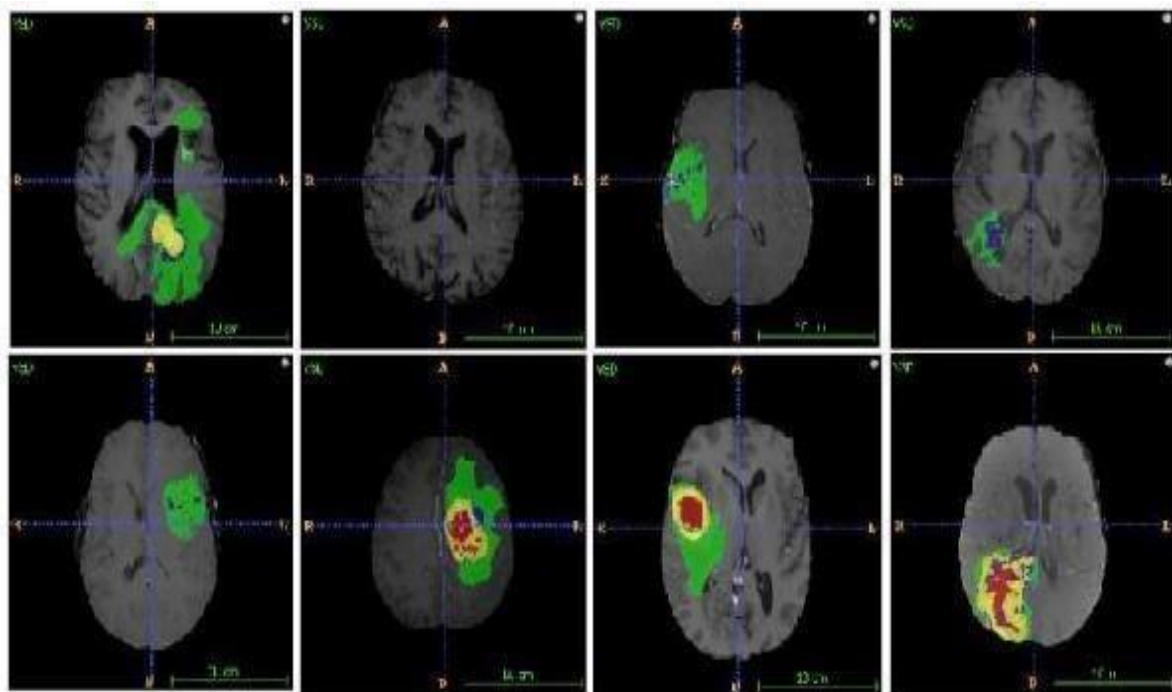


Figure 1.2 Distinct patients with Tumour (BraTS Dataset)

Figure 1.2 shows the same brain slice with help of various patients, exhibiting tumor variety. Each of the eight photographs or patients shown below clearly shows the location of the tumor. Each of the eight photos has a different form and intra-tumor anatomy. There may be possible more than one tumor site. This illustrates the challenges of the automated segment process [16][17].

Therefore, rather than taking the usual path of manual feature extraction, Deep self-learning architecture should be our goal. It is a major motive for the use of deep learning to handle challenges like identifying tumor features using brain images. Tumor identification is an intuitive and tough process because of variability in tumor characteristics such as structure,

form, and location from one patient to another patient. This makes tumor segmentation in MRI challenging [15].

The dice score is utilized to assess segmentation methods or algorithms' performance. The Dice Similarity Coefficient (DSC) is utilized to determine it [5], which computes the imbricate between manual and automatic segment processes.

$$DSC = \frac{2TP1}{FP1 + 2TP1 + FN1} \quad (1.1)$$

Where TP1 stands for True Positive, FN1 stands for False Negative, and FP1 is for False Positive [18].

This study considers certain basic ideas of multilayer perspective in deep convolutional neural networks (DCNNs) and convolutional neural networks (CNNs), which are used to segment brain tumors [19-21]. The most challenging feature of assessing such a segment process is the dice score. This research develops a unique transfer learning approach in combination with a hierarchical dense convolutional neural network to boost the dice score coefficient. In this research, the primary focus is to improve the accuracy of the segmentation algorithm by using GAN, which aids in accurately and precisely localizing the brain tumor for a huge dataset [22-24].

1.2. Brain Imaging

Brain imaging techniques, as opposed to physical incision, use a correlation between different types of power and brain tissue (e.g., particle radiation, or electromagnetic) to record positional information on the anatomy and brain functioning. Imaging investigations offer information regarding routine brain functioning and structure, neuroanatomic aspects of mental and disorders related to neuro, as well as modifications related to neural process linked with diagnosis respond [25].

The goal of clinical applications is often to distinguish between normal biological activity in a healthy brain and disrupted conditions for example Alzheimer's and stroke. The focus of neuroscience-based cognition is to know in which way brain functioning influences human behavior and cognition for example language, vision, and memory. Accomplishing such objectives is dependent on the type of the detected temporal resolution, signal, and spatial, as well as reasonable restrictions such as the invasive nature and expense of each approach. Diffusion tensor imaging (DTI), Magnetic resonance imaging (MRI), functional MRI (fMRI),

PET, electroencephalography (EEG), and magnetoencephalography (MEG) are frequently utilized in image modalities. These modalities use various physiological parameters to represent features of either structure of the brain or its functioning [25].

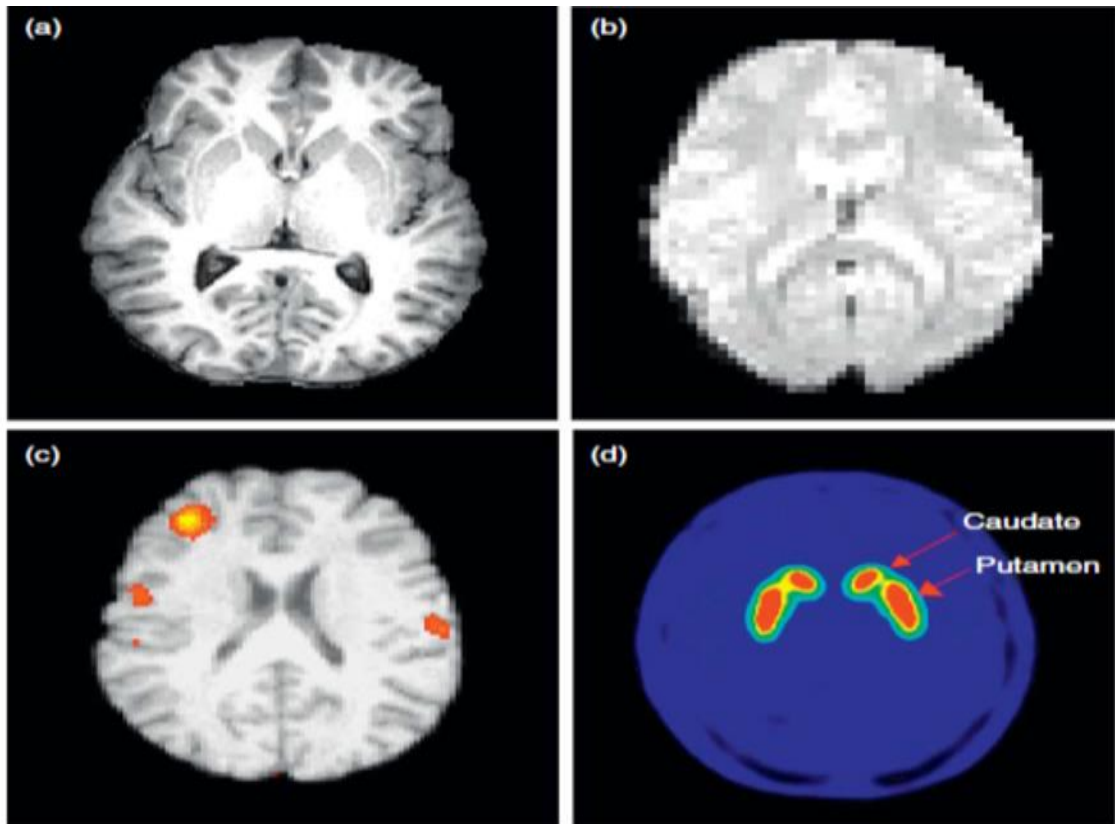


Figure 1.3 MRI shows structures such as deep nuclei, bone, white vs. gray matter by evaluating the oxygen concentration in blood haemoglobin

Conventional MRI pictures Figure 1.3(a) depict the 3D composition of the brain in detail, differentiating among tissues like white matter grey, cerebrospinal fluid, fat, bone, and air, along with the existence of diseased tissues like tumors. Some benefits of the MRI are its great versatility in terms of the variety of signals it can monitor. Diffusion-weighted MRI is very responsive to the motion of molecules during time intervals. The identification of directed diffused signals enables the description of white matter structure, paving the way for the advancement of MRI-centred tractography tools for revealing white matter relation [26].

It is particularly susceptible to alterations that take place soon in neurological illnesses and stroke when used to evaluate overall diffusion. The localized concentration of specific metabolites measured by MRI spectroscopy can signal energy metabolism and brain cell integrity. MRI may also be used to analyze brain circulation and specify blood flow that is a precise indicator for cerebrovascular illnesses and stroke. At last, the most significant use of

MRI in the assessment of brain activity through fluctuations in blood haemoglobin oxygenation [26].

The brain patterns change depending on the sort of stimulus identified. As shown in figure 1.3(a), the signal is generally generated by fluctuations in the magnetic parameters of hydrogen atoms throughout various brain tissues, resulting in superior-resolution structure pictures that define features like white and grey matter, bone, ventricles, and deep nuclei. By monitoring the oxygenation level of blood hemoglobin, MRI may also be used to assess brain activity [26].

As shown in figure 1.3(b), the pictures produced have a reduced resolution but a superior temporal resolution. The regions of task-specific modifications in brain metabolism are revealed by comparing the obtained pictures across tasks or states. The activation maps are overlaid over a structural picture to localize these changes. Figure 1.3(c) depicts another measure of brain function. Using positron emission tomography, the binding capacity of D2 as dopamine receptors for the radioactive tracer fall pride is shown in PET. When compared to other sections of the brain, the receptors density for example hot hues like red and yellow roses in the caudate and putamen elements of the basal ganglia [26].

1.2.1. Imaging modalities

The most efficient way for diagnosing brain tumors and other diseases is medical imaging inspection. Different imaging modalities like digital mammography (DM), MRI, microscopic pictures based on histological, infrared thermography, and ultrasound are utilized for diagnosis. To support radiologists and clinicians in detecting anomalies, these modalities provide pictures that have been shown to cut death rates by 30%–70% [27].

Imaging modalities are often classified according to the mechanism by which pictures are created: radiation, ultrasound for example X-Rays, and MRI. Ultrasound images are created using sound waves and may capture images of both structure and activity (shutting and heart valve opening) in real-time. Devices based on Ultrasound techniques are often compact (similar to tablet computers) and transportable. While air and bone are great conductors of ultrasound waves, soft tissue regions for example the belly are ideal candidates for ultrasound image creation [28].

Radiation-created images are produced by X-Ray equipment, which consists of a particular X-Ray resource that produces two-dimensional pictures. Fluoroscopy units produce passing pictures in real-time as a result of X-Ray contact. Angiography is a common fluoroscopy application that includes the viewing of blood circulation in veins. Dual-energy

X-Ray absorptiometry (DEXA) scanners use X-Ray radiation to detect bone mineral density. Furthermore, computed tomography (CT) scanners have enhanced picture clearness due to the usage of several X-Ray resources and sensors. Mammography is a kind of X-Ray image technique that is specifically used to examine tissue related to the breast. Scanners Monitor used in Positron emission tomography (PET) uses radiation-emitting with modified glucose molecules to capture imaging, which is crucial for cancer diagnosis. PET scanners are frequently used in conjunction with CT scanners to get structural and biological pictures simultaneously [28]. Different imaging technologies used for the segmentation of images are described below [28]:

- Ultrasound
 - Magnetic Resonance Imaging
 - Optical method
 - Bio photonics
 - Positron Emission Tomography
 - Computed Tomography
 - Fluoroscopy
-
- **Computed Tomography**

A CT scan is performed using the huge, box-shaped scanner equipped with a small tunnel. It is a medicinal procedure that generates various two-dimensional and three-dimensional pictures of the interior organs of the human body that may be seen over the computer system. To diagnose an abnormality in every inner region of the body, a picture based on target location is necessary. The CT scan offers extensive information about the region being scanned, which may include soft tissue, organ, and blood vessels. When compared to X-Rays, it is very useful in detecting disorders such as cancer, infectious diseases, and cardiovascular problems. The radiation dosage associated with CT has become a serious concern, and it is the focus of current efforts, coupled with high-speed imaging [29].

Some of its distinctive features are as follows [29]:

- It is ideal for the abdominal and pelvic because it provides a detailed image of the interior of the body along with the cross-section views.
- It is best to pick up cancer in the lung, chest, kidney, ovary, and pancreas.
- It can assess kidney tumors, injuries, and cystic fibrosis.

Advantages:

- Non-invasive as well as painless.
- Cost-effective, simple, and Fast.
- Offers a complete picture of the lung, bone, soft tissue, blood vessels, and liver.
- Pictures based in real-time are used to perform surgery based on invasive techniques like fine needle biopsy and core biopsy.

This is the most effective technique for imaging over cross-section view, which may be utilized for preparation purposes such as biopsies and needle guiding. CT scans provide a 2D image of almost anyone portion of the human body.

- **Ultrasound**

Ultrasound is transportable, affordable, simple-to-use, and noninvasive. The use of ionizing radiation is not required in ultrasound. The time interval ranges between seconds and minutes, and it may be utilized in conjunction with a picture from an alternative modality during the guiding step. However, imaging through hard bones is challenging with ultrasound. Ultrasound creates an image of the inside body components using sound waves. A specialized Doppler ultrasonography approach is a procedure for examining the flow of blood in arteries, arms, legs, and all other body sections, as shown below [30]:

- **Color Doppler:** It represents the velocity and path of blood movement by altering Doppler measurements to a color palette.
- **Power Doppler:** It does not display the path of blood movement, is then color Doppler, and offers detailed data during periods of low blood flow.
- **Spectral Doppler:** It displays a graphical depiction of the bloodstream and may generate a blood movement sound, which can be caught with each pulse.

Advantage

- It investigates the cause of discomfort, edema, and infection.
- It analyzes an infant's kidney, spleen, uterus, brain, hip, bladder, spine, and eyes.
- It directs surgery used needle biopsy to acquire tissue samples from unhealthy areas.
- An echocardiogram detects heart cancer and failure.
- It investigates the motion of the baby in the mother's womb.

- **Positron Emission Tomography**

A radioactive tracer is used in nuclear medicine imaging modalities such as PET and Single-Photon Emission Computerized Tomography (SPECT) to provide a picture of the body's organs and structures. Radioactive detectors are messenger molecules that are only used for the scan process. SPECT generates a three-dimensional image of radiotracer molecules inside the body part. To create a three-dimensional photo, several projected shots of the body at varied time intervals are necessary. Whenever the tracker is introduced into the body, it radiates gamma rays that are identified by a specific camera and utilized to generate a picture. PET is called a nuclear-based medical imaging method that employs radiopharmaceuticals to produce a three-dimensional picture. The kind of tracer employed determines the difference between PET and SPECT. Positrons are particles that are released by the PET tracer. These are similar to electrons; however, they are negatively electric charged [31].

They are eliminated while the positron and the electron unite, releasing radiation in photons forms. This energy is detected by the PET camera, which generates a picture. PET/SPECT imaging modalities may be used with CT and MRI image modality at the core biopsy stage of tumor planning medication, such as PET offers evidence regarding tumor margin and CT provides data related to the anatomical reference. PET uses little quantity radioactive type drug to distinguish into the healthful and sick tissue. Fluorodeoxyglucose is an extremely utilized tracker drug, which is why it's also known as an FDG-PET scan. Positron emission tomography is called a non-invasive image technology with a wide range of clinical and scientific applications [32].

- **Fluoroscopy**

Fluoroscopy is a kind of X-Ray film that exhibits continuous X-Ray pictures over the system. Navigating an intraoperative surgical tool may be quite helpful during surgery. An X-Ray beam is passed over the body during a fluoroscopy procedure, and the images are forwarded to a computer system to examine how the body elements move. Fluoroscopy is used to treat and diagnose a variety of disorders. Some of its applications are as follows [33]:

- It is utilized in orthopedic surgery to replace joints and knees, as well as to treat fractures.
- It gives you a picture of your gastrointestinal system so you may examine your esophagus, stomach, and intestine. The heart problems treatment.
- It is used to open up blocked blood vessels.

The fluoroscopy procedure uses radiation way, which is hazardous to the human body since a high dosage of radiation may cause burn tissues and skin cancer.

- **Optical Method**

The optical method is a non - invasive approach. that uses visible light and particular qualities to see into the body and obtain pictures of tissue and organs, as well as molecules and cells. The two highly often used optics-based techniques are bioluminescence in which light is generated by living organisms [34].

- **Nuclear Method**

Nuclear medicine is called an image modality technique that involves injecting radioactive substances called radiotracers into the human circulation to obtain a photograph of the inside of the body. Such substance travels about the objected region and releases gamma rays, which are taken by the system and the camera and used to form the picture. This is a minimally invasive process that is utilized in several medical products. Nuclear medical scans are categorized by their kind [35]:

- Bone scan: An image of the bones is captured to verify the existence of tumors and infections in the bone.
- Gallium scan: Photographs the specific tissue to assess for disease or cancer.
- Nuclear medicine has a multitude of purposes, some of which are listed here:
 - Cardiovascular function assessment after chemotherapy.
 - Visualizing the blood circulation via the heart and spinal fluid, etc.
 - To Locate infection of unidentified cause.
 - Making treatment strategies for cancer.
 - Identification of biopsy locations.

- **Bio photonics**

Bio photonics is an interdisciplinary branch of study that blends biology with photonics, the assessment of light. It may assist physicians to realize how tissues and cells function. This approach based on light allows for the collection of samples of abnormal and healthy tissue for diagnostic, therapeutic, and surgical purposes. Alexander Gur switch suggested this relationship between photons and living cells in 1923, based on the production of ultraweak

photons from yeast and onion [36]. Scientists from Germany observed similar radiation from alive organisms twenty years later and coined the name "bio photonics".

Several usages of bio photonics include the following [36]:

- To investigate the role of proteins and DNA in biology using additional substances.
- To observe live entities and to investigate how cells interact.
- To aid in the detection of infectious diseases (HIV).
- To transmit information about the body's moving components.
- To offer noninvasive treatments for a wide range of disorders.

1.2.2. Magnetic resonance imaging

Over the previous four decades, MRI has evolved from a promising tool to major diagnostic investigation for a wide variety of clinical conditions. Its application, which was initially restricted to the neuro-axis, has expanded to include all parts of the body. An expanded knowledge base has resulted in a deeper comprehension of how it should be used optimally, either alone or in combination with other techniques, to optimize diagnostic assurance. A short history of magnetic resonance imaging, as well as the fundamentals of magnetic resonance imaging, is explained in this section, its application in the maxillofacial region, and recent advances in MR imaging [37].

MRI can get more precise images of the brain and other cranial structures using magnetic resonance imaging than any other imaging technology because of a combination of a strong magnetic field, radio waves, and a computer. This examination does not involve ionizing radiation and may need an injection of gadolinium contrast material, which is less likely to trigger an allergic response than iodinated contrast material. Brain tumors may be detected using advanced imaging methods. The most often utilized diagnostic technologies are computed tomography scans and magnetic resonance imaging. Magnetic Resonance Spectroscopy can be utilized to assess the chemical composition of a tumor and to reveal the kind of injuries discovered during an MRI scan. PET scans may be used to diagnose recurrent brain tumors. Magnetic Resonance Imaging, a commonly utilized without-invasive technique, generates a huge and diversified array of tissue contrasts in every imaging technique and has been extensively employed by medical experts to identify brain tumors [38].

1.2.3. Magnetic Resonance Imaging Principle

The fundamental idea behind MRI is that everything is composed of atoms, as well as the human body. Every atom is composed of a nucleus that is surrounded by electrons. Protons and

neutrons are subatomic particles that exist inside each nucleus and are responsible for the structure of the nucleus. Neutrons are electrically neutral, while protons have a positive (+) charge. The atomic number is determined by the total amount of protons present inside the nucleus, and atomic weight is calculated by the sum of protons and neutrons. Nuclei can be thought of as the nucleus of magnetic resonance, where atomic nuclei rotate around one another. Many components include no less than one isotope with a spin greater than zero. These nuclei are referred to as magnetic resonance active nuclei [39]

Electromagnetic induction is governed by three principles: motion, magnetism, and charge. Magnetism is induced while charge and motion are together. Magnetic moments are naturally acquired by active nuclei of Hydrogen that have a total electric charge and are spinning motion. Carbon (^{13}C), sodium (^{23}Na), Hydrogen (^1H), fluorine (^{19}F), and phosphorus (^{31}P) are all illustrations of active nuclei of MR. Hydrogen nuclei are composed of only one proton and have a strong magnetic moment field. The primary active nuclei of MR employed in the creation of the MRI technique due to their large quantity of fat molecules and water, which together account for greater than 75% of the total human body weight. Thus, MRI technology makes use of the magnetic properties of hydrogen nuclei found in the body. When no outer magnetic field exists, hydrogen nuclei's magnetic moments are aligned in a random direction. When hydrogen nuclei are put in a strong exterior Static Magnetic Fields (SMF), it comes to the magnetic field, their moments line up perfectly. According to Plank's quantum field theory, nuclei hydrogen can exist in one of two unique energy states [39]:

- spin-up nuclei (lower energy), whose magnetic moments are in the same direction as the external magnetic field,
- spin-down nuclei (higher energy), whose magnetic moments are anti-parallel to the applied magnetic field.

The externally applied field's strength and thermal energy govern the relative abundance of spin-up and spin-down nuclei. The thermal energy of a nucleus is mostly determined in clinical applications by a patient's temperature. The proportion of spin-up nuclei slightly surpasses the count of nuclei at thermal equilibrium. In the existence of SMF, this little excess provides a net magnetism that shows the comparative balance of spin-down and spin-up nuclei.

At resonance circumstances (Larmor frequency), external oscillating RF pulses may be used to orient the available longitudinal equilibrium magnetization so it can be detected. Due to the resonant and transverse magnetization created by this, when a receiver coil or conducting loop

is placed near these oscillatory magnetic fields from hydrogen nuclei, a voltage is formed in the reception coil, which produces an MR signal. The magnetic resonance signal intensity is measured by the intensity of magnetization in the transverse plane. Thus, MR active nuclei signals may be obtained in homogeneous SMF using an appropriate Radio Frequency (RF) [40].

Whenever the RF is shut off, the energy in the MR active hydrogen nuclei is lost given by the RF pulse, which is referred to as relaxing. Certain spin-down nuclei change into spinning nuclei during relaxation, aligning the magnetization in the same direction as the spin-up orientation. Simultaneously, the quantity of transversal magnetization progressively decreases a process called decay. Thus, relaxing occurs in the restoration of longitudinal magnetization while the transverse plane magnetization decays. The restoration of longitudinal magnetization occurs because of a process known as T1 restoration or spin-lattice relaxing, it involves the transmission of radiation by "high-energy atomic nuclei" to the physical conditions. The reduction of transverse magnetization against the direction of SMF is induced by a procedure called T2 decay or spin-spin relaxing, which occurs because of nuclei sending and receiving radiation with nearby nuclei and communicating with one another. The T2 decay and T1 recovery rates are determined by the tissue's fundamental structure and the movement of molecules [40].

Two events must occur concurrently for stimulating magnetization in a particular slice/section of the body [40].

- The RF pulse must have a set bandwidth that excites spins exclusively within a certain frequency range.
- Simultaneously with the communicated RF pulse, a straight rising

GMFs should be provided to change the regional frequency in the slice/section direction. Usually, linear Gradient Magnetic Fields (GMF) is used to transform the magnetization of an item spatially. The imaging pulse sequence is distinguished by various elements, which include the given below [40].

- It is possible to use many pictures or slices of the same picture or slice with different RF pulsations within the same repeating time (TR), which would be determined in milliseconds. The TR also calculates how much T1-contrast and T1-relaxation are there.

- The echo time, which is the time interval between the distribution of the Rf field and the reception of a signal (measured in milliseconds), regulates the amplitude of the T2 contrast by determining how much transverse magnetization degradation happens.

The intrinsic variability in protons compactness, T1, or T2 in diverse tissues results in enough contrast in MRI images. Nonetheless, immediately after the introduction of commercialized magnetic resonance equipment in the mid-1980s, extrinsic MR contrast agents were developed to enhance the inherent contrast between normal and sick tissue. Contrast agents in MR operate by selectively influencing the T1 and T2 excitations in diverse tissues via spin interaction between the various electron spins of metals, particularly proton and contrasting agents in the water. MR contrast agents' function by selectively altering the T1 and T2 relaxing durations of specific tissues via spin interactions between both the electron spins of metal-containing proton and the distinction agent in the water [41].

However, numerous other forms of agents have begun to enter the market. Various forms of the contrast agents may be described based on [41]:

- The agent's magnetic property,
- The agent's predominant impact on the signal intensity is defined
- The agent's major influence on signal intensity.

During the MRI operation, which may take many few minutes, the patient rests over the table and particular areas of a body are subject to the three elements of an electromagnetic field, namely, time-variable GMF, SMF, and the pulsed RF, to obtain pictures [41].

- Longitudinal magnetization is obtained using a high-level SMF
- The quickly switching time variable GMF enables geometric encoding.
- The magnetization is excited by resonant pulsed RF, which results in a quantifiable signal. While an SMF is always obtainable even when the MRI scan is not in use or functioning, the moment pulsed RF or GMF are only conveyed during the imaging process.

1.3. GAN

A generative adversarial network (GAN) is made up of two networks that are both trained at the same time. The discriminator is trained to categorise whether images are from the training data or not, while the generator is educated to learn the distribution of the training data. Several efforts have improved GANs' ability to generate high-resolution, realistic-looking images since the GAN's proposal [42].

1.4. Research Motivation

Brain tumors are among the most dangerous forms of malignancies in the world. Glioma, the most frequent kind of primary brain tumor, is distinguished by numerous histological and malignancy grades, with glioblastoma patients having an average survival duration of fewer than 14 months later diagnosis. It has become more important to use segmentation methods in quantitative analysis of medical images in recent years. Commercial imaging and analysis systems are currently using a wide range of imaging modalities. Every segmentation technique has its limitation and its advantages. There is a need for real-time automated brain tumor image segmentation to enhance treatment options and improve patient survival lifespan. Basis motive of research is to fulfill this technological gap in the segmentation technique by building the most efficient algorithms which not only automatically define tissues, organs, and tumor volumes in real-time but also enhance the accuracy of segmentation algorithm by using GAN that helps incorrectly and more precisely localizing the brain tumor for a large dataset.

1.5. Research Objective

The current research program's objective is to build up an effective brain tumor segmentation techniques for use in real-world scenarios.

1.5.1 Sub-Objectives

At the start, the following sub-objectives were developed, defining the key characteristics of the research endeavour. The following stages are involved in the development of an algorithm for automatically segmenting brain tumors:

1. Developing a robust, efficient and rapid deep learning algorithm for segmentation of tumors from MRI images.

- Finding research gaps in current automatic brain tumour segmentation techniques.
 - Gaining a deep understanding of typical deep learning-based brain tumor segmentation methods.
2. Implementation of the proposed algorithm in the real-time scenario.
 - Developing a robust, comparatively efficient, and fast deep learning-based algorithm, which can clearly distinguish between core, active, and whole tumors.
 - Developing a transfer-learning algorithm based on the GAN network.
 - Implementing the proposed DH-CNN and RT-GAN in real-time scenario.
 3. Performance testing of the newly developed deep learning algorithm for brain tumor segmentation, as well as comparisons with current methods to demonstrate the new algorithm's efficacy.

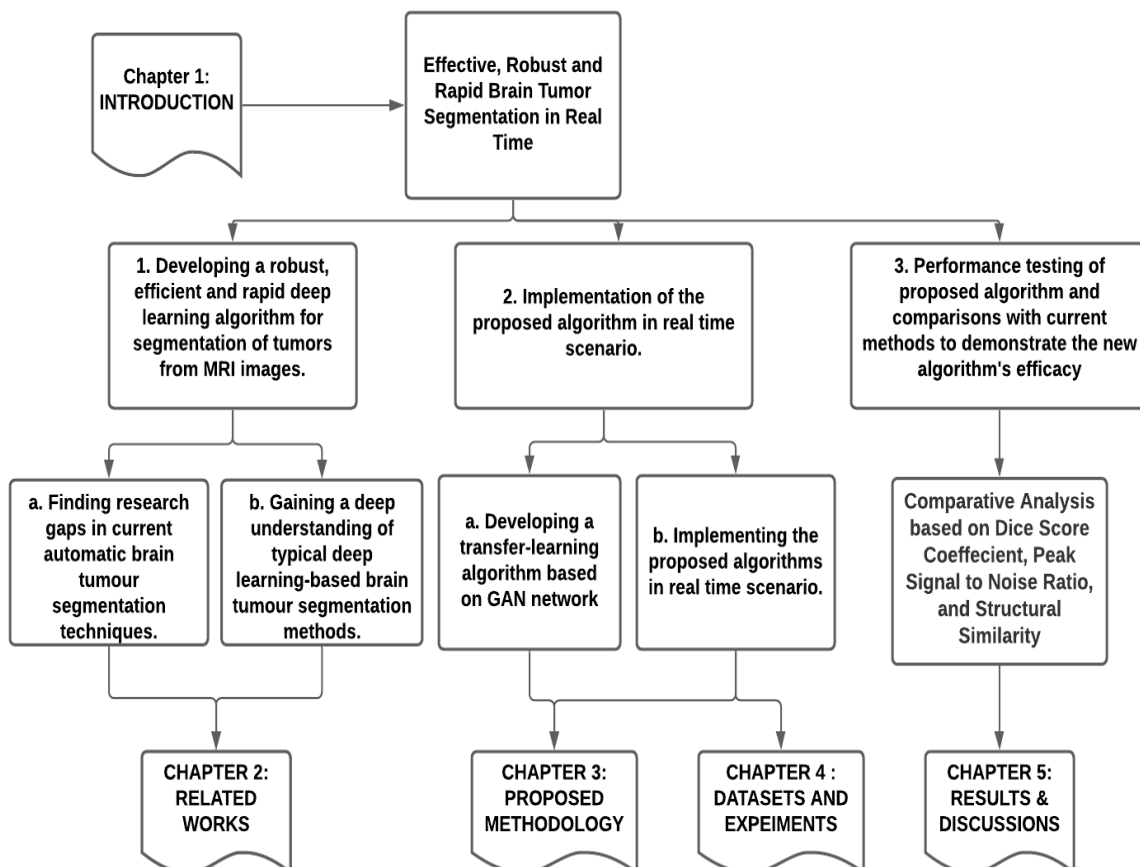


Figure 1.4 Outline of Research Objective and Sub-Objectives

1.6. Research Overview

Brain tumor segmentation deals critically in distinguishing between the tumorous and healthy areas in order to utilize the information in clinical settings. IT can forecast the accuracy of brain tumor segmentation algorithms using dice score coefficients.

According to the literature review, the technique should be relatively resilient, have a high processing speed, be less complex, and have good precision. A high dice score coefficient and structural similarity index indicate that brain tumors were efficiently and reliably segregated from MRI data. The purpose of this study is to develop a faster, robust, and less complex approach for segmenting brain tumors in real-time

In the suggested research approach, three algorithms are implemented to check the comparatively efficient brain tumor segmentation technique. The first algorithm is T-net algorithm, which is based on the transfer-learning model that does not require a high training dataset. The second algorithm is hierarchical dense CNN technique is planned for the brain tumor segment process utilizing MRI images. The planned approach includes a pre-processing step with bias field rectification and concentration normalization. The third algorithm is RT-GAN beneficial for small training labelled datasets. Additionally, this work enhances the effectiveness of segment process techniques by combining qualitative indicators like dice score coefficients with quantitative characteristics including mean square error & peak signal to noise ratio. Because segmentation algorithms' precision helps to reduce mortality, it is vital to enhance their precision.

An upgraded deep learning approach combining the transfer learning based GAN model improves the computational efficiency and competency of the tumor detection technique for future study. All the algorithms went under comparative analysis on the basis of parameters as dice score coefficient, structural similarity index, peak signal to noise ratio, and mean square error. This research is proven to be highly efficient based on the T-test performed on RT-GAN and DH-CNN.

1.7. Thesis Organization

Chapter1: Introduction

This chapter introduces the concept of real-time segmentation of medical images and their applications focusing specifically on automatic segmentation of brain tumors using MRI. It

discusses the different imaging modalities and its relevant advantages and disadvantages. It also discusses the research motivation and objectives (sub-objectives). The chapter also details about image segmentation thesis.

Chapter 2: Literature Review

In this chapter, we can find contextual information & understanding of the field of concerning research. It discusses the various research gaps from the various medical image segmentation techniques and also analyses each technique on the basis of some parameters. This helps in understanding the latest algorithms and developing the proposed methodology. Based on the literature survey conducted, it helps in fulfilling the sub-objectives for this research work.

Chapter 3: Methodology

In this chapter, we can discuss the methodology part of the model Machine learning-based training and detection. This section discusses all the algorithms proposed for the research work to be carried out. It discusses the implications of the research. All the phases like pre-processing, feature extraction with their methods will be discussed in this section.

Chapter 4: Datasets & Experiments

This chapter discusses the datasets involved in the presented research work. It also discusses the set-up of the BraTS dataset and the experiments performed on the BraTS grading for this research work. This research work discusses the feature acquisition from the multimodality image dataset and the preparation of the dataset the experimentation.

Chapter 5: Results & Discussion

This chapter explores & assesses the empirical results of experimentations in order to justify the theory offered in Chapter 3. The research is inspired by this chapter and it discusses the outcomes attained from all the algorithms and then performed a comparative analysis of the same. The technique then gives effective outcomes & analyses of every information or test. The techniques underwent t-tests as well for proving them comparatively efficient from other techniques.

Chapter 6: Conclusion & Future Directions

This chapter will include concluding remarks of the task performed during the thesis and criticism to show the direction of future research to enhance the proposed technique for the Real-Time Segmentation of Medical Images.

CHAPTER 2

BRAIN TUMOUR SEGMENTATION RELATED WORK

2.1 Overview

In the past years, many researchers have done a significant survey in the field of medical applications, where automatic and semiautomatic methods have been suggested for the segmentation of medical Images. Medical adoption of partition has been contingent upon the computation's simplicity and the level of user monitoring. Interactive or semiautomatic approaches are likely to continue to be popular in practice for some time, particularly in situations where incorrect interpretation is undesirable. This chapter gives an overview of the most significant real-time segmentation approaches for medical pictures currently available.

2.2 Literature Survey of Automated Medical Image Segmentation

Multiple approaches have been used to segment and identify brain tumors. In general, Magnetic Resonance Imaging (MRI), Computed Tomography (CT) can be effective methods to find the various types of diseases in the human body. The brain tumor is occurred by the unnecessary abnormal cell growth in the brain part of the human body in a disorder method. The brain tumor is detected using MRI image processing according to its size, form, and position. At present many image processing techniques were presented to find and segment the brain tumor from the MRI. Brain tumors are developed as Benign and Malignant Tumour. While benign tumors do not influence other regions of the body, malignant tumors are cancerous that can spread throughout the brain. At present, MRI has become better technology to scan the brain on the medical side. The MRI technique can take the image of the brain. Therefore, image processing and segmentation must be needed to detect the tumor in the brain. The purpose of the review of various MRI image segmentation and classification methods.

In this chapter, computer vision-based and image processing methods for brain tumor detection can be surveyed, and several brain tumor segmentation methods, feature extraction, tumor classification, and deep learning algorithm can also be examined. An effort can be made to survey and analyze the current knowledge in automatic brain tumor detection using an

effective segmentation method. The importance of accuracy and tumor classification has been extensively discussed in this literature. Different research works are obtainable on brain tumor detection utilizing an effective image classifier in this survey. Only some of the present works are assessed for brain tumor segmentation methods.

The literature survey is organized in following steps:

- Segmentation of Medical Images through Convolutional Neural Networks
- Deep semantic segmentation of medical images
- Real-Time Interactive 3-Dimensional segmentation
- Segmentation of Medical Images Using Hybridized Technique
- Generative adversarial network GAN based image segmentation

Above-mentioned literature survey is concluded in section 2.3, which discusses the detail the specific brain tumor segmentation algorithms based on the deep learning techniques.

2.2.1. Segmentation of Medical Images through Convolutional Neural Networks

Convolutional Neural Networks have proven to be the state of art in medical image processing, analysis and segmentation. CNN's being associated with automatic feature extraction based on the training inputs has accelerated its usage in medical image analysis. The layers defined within the CNN such as convolutional layer, pooling layer, etc. only fetch those parameters, which are relevant to the required tissues whether healthy or unhealthy. When dropout layer is included in the CNN makes it more suitable for extraction of important and relevant parameters only. CNN's can also be merged with fully convolutional layer, which acts as the final decisive layer in the whole network. This literature survey indicates the frequent and rapid usage of CNN's in medical image analysis and segmentation.

Garcia et al., (2017) introduced an innovative cross and comprehensively stacked CNN model based on the Dice error function, which enables true instrument separation in robotic surgery at an fps of about 29Hz. It utilizes outperform strategies such as 9 times sampling the precise details (the stipulation for a feature extraction which also respects the edges of robotic systems devices for contour being used accurately for process control and the details) as they account for the limitations imposed by prior optimization techniques. The positive findings from the testing dataset indicate that combining neural projection from both different values of the CNN's aids in the isolating of robotic surgical equipment and that giving deep supervision to all input units further enhances segmentation performance [43].

Hajabdollahi et al., (2018) stated that for Segmentation of the retinal vessels provides clinicians with vital information about the vessels and can be utilized for ophthalmic surgery and visual diagnostic procedures. Convolutional layers (CNNs) are highly effective techniques for medical picture categorization and segmentation. However, because of the complexity of CNNs, implementation in wearable electronics such as monocular indirect ophthalmoscopes is challenging. The objective of that first essay is to suggest a method for simplifying CNNs that combines quantization and pruning. To achieve a basic and efficient network topology, fully linked layers are quantization, and convolution layers are trimmed. Experiments on pictures from the STARE dataset demonstrate that their reduced network is capable of segmenting retinal vessels accurately and with a minimal degree of complexity. The simplified CNN suggested herein might be used to segment vessels automatically in compact retinal diagnostic equipment [44].

Li et al., (2019) depicted that medical pictures are distinguished from regular photos by their unique properties. As a critical aspect, there is typically a disparity in data distribution between the source and target domains to account for sparsity and privacy concerns. The purpose of this work is to offer a framework for domain adaptation of medical images called CLU-CNNs. CLU-CNNs enhance domain adaptation capabilities without requiring domain adaptation training. ANCF is a novel approach to domain adaptation probability distribution assumptions about network output. Additionally, to increase stability, the BN-IN Net is incorporated in fully convolutional networks. There are two particularly noteworthy contributions: 1. A novel strategy for domain adaptation was presented that does not require further training. 2. BN-IN Net was created to effectively increase the model's stability. CLU-CNNs are easily extensible to handle a variety of tasks. Additionally, it avoids most of the unnecessary computing expense associated with medical pictures, because it is created around medical image properties [45].

Schlemper et al., (2019) stated that for medical image analysis, they offer a unique attention gate (AG) model that extrapolates to focus on structures of varied forms and sizes. Models trained using AGs learn implicitly to suppress unnecessary areas in an input picture in favor of emphasizing key characteristics important to a particular task. When convolutional neural networks are employed, thus eliminate the chances for specific artificial vascular identification features. AGs may be easily included in well-known Convolutional network topologies such as VGG or U-Net at a low computational cost, while simultaneously improving model reactivity and prediction accuracy. To demonstrate the use of AGs in detecting scanned surfaces during prenatal ultrasonography monitoring. They demonstrate that the suggested

attention strategy is capable of effectively localizing objects while also improving prediction performance through the elimination of false positives. Segmentation of the designed system is evaluated using two massive 3D CT abdominal datasets tagged explicitly for various organs. Experiments show that AG models consistently beat foundation architectural style in forecasting throughout a spectrum of datasets and retraining size combinations while being computationally efficient [46].

Zhang et al., (2020) stated that in a typical label acquisition approach, numerous human experts assess the "real" split labels based according to their preconceptions and levels of expertise. Segmentation and classification algorithms are restricted in their efficacy because they inaccurately rely on such noisy classifications as reality. Through, the use of two linked CNNs, techniques describe an approach for complementing the reliability of labeled data and the accurate classification labeled distribution via essentially noisy data independently. The two are separated by allowing the estimated dataset to be as inefficient as feasible while achieving a high degree of precision with a noisy learning algorithm. They begin by constructing a practice dataset for classification based on Microarray datasets and examining the tentative algorithm's features. Following that, the technique is demonstrated using three publicly available computed tomography delineation datasets with both simulated and realistic varying observations: 1) lesions associated with multiple sclerosis 2) tumors of the brain 3) anomalies of the lungs. In every scenario, technique beats competing for methods and comparable baselines, exponentially with the number of annotations is limited and the degree of disagreement is high. Additionally, the trials demonstrate a high capacity for capturing the complicated spatial aspects of annotators' inaccuracies [47].

Ahammad et al., (2020) suggested that the prediction of spinal cord illness using a convolutional network (CNN) has established itself as a trustworthy approach in computer vision applications. Detecting spinal cord injury (SCI) is a significant challenge for disease segmentation and classification. Historically, radiologists manually analyzed SCI pictures to diagnose aberrant spinal abnormalities. Manual interpretation of a high-dimensional feature space makes predicting the precise category and severity level challenging. On the other hand, a deep learning system enables accurate and rapid diagnosis. Automatic classification of normal abnormal SCI photos is performed using a deep learning method. This article proposes a methodology for using deep learning to aid in the diagnosis of SCI especially appealing to the segmented regions. On-sensor SCI image data, this work applies a unique CNN-deep segmentation-based boosting classifier. A true test to check is used to record data about spinal

cord disorders of various forms and orientations. The experimental findings demonstrate that the new CNN-deep segmentation-based boosting classifier outperforms previous CNN-based classifiers in terms of computational SCI disorder prediction [48].

Hao et al., (2020) stated that the distinction between binocular and stereoscopic vision has been proven to be rather small. This observation supports the argument that stereoscopic vision has no discernible impact on the vision threshold. Another notable component of the findings is elderly observers' near-complete blindness to reddish inputs, which adds to the inadequate dark acclimation. About Blackwell's work, it is critical to stress distinguishing features. Blackwell's experiment demanded a significant exertion in terms of manpower, which was not accessible in this instance. Using a rigorous time in developing, a greater number of conditions were evaluated. Additionally, the number of veterans is significantly higher (45 versus 19), with a special emphasis on demographic characteristics dispersion. The findings imply that it is critical to consider the biological being's aging (e.g., in anthropomorphic robotics autonomous automobiles operating in low light on highways shared with people driving cars), but stereoscopy can be deemed less significant, particularly in low light. Accompanies could be made in low-light photography, for example, enabling aesthetic analysis of photographs; color mapping can be used to create a picture obtained during the day that appears to be shot at night, taking into consideration the peculiarities seen in the standard tests [49].

Qin et al., (2021) proposed a technique for computing and visualising the position of a custom Image acquisition instrument and carried out an experiment on a preserved kidney utilising deep CNN-based image processing. The design and operation of the system are cost-effective in terms of price, ease of use, precision, and speed. They demonstrated that their hardware or software versions are capable of not only monitoring and controlling the probe location with great accuracy and control, but also of visualising and evaluating 2-dimensional optical images with their 3D location in a simple and straightforward manner. Physicians will have access to substantially more data and a better knowledge of the tissue medical condition if the researchers provide them with the probe longitude and latitude for each 2D OCT image, as well as the intensity or size distribution maps generated by their method. Additional information can be acquired from the same process without requiring physicians to change their current process flow by combining approaches from the virtual and augmented reality (AR/VR) sectors with machine learning. Furthermore, the additional data and visualisations can provide clinicians with valuable insights into the obtained data during the records evaluation process, perhaps leading to a much more conclusive diagnosis [50].

It illustrates that the approach employed by the author is sufficient and simply generalizable to completely undiscovered surgical techniques and video recording environments. The design is generic and anticipates that it will be beneficial for investigating issues like those encountered while classifying medical devices, such as tool identification or operating phase identification. Additionally, the suggested CNN design has up to 15 times fewer parameters than the commonly utilized FCN architecture, which is critical for real-time performance. Additionally, their model's considerable decrease in size enables easy distribution to end-users and implementation to embedded devices.

Table 2.1 shows the summary of the literature survey conducted for the medical image segmentation basis on the convolutional neural networks.

Table 2.1 Summary of CNN based Medical Image Segmentation

Author and References	Technique	Outcomes
Garcia et al., (2017)	2 deep learning architectures for the automated identification of non-rigid surgical instruments	Increase the network's regularity while retaining segmentation accuracy
Hajabdollahi et al., (2018)	CNN's based on a quantization-pruning strategy	Reduced network is capable of segmenting retinal arteries accurately and efficiently.
Li et al., (2019)	A framework for domain adaptation termed CLU-CNNs	CLU-CNNs achieve great placement accuracy and speed.
Schlemper et al., (2019)	Revolutionary attentiveness gate (AG) approach	Efficiently localize object and enhancing prediction accuracy by eliminating false positives.
Zhang et al., (2020)	2 linked CNNs, we can get annotators and the genuine segmentation label distributions.	High capacity to capture the intricate spatial aspects of annotators' errors.
Ahammad et al., (2020)	CNN-deep segmentation-based boosting classifier	Efficient Computation of SCI disorder prediction.

Hao et al., (2020)	Multi-scale convolutional network (MSCNN) model.	Segmenting the cerebral lesion tissue efficiently and increased generalization ability.
Qin et al., (2021)	Visual odometry (VO) based on a camera and concurrent mapping and localization (SLAM)	High degree of precision in tracking the probe's location, user-friendly visualization tool for reviewing OCT 2D pictures in 3D space.

Table 2.2 indicates the comparison between the various proposed techniques based on three parameters i.e accuracy, processing speed, real-time, and complexity.

Table 2.2 Comparative Analysis of various CNN Frameworks

Frameworks	Accuracy	Processing Speed	Real Time	Complexity	Remarks
Garcia et al., (2017)	✓	✓	✓	✗	High complexity
Hajabdollahi et al., (2018)	✓	✗	✗	✓	Low processing speed
Li et al., (2019)	✓	✗	✗	✗	High complexity
Schlemper et al., (2019)	✓	✗	✗	✗	High complexity
Zhang et al., (2020)	✓	✗	✗	✗	High complexity
Ahammad et al., (2020)	✓	✓	✗	✗	High complexity
Hao et al., (2020)	✓	✗	✗	✗	High complexity
Qin et al., (2021)	✓	✓	✓	✗	High complexity

2.2.2. Deep semantic segmentation of medical images

Semantic Segmentation of medical images helps in understanding the depth and variety of the damaged tissue in any human organ. Semantic segmentation involves separation of all the tissues and sub-tissues minutely. Below literature survey, illustrates the framework or techniques used for the in depth semantic segmentation of medical images.

Cunningham et al., (2016) stated that despite the widespread availability of echocardiography and the increasing need for personalized muscle diagnosis (chin injury, work-related issue, dystrophies, and nerve damage), current techniques struggle to reliably identify muscles within complex groupings. Cervical Dystonia (CD), for example, is a common neurological disorder that results in painful dystonia in one or more members of the neck muscular system. Therapists generally possess a method for directing and monitoring muscle pain stimulation. Physicians would have been able to verify, activate, and test the thoracolumbar tissues by ultrasound using computerized muscle segment procedures. They have devised a technique for real-time segmentation of 5 contralateral neck musculature and the spine using just ultrasonography. To get ultrasonic muscle segments labels, a novel multifunctional registration approach was devised that involved the identification of MRI scans and contour registrations to MRI-matched ultrasound pictures by approximations of tissue distortion. After transforming the annotation and texturing into a mean space using polynomial regression, they generated a texture-to-shape dictionary using shape statistics. To do segmentation, researchers compared test photos to dictionary textures, which provided a preliminary fragmentation, and then refined the fitting to use a customized Active Shape Model. The approach presently segments a single picture in 0.45 seconds with an accuracy of approximately 86 percent using ultrasound alone on observed individuals. They argue that this technique is relevant to segmenting, extrapolating, and visualizing deep muscle anatomy in general, as well as analysing statistical aspects online [51].

Malviya et al., (2017) suggested that lung cancer is becoming the world's most significant health concern, claiming thousands of lives each year. There are several approaches available for diagnosing lung cancer, including CT imaging, MRI imaging, and X-Ray imaging. However, the CT scan picture offers more data about the lungs' complex organs. As a result, medical pictures of millions of pixels are being created increasingly often as part of their regular duties. Retrieving medical pictures from a huge collection is a difficult task; hence, a content-based medical image retrieval (CBMIR) system is developed. Clustering-based segmentation was proposed by the retrieval system for lung cancer diagnostics. It consists of three distinct stages. The first phase describes segmenting the lung image into distinct regions; the second phase describes extracting texture features from the lung regions; and the third phase describes clustering, which has been used to classify and organize images into distinct clusters, thereby increasing the system's speed and accuracy when retrieving images. It is an analysis that quantifies accuracy and recalls concerning time [52].

Kalshetti et al., (2017) stated that segmentation is frequently used on medical pictures to aid in the diagnosis of disorders during a clinical examination. As a result, it has developed into a

significant area of research. Standard digital segmentation techniques are unable to generate sufficient discriminative power due to irregularities evident in medical data. Before segmentation, they must be pre-processed. They provide MIST (Medical Image Segmentation Tool) as a two-stage method to produce the most appropriate strategy for segmenting medical pictures. The first stage uses mathematical morphology to automatically build a binary marker picture of a region of interest. This marker acts as the mask picture for the second step, which employs GrabCut to produce a segmented output efficiently. The acquired result can be fine-tuned further by user input, which can be accomplished through the usage of the suggested Graphical User Interface (GUI). The proposed technique is accurate and produces high-quality segmentation results from both healthcare and instinctive image with minimal user participation [53].

Iqbal et al., (2018) suggested a novel Generative Adversarial for Medicinal Imaging (MI-GAN) architecture for segmentation and creation of retinal vasculature images. These computer-generated visuals appear to be genuine. When employed as an extra training dataset, the architecture aids in improving the performance of picture segmentation. From a limited training set, the suggested algorithm can understand relevant characteristics. The training set in their case comprised of ten samples from each dataset, namely DRIVE and STARE. In terms of AUC ROC, AUC PR, and Dice co-efficient, the model beat other current models. In comparison to other approaches, this method generates fewer false positives at small vessels and drew more precise lines [54].

Anas et al., (2018) stated that prostatectomy biopsy has become targeted prostate surgery, which utilizes multiparametric magnetic resonance and ultrasonography. Targeted biopsy techniques rely heavily on accurate computed tomography segmentation for verification. Segmentation is often conducted automatically or semi-automatically online before the beginning of the biopsy. They offer a real-time prostate segmentation approach based on deep neural networks during the biopsy operation in this article, opening the path for dynamical registrations of mp-MRI and ultrasound data. Along with convolutional networks for spatial data extraction, the proposed technique employs recurring models to extract temporal data from a succession of MRI images. One of the most significant advancements in technology is the use of remnant inversion in machine learning algorithms to enhance optimization. Additionally, they exploit contextual data more efficiently by using recurrent connections inside among layers of convolutional models. Additionally, sample the source ultrasound sequence densely and sparsely to make the system resistant to ultrasonic artefacts. The topology was generated using 2,238 labelled transrectal sonography pictures, with further confirmation

using 634 and 1,019 images. The average Dice similarity coefficient is 93%, surface distance error is 1.10 mm, and Hausdorff distance error is 3.0 mm. A comparison of the provided findings to those of a state-of-the-art technique shows that this method strategy achieves statistically significant improvement [55].

Siam et al., (2018) stated that Real-time segmentation is critical for robotics applications such as automated cars, assisted driving, and traffic monitoring using imagery from unmanned aerial aircraft. They present a unique two-stream convolutional network for motion segmentation that balances the accuracy and computational efficiency trade-offs by utilizing flow and geometric signals. Mathematical cues leverage the application's domain knowledge. In the case of mostly flat pictures obtained from high height unmanned aerial vehicles, holography-adjusted flow is used. While scarce projection depth estimates and dead-reckoning data are utilized in the terms of local scenes in autonomous driving because GPS/IMU sensory data is not accessible, weak planned depth assessments and odometry data are used. The network reduces segmentation time from 160 ms to 39 ms about 4.7x, albeit at the expense of pixel boundary classification precision. This enables real-time operation of the network on a Jetson Tx2. Geometric priors are employed to recover part of the accuracy loss while maintaining a much-enhanced computing efficiency above the state-of-the-art [56].

Robinson et al., (2018) [57] suggested that true performance with sentient accuracy is now possible because of advancements in deep learning-based segmentation technologies. Even the greatest approach, however, may fail occasionally owing to poor image quality, artifacts, or unexpected results of data recorder algorithms. It is crucial to be able to forecast partition integrity in the existence of test datasets in clinical practice and large-scale research to avoid include wrong data in subsequent analyses. They offer two ways for real-time automatic quality management of cardiovascular magnetic resonance image categories using deep learning. To begin, researchers train a neural network on 12,880 data to predict individual Dice Similarity Coefficients (DSC). On 1,610 test samples, they report an average mean error (MAE) of 0.03 and a binary classification accuracy of 97 percent for differentiating low- and high-quality segmentations. Second, in the absence of manually annotated data, they train a neural network to predict DSC scores using quality estimates derived via a backward testing technique. Now, these networks accurately predict if segmentation is 'excellent' or 'bad' based on some threshold, but they cannot safely discriminate between two groupings of comparable quality [57].

Stefaniga et al., (2019) [58] depicted that image enhancement in medical imaging has evolved to the cutting edge in medical picture interpretation and processing, according to the study. In

this experimental procedure, they employ Deep Learning GPU Training (DIGITS) to provide a high-level technique of densely integrated deep neural networks used in healthcare picture segment (lung CT scans), while avoiding mathematically rigorous formalism of neural networks. The goal of this experimental study is to build an analysis of various methodologies in lung CT scan delineation using the U-NET design, which is among the most frequently utilized architectures in machine learning for medical feature extraction techniques. This will result in the leading edge achieving a statistical equation for training to locate valuable results when given data input. It can also demonstrate how and when to prepare a Deep Convolution Network (DCN) structure like U-NET utilizing edge detection for lung malignant cells received from a Computed Comprehensive look (CT) console on peritoneal image features using GPU calculation with Nvidia Digits [58].

Nguyen et al., (2019) suggested that picture segmentation identifies objects and boundaries. It is crucial in several clinical contexts, including liver pathology, therapy planning, and postoperative evaluation. Fuzzy boundaries, diverse backgrounds, and shifting appearances of items of interest challenge segmentation. Success in the procedure remains fully reliant on the operator's experience and hand-eye coordination. As a result, their research was inspired by the demand in medical imaging for rapid and precise object recognition. This research employs a unique adenoma segmentation technique called CDED-net that is built on many deep encoder-decoder networks. Along with storing multi-level contextual data, the architecture may gain rich information features during the training phase by acquiring missing pixels. Additionally, by utilizing multiscale effective decoders, the network can record object boundaries. Additionally, they present a novel methodology for boosting the system's classification model by implementing a method for enhancing data with a novel treatment dice gradient descent. This approach attempts to offer access to a network of computer intelligence by utilizing imprecisely defined object boundaries formed by the non-specular subtropics between binarization areas. To fully show the proposed technique, they trained and evaluated their network on three well-known polyp data - sets: Patient identification, Catheterization, and Advancing PolypDB [59].

Girum et al., (2020) stated that the determination of the clinical target volume (CTV) for permanent prostatic irradiation using surgical transrectal ultrasonography (TRUS) imaging guidance. The development of an effective and automated method for identifying the CTV on postpartum TRUS images is crucial for patient flow efficiency and patient safety. They propose a cross-deep learning technique for automatically recognizing the prostate CTV boundary in perioperative TRUS pictures by combining low-level and elevated information. This approach

for rectal intervention and transformation comprises a communication feature calibration mechanism that allows for restricted feature extraction and attempts to learn previously learned models. It employs curve reconstruction from instantly analyzed bounding exterior parameters (pseudo-landmarks) to recognize negligible and complicated provinces from across the prostate line of demarcation, while still being less affected by partial shading, intrinsic stippling, and aberration signals from the needle or implanted radioactive seeds [60].

Park et al., (2020) stated that the pig and human corneas have a comparable layer structure and biomechanical qualities, the swine cornea's core thickness is greater than that of the human cornea. As a result, when the porcine cornea is used, it is simpler to implant the needle deeply. As a result, they not only measured the thickness ratio in porcine instances, but also the leftover implant depths of 50 m. The second issue is that the analysis can't compensate for eye movement. In a clinical setting, the patient's eye is not stationary, and the syringe implantation energy may trigger eye movement. In this instance, the needle tip might well be situated just outside of the frequency range, and the suggested approach cannot ensure the needle tip's position to be accurate. In potential treatments, active scanning range modification and probe pose adjustment should be considered. The suggested technique for OCT image processing, which incorporates deep learning-based segmentation and distortion correction, may give adequate information to accurately place the needle within the cornea. The imaging range can be reduced while still guaranteeing that the needle is inserted to a required level using automated needle insertion [61].

Jha et al., (2021) suggested methods for computer-aided recognition, positioning, and segments that have been presented can help to improve colonic operations. Following the emergence of numerous strategies for automated adenoma recognition and division, evaluating systems remains an ongoing problem. This is because an expanding number of computer vision methods have been investigated and may be used to neoplasm feature sets. The advancement of automated polyp identification and segmentation tasks can be guided by the benchmarking of emerging approaches. Furthermore, it assures that the community's created findings are repeatable and allow a valid comparison of established approaches. It assesses multiple new algorithms for adenoma identification, placement, and delineation u, evaluating procedure quality and consistency on an overall basis. While most current techniques highlight speed over exactness, they indicate that the suggested ColonSegNet achieves a good trade among both average accuracies of 0.950 and mean IoU of 0.650, as well as the quicker speed of 200 frames per second, for this kind of detection and regulatory factor. Similarly, for the segmentation challenge, the suggested ColonSegNet obtained a respectable partition factor of 0.8206 as well

as a maximum speed of 182.38 fps. This extensive comparison with several province algorithms highlights the need for gauging deep neural networks for computer-controlled authentic polyps' classification and differentiations, which have the potential to alter existing diagnostic tests and reduce miss-detection rates [62].

Ouahabi et al., (2021) suggested that to increase segmentation efficiency while maintaining high accuracy, a real-time architecture for medical image text categorization dubbed Purely Computational complexity dense Distended Network is developed. Despite different resolutions and contrast, shadow interference, and changes in the position and size of nodules, effective ultrasonography picture identification is difficult. As a result, a unique structure is presented that blends the benefits of extensive connectivity, stretched convolutions, and normalized filters to maintain outstanding accuracy. Complex interconnectivity integrates fine segmentation at the low level alongside rough fragmentation at the top standard to extract more information from ultrasound images. Distended inversion can be used to increase the perceptron of a filter, and various filtration system sizes can be used to address the issue of particle size and positioning inequalities. Additionally, this approach integrates quantized filtration into the networks to further optimize the model's efficacy. Additionally, a deficit algorithm to solve technique is given to address the binary classification problem in medical picture text categorization, which further enhances the network's accuracy. The suggested framework features state performance of robustness and efficiency, as evidenced by a detailed series of tests using the thyroid dataset [63].

Table 2.3 shows the summarize literature survey for the deep semantic segmentation techniques of medical images.

Table 2.3 Summary of Deep semantic segmentation techniques of medical images

Author	Technique	Outcome
Cunningham et al., (2016)	A unique multimodal registration approach based on MRI image annotation	To segment, extrapolate, and visualize deep tissue anatomy, as well as to perform online statistical analysis
Malviya et al., (2017)	Content-based medical image retrieval (CBMIR) system.	Categorize and organize photos into clusters, which improves the system's speed and accuracy by retrieving images.

Kalshetti et al., (2017)	2 stage MIST (Medical Image Classification Tool).	On medical and natural photos, the suggested technique is accurate and produces good segmentation results with minimal user intervention.
Iqbal et al., (2018)	Novel Adversarial Generative Networks for Magnetic Resonance (MI-GAN)	Produces more exact segmented pictures than previous approaches.
Anas et al., (2018)	Real-time prostate segmentation approach based on deep neural networks	Robustness towards aberrations in the input ultrasonic sequence by a combination of dense and scattered sampling
Siam et al., (2018)	Unique two-stream convolutional network	By comparing the IoU measure to the baseline network, they enhanced segmentation in UAV images by 5.2 percent.
Robinson et al., (2018)	Automation of cardiovascular MR segmentation quality control in real-time using deep learning	Permits novel uses of picture acquisition optimization for the best possible analysis outcomes
Stefaniga et al., (2019)	Deep Learning GPU Development System (DIGITS)	The experimental results indicate that after 50 epochs, a satisfactory benchmark was obtained.
Nguyen et al., (2019)	Deep encoder-decoder networks dubbed CDED-net	Enhancing the product's segmentation performance using a boundary-emphasizing data augmentation technique in conjunction with a novel therapeutic dice loss function
Girum et al., (2020)	With transrectal ultrasonography (TRUS) image-guided intraoperative prostate brachytherapy, the clinical target volume	The technique has an average accuracy of 0.96 and a mean surface distance inaccuracy of 0.10 mm.
Park et al., (2020)	Deep learning-based picture segmentation in real-time computed tomography	Traditional difficulties with OCT pictures include vision problems, optical interference from surgical equipment, and sluggish volumetric scanning speed can be solved by a marginal insertion depth in the OCT scanner.

Jha et al., (2021)	Detection, location, and segmentation of polyps using Kvasir-SEG, an accessible database of colonoscopy images	Achieved the best actual pace of 182.38 fps and a competitive dice factor of 0.8206 for the segmentation task.
Ouahabi et al., (2021)	The Fully Convolution Dense Distended Network architecture.	Incorporates factorized filters into a network in order to better increase the model's efficiency

Table 2.4 discusses the comparative analysis of deep semantic segmentation frameworks for medical image analysis based on the accuracy, processing speed, complexity and real time.

Table 2.4 Comparative Analysis of Deep semantic segmentation frameworks

Frameworks	Accuracy	Processing Speed	Real Time	Complexity	Remarks
Cunningham et al., (2016)	✓	✓	✓	✗	High complexity
Malviya et al., (2017)	✓	✓	✗	✗	High complexity
Kalshetti et al., (2017)	✓	✗	✗	✗	High complexity
Iqbal et al., (2018)	✓	NR	NR	✗	High complexity
Anas et al., (2018)	✓	✗	✗	✗	High complexity
Siam et al., (2018)	✓	✓	✓	✗	High complexity
Robinson et al., (2018)	✓	✗	✗	✗	High complexity
Stefaniga et al., (2019)	✓	✓	✗	✗	High complexity
Nguyen et al., (2019)	✓	✗	✗	✗	High complexity
Girum et al., (2020)	✓	✗	✗	✗	High complexity
Park et al., (2020)	✓	✗	✗	✗	High complexity
Jha et al., (2021)	✓	✓	✗	✗	High complexity
Ouahabi et al., (2021)	✓	✗	✗	✗	High complexity

2.2.3. Real-Time Interactive 3-Dimensional segmentation

Automated medical image segmentation based on deep neural networks also require the need of its real time implementations so that these techniques could assist the radiologists in performing the diagnosis task in real time. Below survey states the various real time 3 D segmentation techniques.

Egger et al., (2014) stated that the current contribution provides a scale-invariant image segmentation approach that, by its participatory feature, encompasses its computation parameter for users, avoiding the usage of "arbitrarily chosen" values which the user cannot completely grasp. As a result, they devised a unique graph-based segmentation technique that demands just a single origin location within the template from either the user, providing it especially suited for exceptional productivity or interactive experience, for real-time user customization. Additionally, the technique's required color or grayscale value information may be automatically retrieved everywhere around a user-defined seed point. Furthermore, the network is organized in such a way that the segmentation result may be obtained in a split second using a binomial computation on a contemporary computer. To test the technique, researchers used two-dimensional or four medical picture data containing neurological diseases, cortical abnormalities, and vertebral bodies. When compared to the more costly manual compression segmentations conducted by skilled specialists, this participatory method offers better healthcare [64].

Chitiboi et al., (2014) used an artificial object-based segmentation system to demonstrate a strategy for recognizing left ventricular tissue in short cardiac image series. Using this method, they were able to completely divide the cardiovascular system in each frame and observe the heart function over time. The technology paves the way for a more extensive clinical application of true cardiac magnetic resonance imaging. The demand for separate two-dimensional heart sections is now a restriction, as real-time images are collected as serial pass pictures that cannot be instantaneously stacked to create the left ventricle. On the other hand, future improvements will stitch the various segments together via equivalent cardiac cycles to generate a 3D volumetric picture [65].

Kurzendorfer et al., (2017) drew attention to the need for segmentation in mental image analysis. Manual segmentation is hard, time-intensive, and sensitive to inter-observer variability. Completely automatic segmentation algorithms require a large number of data

points and may fail under difficult or uncommon conditions. In this research, they demonstrate a unique technique for two-dimensional identification of individual segments and three-dimensional estimation of fragmented slices. Using a two-dimensional slice, Smart Brush quickly splits the items of interest. Customized Hermite nonlinear activation variable formulations reconfigure a layer from certain labeled sections. Effective interaction with fewer equations improves performance, enabling real-time and comprehensible segmentation of three-dimensional objects through participatory segmentation. The proposed approach is evaluated by comparing it to platinum normal medical expertise labeling of the left ventricle using 12 medical 3D computerized CT neuroimaging data sets. For the various slices, the algorithmic evaluation of the 2D Smart Brush resulted in an overall Linear discriminant analysis of 0.88. For 3D interpolation with Hermite radial basis functions, an average Dice factor of 0.94, 0.02 is found. The benefit of this approach is that the user may easily remedy the outcome of the three-dimensional segmentation by segmenting an additional two-dimensional slice with the highest mismatch. Furthermore, as no prior knowledge is necessary, any three-dimensional data gathering can be split arbitrarily, independent of the imaging modalities, visible organ, or medicinal use [66].

Wei et al., (2018) stated that a real-time image processing strategy for detecting tiny and weak targets. For the improvement of 2D images and selective target detection, mathematical morphological procedures using 1D structural components were used. The single-layer image processing technique is incorporated in hardware and is used to process the picture region by a couple of rows during data readout. The ERS approach is also used to create breakthroughs in hyper-frame temporal resolution. The recovery and determination of small and weak targets are investigated for positioning accuracy. An investigation has shown that the approach based on 1D morphology is extremely resilient under a variety of work settings. Moreover, laboratory and field tests revealed that the suggested technique is capable of accomplishing target placement with the dependability of fewer than 0.1 pixels. The entire latencies time for this approach is 3 seconds when utilizing a 25 GHz readout clock and is nearly constant as the pixel size of the picture, namely the sequence number, rises. The suggested step in image analysis is intriguing for biological-image analysis, infrared monitoring, and targets measurement and tracking applications because of its performance advantage, high accuracy, and resilience [67].

A brain aneurysm, according to **Zhai et al., (2018)**, is a weakening in a blood vessel that can expand and leak into the surrounding area, resulting in a potentially fatal condition. As a result, identifying aneurysms early and precisely is crucial in assisting doctors in deciding the

appropriate treatment. On the Microcontroller system-on-chip (SoC) and virtual servers, this research intends to create a real-time robotic segmentation approach for cerebral aneurysms. The results are on a 3D plane, with virtual reality (VR) tools like the Oculus Rift being used to create an exciting training environment. The segmentation method is built using hard thresholding and the Har wavelet transformation. The split masks and 3D generated volumes produced satisfactory results, according to both subjective and quantitative evaluations. Furthermore, the hardware implementation findings show that using the Zynq SoC, the proposed implementation can process a photo in an average time of 5.2 Ms [68].

Wang et al., (2019) suggested that tongue diagnosis, one of Traditional Chinese Medicine's (TCM) key diagnostic procedures, is regarded as an ideal option for remote diagnosis methods due to its simplicity and non-invasiveness. The exchange between accuracy and efficiency, as well as the variability of tongue pictures, represent significant obstacles in true tongue image segmentation. To address these issues, the work introduces a super lightweight design on the encoder-decoder structure. The tongue image feature extraction (TIFE) module is intended to provide features with broader receptive fields while maintaining spatial resolution. By collecting multi-scale contextual information, the context module improves performance. The decoder is intended to be a simple and effective feature up sampling module for combining distinct depth data and refining segmentation accuracy along tongue borders. To cope with misclassifications caused by class imbalance, the loss module is offered. During modeling training and testing, novel tongues image data (FDU/SHUTCM) with 5,600 tongue pictures and their accompanying high-quality masks is prepared [69].

Zeng et al., (2020) depicted that cardiovascular MRI scan in real-time has become an increasingly significant tool for directing various heart procedures. To enhance visual aid, cine MRI frames must be split on the fly to eliminate apparent visual latency. Additionally, for the sake of dependability and the protection of patient data, computations should be performed on local hardware. Modern MRI segmentation algorithms are primarily concerned with accuracy and are thus rarely applicable in real-time or on local equipment. The very first equipment cross neural architecture search (NAS) system for 3-dimensional cardiac cine MRI delineation in this paper. To account for real-time restrictions, the proposed architecture adds a latency control parameter into the loss function, while considering the underlying hardware. Additionally, because the formulation is completely discrete following the architectural parameters, it may be optimized using a back propagation algorithm to minimize computing costs while upholding optimum quality. Experiments using the Collaboration MICCAI 2017

dataset reveal that their equipment multiscale Network storage arrangement can substantially decrease latency and meet real-time restrictions while maintaining competitive segmentation accuracy when compared to the state-of-the-art NAS separation framework [70].

AlZu'bi et al., (2020) stated that due to the algorithm's success, using 2D Clustering has been widely used for differentiating medical pictures. Throughout decades, many expansions have been planned. They present a customized form of Classifier for dividing 3-dimensional collections therefore in research, that has been utilized to 3D medical imaging segmentation only sporadically. The suggested algorithm's parallel implementation utilizes Graphics Processing Units (GPU). According to the research, one of the primary issues with employing FCM for diagnostic devices is efficiency while interacting with 3D models. As a result, a hybrid adequate way of FCM is suggested to elicit capacity objects from medical information. The suggested approach was validated using both real-world medical data and phantom data. The reliability of separation on prescribed and genuine case information was critical for system validation. The parallelized versions' processing times are compared to demonstrate the efficacy of each method. According to the obtained findings, the parallel solution is 5X quicker than the customers and implement the identical task [71].

Table 2.5 shares the summary of all the mentioned real time interactive 3 dimensional algorithms used for medical image segmentation.

Table 2.5 Survey on Real-Time Interactive 3-Dimensional segmentation

Author	Technique	Outcome
Egger et al., (2014)	Graph-based segmentation approach	Holds high medicinal significance.
Chitiboi et al., (2014)	a region-based automated approach for segmenting the myocardium	Easier to do a multicore cardiac function analysis that is unaffected by breathing or arrhythmia.
Kurzendorfer et al., (2017)	Hermite radial basis formulation (HRBF)	The 2D Smart Brush's algorithmic evaluation produced an average Dice factor of 0.88 ± 0.09 for both the individual slices.
Wei et al., (2018)	One-dimensional morphology-based structure elements	The stability and precision of the real-time detection approach make it desirable for use in all sorts of real-time tiny target detection systems.

Zhai et al., (2018)	Brain rupture segmentation on the Zynq scheme (SoC)	The information accumulation events unfold that the segmentation masks and three-dimensional generated volumes produced acceptable results.
Wang et al., (2019)	MSU-Net for real-time 3D Neuroimaging features extraction in cardiac surgery	Achieves 268 and 237 percent speedup with 1.6 and 3.6 percent Dice score improvement
Zeng et al., (2020)	NAS architecture for real-time 3D ventricular motion MRI segmentation	Minimize latencies by down to 3.5 and meet real-time requirements
AlZu'bi et al., (2020)	Parallelization of the control scheme utilizing Graphics Processing Unit (GPU).	The findings show that the concurrent implementation is 5X quicker than the sequential version.

Table 2.6 discusses the comparative analysis of the real 3 dimensional frameworks used for medical image segmentation based on the four parameters such as accuracy, complexity, real time and processing speed.

Table 2.6 Comparative Analysis of Real-Time Interactive 3-Dimensional segmentation Techniques

Frameworks	Accuracy	Processing Speed	Real Time	Complexity	Remarks
Egger et al., (2014)	✓	✗	✗	✗	High complexity
Chitiboi et al., (2014)	✓	✗	✓	✗	High complexity
Kurzendorfer et al., (2017)	✓	✗	✓	✗	High complexity
Wei et al., (2018)	✓	✓	✓	✗	High complexity
Zhai et al., (2018)	✓	✗	✓	✗	High complexity
Wang et al., (2019)	✓	✓	✓	✗	High complexity
Zeng et al., (2020)	✓	✗	✓	✗	High complexity
AlZu'bi et al., (2020)	✓	✓	✓	✗	High complexity

2.2.4. Segmentation of Medical Images Using Hybridized Technique

Automation of medical image segmentation requires maximum efficiency, accuracy and precision such that the automated techniques are able to assist radiologists in real time scenario. For this purpose, researchers focussed on hybrid techniques to make automated segmentation techniques highly efficient. The combination of neural networks with fuzzy logic is considered as one of the hybrid techniques for medical image segmentation. The reason of merging fuzzy logic is that it helps in acquiring indefinite inputs from the images as well which can precisely identify the unhealthy tissues and can accurately guide the neural networks to predict the disease. Below mentioned literature survey discusses such hybrid techniques utilized in the medical image segmentation.

Kashyap et al., (2015) stated that applications in health care have been a benefit to the healthcare business. It requires proper segmentation of medical pictures to provide an accurate diagnosis. This ensures that healthcare photos are segmented accurately. While the level set method (LSM) is a capable methodology, it is still challenging to perform a fast procedure while utilizing the suitable segments. For intensity irregularity pictures, the region-based approach is insufficient. They offer a more advanced region-based level set approach that incorporates the changed signed pressure function because of geometric active contour models and the Mumford-Shah model. As a result, the technique for re-initializing the historical level set model is eliminated, as well as the computationally expensive re-initialization. In comparison to the ancient model, the approach is more resistant to pictures with weak edges and erratic intensity distributions. This approach is new in that it assists users in locally computing an upgraded Signed pressure function (SPF), which utilizes local mean values to find boundaries within homogeneous areas. In comparison to existing active design models, the suggested technique achieves significant benefits by including a rapid procedure, automation, and the proper segmentation of medical images. Numerous analytical experiments have been conducted to demonstrate this method's utility in medical picture segmentation [72].

Nelakuditi et al., (2015) stated that Segmentation of medical pictures is critical for image processing. Due to the low contrast of medical pictures and the dispersion of organ or tissue borders, fragmentation of CT scans is a difficult process. Numerous medical diagnostic processes are automated via the use of image analysis principles because of new engineering technology developments. As a result, this research utilizes the Xilinx System Generator (XSG)

to achieve hardware segmentation of brain tumors. Due to its high level of multiplexing and pipelining, it outperforms typical programmable Digital Signal Processing (DSPs) and even PC integrated coprocessors in terms of performance, design time, and cost. The use of XSG in healthcare image processing applications substantially lowers the complexities inherent in architectural design and adds the capability of hardware co-simulation [73].

Hamdaoui et al., (2015) depicted that Particle Swarm Optimization (PSO) is an optimization approach for continuous search problems that are based on metaheuristic algorithms. It is one of the most widely utilized algorithms in a wide variety of applications. Its popularity has grown to encompass real-time difficulties requiring the use of embedded systems. Numerous researchers have developed and refined several practical examples, such as mobile robots and medical image analysis, by utilizing PSO. In prior research, they successfully implemented true classification of MRI image data using the PSO method. In this research, they attempt to enhance the work by including a monitoring system that manages the many tasks performed by the architecture's numerous parts. As a result, the newly developed synchronous design of MRI image segmentation-based PSO enables time savings and hence simplifies the search for the best threshold. The performance of the proposed synchronous hardware architecture is evaluated and validated using a set of medical MRI images [74].

Dergachyova et al., (2016) stated that the medical profession has demonstrated an increasing interest in context-aware technology intending to expand surgical staff's awareness and activity within the operating theatre. These systems, which require precise identification of the operating process, make use of data collected from a diverse array of accessible sensors. They give a comprehensive set of data and a structural equation modeling for segmenting and identifying surgical phases utilizing a mix of video feeds and instrument usage indications, without the need for prior knowledge. Additionally, they provide additional validation indicators for the examination of workflow detection. These operations of separation and identification are carried out in four stages. To begin, a computerized Postoperative Procedural Framework is designed during the training phase, employing useful comments to guide its succeeding procedure. Secondly, sensor readings are characterized in terms of a mix of low-level experiences that connect and equipment information. The third stage uses this description to train an Ensemble classifier capable of differentiating between surgical stages. Finally, the Ada Boost responses are put into a Concealed tractor-trailer Model for decision-making [75].

Kashyap et al., (2016) stated that medical image processing provides potential for researchers, as precise segmentation remains a challenge, and automated segmentation is necessary for

improved picture analysis. While energy-based approaches such as leveling set with active contours are viable possibilities, processing data quickly and accurately remains a barrier. The existing research suggests a new technique that uses the conjugate gradient method to determine the future level set equation and an augmented Laplace Transform technique to solve the subsequent partial differential equations. The suggested technique has various advantages, including the ability to create high-quality results, automation, and partial interpretability for intensity anisotropy. This approach has been subjected to a variety of evaluation procedures to establish its use in image analysis. When compared to an older model, it is more robust against pictures with weak edges and noise. The peculiarity in their technique seems to be that can solve partial differential equations quickly using an upgraded lattice Boltzmann method that takes advantage of localized mean properties to discover limits and leverage patterns for object extraction. To reduce computing time, the suggested technique makes use of complicated partial differential equations [76].

Sharma et al., (2017) stated that Hybrid RGSA-SVM classifier, hybrid ACO-GWO-PSVM classifier, EGSO-based RBFNN classifier, and KSCA modeling were used in simulations to achieve effective and reliable classification while avoiding stagnation, local minima, and other restrictions. Most of these suggested techniques are focused on streamlining and successfully executing the variable selection, categorization, and segmentation on the brain and liver images in question. Each of these proposed solutions makes use of a distinct approach for completely utilizing the search area, retraining the neural network architecture, or constructing the KSCA method to arrive at more convergent results and the requisite diagnostic procedure. All the techniques operate on a helpful and cooperative basis instead of an aggressive basis. Each one of these hybrid recommendation strategies developed and executed is dependable and demonstrates a greater number of iterations in locating the optimum solution and determining the fitness values, which is most likely the standard error. The simulation findings are much more intelligent and resilient, resulting in superior solutions when compared to those produced by established conventional methodologies [77].

Gueziri et al., (2017) stated that segmentation of images using interactive scribbles is quite liberal in terms of user efficiency. Similar segmentation results may be obtained using a variety of label designs and human effort throughout the segmentation job. Thus, the context in which the user gets segmentation feedback influences his or her performance. They examined the user's performance under two different scenarios of latency fluctuation in this study: the latency level: between 100 ms and 2 s; and the kind of delay: Systematic or multi latency are

characterized by an automatic refresh of the segment information and a consumer reconfiguration, respectively. Latency increases have a negative influence on overall efficiency. However, this has a varying effect on user performance depending on the delay and refresh technique used. They discovered non-linear volatility in the user while employing the automatic refresh strategy, as well as a reduction in drawing performance for very short latencies. The user is listening closely to the segmentation changes, which occur often. For longer latencies, it appears as though the entire segmentation time increases steadily with the delay. Although the user is less aware of the changes, the drawing performance is increased. Increased latency has a lesser effect on the user's behavior when the refresh is triggered by the user. In this scenario, the process of drawing and interpreting the outcome updates is separated into two distinct processes. Concentrating the user's focus on a particular task at a time improves performance. The user-initiated refresh approach surpassed the default strategy in terms of labeling time [78].

Labrunie et al., (2018) suggested that the auditory and articulatory traces of speech production processes can be used to describe them at a peripheral level. As a result, researchers have made significant attempts to assess articulation. Real-time MRI Scan (RT-MRI) currently gives frame rates closer to those reached by magnetic articulography or ultrasonic echography while providing highly comprehensive geometric properties about the whole vocal tract, thanks to amazing advances made in the previous decade. Thus, RT-MRI has become unavoidable for studying the motions of speech articulators. However, making optimal use of vast collections of pictures to define and model speech activities necessitates the development of automated algorithms for accurately segmenting articulators from such images. The emerging research describes their approach to developing an automatic segmentation method based on supervised machine learning techniques. This work's key contributions are as follows. Throughout this research, they created the first big database of French speakers' RT-MRI midsagittal pictures. It was manually segmented for a limited training set of roughly 60 photos picked by cluster analysis to reflect the total library as faithfully as feasible. These data were utilized to train image and contouring models for autonomous articulatory segmentation [79].

Mahmood et al., (2018) stated that to fully use the promise of pattern recognition for medical imaging, substantial, annotated training datasets are necessary. Similar databases are difficult to get due to privacy concerns, a scarcity of professionals accessible to annotate them, the underrepresentation of uncommon diseases, and a lack of standardization. In conventional vision applications, the absence of datasets has been addressed by improving synthetic data to

resemble actual objects through unsupervised adversarial training. They suggest a framework solution to the issue of insufficiently captioned medical photographs. They created a unique unmanaged reverse domain adaption approach for transforming authentic photos to an artificial domain suited for usage with a network trained on a vast collection of synthetic datasets. They demonstrate that by combining adversarial and self-regularization training, reverse subdomain adaptation may be used to maintain diagnostic data (quality and organ topography) in changed images. Concurrently, their domain adaptation removes physician characteristics from real-world test images, permitting them to be used in conjunction with a network trained entirely on synthetic data. Additionally, this method addresses the issue of networking adaptation across patients, which occurs when a system trained on one individual failed to generalize to other patients owing to the system learning from the patient's distinctive texture or color. Eliminating patient-specific material does not affect diagnostics since clinicians are not seeking distinct patient information (as with fingerprinting), but for qualities associated with a healthy or sick domain. Their investigations reveal that when healthy and pathological qualities can be recreated in synthetic images, the descriptor is likely to be fooled when clinically relevant aspects are removed by the transformer. They illustrate quantitatively, using genuine endoscopic images from a pig colon, that the key properties necessary for depth estimation are preserved during identity transition to a synthesized sample domain [80].

Liu et al., (2018) suggested a Two-step weighted variational selective picture segmentation model. The very first stage is to produce a smooth approximation to the targeted area in the input picture using the Mumford-Shah model. The approximation delivers a bigger value for a specific region and lower values for other locations by using a weighted function. They subsequently utilize that approximation and a thresholding approach to acquire the item of interest in the second step. The approximation may be derived using the alternating direction multiplier approach, and the method's convergence analysis can be developed. The experimental results for selective segmentation of images are shown to demonstrate the suggested method's utility. Additionally, they conduct additional comparisons and demonstrate that the suggested technique outperforms the other test method [81].

Yu et al., (2019) stated that in the medical industry, reliable segmentation of medical pictures remains tough due to poor contrast, complicated noise, and intensity inhomogeneity. To address these issues, this article proposes a unique edge-based active contour model (ACM) for segmenting medical images. Specifically, an accurate regularisation technique is described for maintaining the level set function's signed distance property, which ensures the evolution

curve's stability and the numerical computation's accuracy. Substantially, an adjustable perturbation is incorporated into the edge-based ACM architecture. The perturbation approach can achieve a balance between conceptual framework stability and segmentation accuracy, which is critical for segmenting medical pictures with intensity inhomogeneity. Several experiments across both synthetic and actual medical images revealed that the proposed segmentation model outperforms state-of-the-art techniques in improved noise tolerance and segmentation efficiency. Extensive trials comparing the model to certain other classic approaches also using synthetic and medical photographs indicate substantial improvements in both segment and anti-noise performance [82].

Choi et al., (2019) stated that for the real-time delineation of microscopic fractures in facades, a radical deep learning architecture called SDDNet-V1 was presented. The SDDNet was constructed using conventional convolutions, various DenSep modules, a customized ASPP component, and a decoding module. The focus of this research was to partition cracks in photos using a variety of different backdrop elements. However, at the commencement of the study, no freely released datasets met this purpose. As a result of this, the Crack200 dataset was developed manually. To increase the performance of the SDDNet, it was pre-trained on the revised Cityscape information and then conditioned on the Crack200 dataset. The training model was validated against the Crack200 test set, and numerous photographs illustrating the findings were displayed and discussed. The results revealed that it would be preferable to construct a domain- and detail model and that developing a model on images with repeating backgrounds would be useless in real-world settings. Despite being 88 times less in size than the reference models, the SDDNet model surpassed them in every way. The SDDNet achieved a performance outcome (36 fps) on images with such a density of 1025512 pixels, 46 times faster than a prior development [83].

Chen et al., (2019) suggested that cortical thickness nucleus of the nervous system is directly correlated with pessimism's emotional choice, this is crucial for increasing the knowledge and management of mental health diseases; and categorization of the subcortical nucleus is the first and most essential method to analyze and testing this region. To initiate, researchers capable of attracting for fragmentation of the nucleus accumbency in brain Magnetic Resonance (MRI) images using Location Regularized Template Matching Evolution, Region-Scalable Fitting (RSF), and Local Feature Fitting (LFF), and researchers compare the segmentation accuracy using selected evaluation indices. Each of the three recommended strategies has an average Correlation Coefficient value of more than 84 percent and an average Jaccard Similarity

Coefficient (JS) value better than 77 percent. While all three methods are capable of segmenting medical images with non - homogeneous filled and meeting the overall segmentation requirements, the recommended DRLSE model is better [84].

Feng et al., (2020) stated that Colon cancer, which is commonly caused by intestinal polyps, is one of the most fatal kinds of cancer. Clinical colonoscopy, which is typically conducted in real-time, is a good technique for finding polyps early. Rectal analysis, on the other hand, is time demanding and has a high rate of false positives. They describe a revolutionary handrail design for segmentation of genuine adenomas in colon pictures, rather than only detection, in this research. The suggested model is not only substantially faster than U-Net but also significantly more accurate at polyp segmentation. At the encoder step, the model first extracts spatial attributes using four parts. Following that, a bypass linkage with a Parallel Awareness Mechanism for each block and a culminating Mega Federation Module is utilized to completely fuse features at various scales. The encryption algorithm may gain significantly more parameters for polyp classification due to substantial data augmentation and frequent monitoring of instructive losses. This novel polyp segmentation approach outperforms state-of-the-art algorithms on multiple datasets (Central venous catheters, CVCClinicDB, and Endo Scene). Additionally, this network may be used for neuroimaging activities such as categorization in real-time and medical care [85].

Guo et al., (2020) suggested that enrichment and fragmentation of blood arteries in computer-aided diagnosis are addressed. To begin, the photos of the blood vessels are pre-processed. The Gray-scale conversion method is utilized to improve the contrast in this article, followed by an analysis of the region growth concept and its pros and downsides. It is discovered that there are two critical stages in fragmenting the blood vessel picture using the region growth method: the first is the seed point selection. Due to the time and labor involved in carefully determining seed points, this research opts to set the initial centroids in the image's center. The second step is to establish the threshold T. The proper threshold is eventually identified in this work after many group experiments. Experiments indicate that the suggested vascular segmentation can efficiently way segment regional blood arteries while eliminating human interference and sustaining a high level of resilience [86].

Memon et al., (2020) stated that Accuracy of delineation is a critical criterion for evaluating the utility of algorithms that users locate local attractions in images. Visual distortions such as lighting, on the other hand, may impair discriminative capacity, making it more difficult to recall things with inhomogeneous intensities. Such research offers a robust zone-based

technique for the segmentation of inhomogeneous pictures to overcome this issue. The suggested distributed generation practical mixes domestic and international intensity functions; a weight function is added that is calibrated as per localized dynamic range. By including the scale factor, the shapes at the intersections of various saturation levels are flattened, resulting in enhanced segmentation. The weight function weeds out erroneous pattern development and verifies entity constraints. In comparison to other state-of-the-art approaches, the suggested methodology surpasses them on both synthetic and real-world photos. A quantitative analysis of the mini-MIAS with Resampled datasets demonstrated that the proposed model outperformed the ground facts in high recognition performance. Additionally, when the suggested model was being used, the time taken for picture segmentation is faster than when other approaches are used [87].

Table 2.7 discusses the summary of the literature review conducted on hybridized techniques for medical image segmentation.

Table 2.7 Summary of Hybridized Techniques for Medical Image Segmentation

Author	Technique	Outcome
Kashyap et al., (2015)	Level set method (LSM)	Enhanced Stochastic pressure factor (SPF), which makes use of neighbourhood mean values to detect borders within homogeneous areas.
Nelakuditi et al., (2015)	Xilinx System Generator (XSG) and FPGA.	Significantly lowers the complexities inherent in the design process and adds the capability of hardware co-simulation.
Hamdaoui et al., (2015)	Particle Swarm Optimization (PSO) algorithm	The synchronous design of MRI image segmentation-based PSO enables time savings and hence simplifies the search for the best threshold.
Dergachyova et al., (2016)	The AdaBoost replies are fed into a concealed semi-Markov model.	With the effect that makes and instrument signals, it is helping to increase segmentation, reduce detection latency, and identify the proper phase order.
Kashyap et al., (2016)	Steepest descent method and improved lattice boltzmann's method	Fast processing speed, accuracy, automation and invariance of intensity inhomogeneities.

Sharma et al., (2017)	RGSA and SVM classification, hybrid ACO - GWO classification and PSVM classification, and KSCA modelling	Heuristic action in a supporting and helpful way rather than an assertive one is dependable and demonstrates their better convergence rate in locating the optimum solution and obtaining the fit function value, which is most likely the mean square error.
Gueziri et al., (2017)	Interactive segmentation using scribbles and calculation time	This effect diminishes as latency increases, as well as the two refresh algorithms, provide comparable user experience at the highest latencies.
Labrunie et al., (2018)	Real-time Magnetic Resonance Imaging (RT-MRI)	The tongue MSD inaccuracy is a tiny 0.55 mm 0.68 mm when using the upgraded version of Active Appearance Models (mASM).
Mahmood et al., (2018)	antagonistic training in a reverse flow framework	a depth estimates on a dataset of synthetic pictures obtained by an endoscope with an efficient forward model and an anatomically realistic colon
Liu et al., (2018)	An image segmentation model with weighted variation	Examination of the convergence of the alternating-direction multiplier technique
Yu et al., (2019)	Medical picture segmentation with an edge-based active contour approach	Balancing curve evolution stability and segmentation accuracy, which is critical for segmenting medical pictures with intensity inhomogeneity
Choi et al., (2019)	The semantical fault diagnosis system (SDDNet) was trained on a crack dataset that was manually generated.	The model analyses pictures at 1025×512 pixels in real-time (36 frames per second), which would be 46 times quicker than a previous effort.
Chen et al., (2019)	Caudate nucleus delineation models in brain Magnetic Resonance (MRI) images employing Directional Regularized Level Set Evolution (DRLSE), Area Matching, and Local Image Fitting (LIF).	All three of these models are capable of accurately segmenting medical images with heterogeneous intensities and meet the fundamental segmented requirements.

Feng et al., (2020)	A unique stair-shape network (SSN) is used to segment polyps in real-time.	With extensive data augmentation and rigorous oversight of auxiliary losses, the algorithm can acquire additional information for polyp segmentation.
Guo et al., (2020)	Region-growth technique using threshold segmentation and the K-means segmentation method	The arterial segmentation method can separate regional blood arteries efficiently and accurately, minimising the need for human involvement, while maintaining a high level of resilience.
Memon et al., (2020)	Hybrid region-based contour-based model for inhomogeneous picture segmentation	The processing time required for picture segmentation is significantly less than that required for other strategies.

Table 2.8 discusses the comparative analysis of hybrid techniques used for medical image segmentation based on the four parameters as accuracy, processing speed, real-time and complexity.

Table 2.8 Comparative Analysis of Hybridized Techniques for Medical Image Segmentation

Frameworks	Accuracy	Processing Speed	Real Time	Complexity	Remarks
Kashyap et al., (2015)	✓	✓	✗	✗	High complexity
Nelakuditi et al., (2015)	✓	✓	✗	✓	Not real time
Hamdaoui et al., (2015)	✓	✗	✓	✗	High complexity
Dergachyova et al., (2016)	✓	✓	✗	✗	High complexity
Kashyap et al., (2016)	✓	✓	✗	✗	High complexity
Sharma et al., (2017)	✓	✓	✗	✗	High complexity
Gueziri et al., (2017)	✓	✓	✗	✗	High complexity
Labrunie et al., (2018)	✓	✓	✗	✗	High complexity
Mahmood et al., (2018)	✓	✗	✗	✗	High complexity

Liu et al., (2018)	✓	✓	✗	✗	High complexity
Yu et al., (2019)	✓	✗	✗	✗	High complexity
Choi et al., (2019)	✓	✓	✗	✓	Not real time
Chen et al., (2019)	✓	✓	✗	✗	High complexity
Feng et al., (2020)	✓	✓	✗	✗	High complexity
Guo et al., (2020)	✓	✗	✗	✗	High complexity
Memon et al., (2020)	✗	✓	✗	✗	High complexity

2.2.5. Generative adversarial network (GAN) based image segmentation

GAN have supported a lot in medical image segmentation and have reduced the need of large labelled datasets, which is still a challenge in medical field. GANs have the capability to excerpt more high-end features, making them ideal for semantic segmentation. GANs have the potential to be used for synthesizing training data with high accuracy. Below mentioned literature survey shows the various GAN based networks along with its advantages in the field of medical image segmentation.

Neff et al., (2017) suggested modern deep learning algorithms excel in many computer vision applications. While deep learning algorithms do well on big datasets, they suffer from classifier and lack of generalisation on smaller datasets. The manual annotation of data is time-intensive and costly, especially in medical picture analysis. In this work, they propose a novel type of Generative Adversarial Networking (GANs) that creates segmentation masks for use in supervised computer-aided diagnostic applications. We assess our method using thorax X-Ray pictures to segment lungs and show that GANs may be utilized to synthesize training examples in this specific application [88].

Automatic biopsy segmentation using computed tomography (CT) images has been actively researched in recent years as a critical topic in imaging analysis, according to **Tang et al., (2019)**, but it remains exceedingly hard due to a lack of suitably labeled training data. Manually annotating a large number of lymphadenopathy categories is time-consuming and expensive. As a result, data augmentation might be considered a replacement for data enrichment. Many traditional augmentation approaches, on the other hand, change the data using a combination

of affine transformations, which can't improve the variety of contextual information in the data. This study proposes a strategy-focused GANs for constructing numerous CT-realistic pictures using customised lymph node masks to overcome this issue. Because of its power in picture formation and capacity to learn both structural and contextual knowledge about lymph glands and their surrounding structures from CT images, the pix2pix GAN model is used in this study. A strong U-Net model for lymphadenopathy segmentation is learned with the addition of these improved photos [89].

Rezaei et al., (2020) suggested a novel recurrent generative adversarial architecture, dubbed RNN-GAN, to address the unbalancing computational problems in medical image semantic segmentation, in which the number of pixels corresponding to the desired object is significantly less than the number of pixels corresponding to the background. A model trained on unbalanced data tends to favor healthy data, which is undesirable in clinical applications, and these networks provide outputs with a high degree of accuracy and low recall. To offset the effect of unbalanced training data, we train RNN-GAN with both the suggested complementary segmentation mask and standard segmentation masks. Two components comprise the RNN-GAN: data generators and a classifier. Researchers demonstrate that the suggested framework is suitable for a variety of various types and sizes of medical photographs. They see consistently improved outcomes in our studies using the ACDC-2017, HVSMR-2016, and LiTS-2017 benchmarks, indicating the usefulness of our strategy [90].

Xiong et al., (2020) stated that recent advances in semantic segmentation have been made possible by the creation of deep CNN. They offer an edge Bayesian segment network for remote sensing pictures that are built on generative models (GANs). To begin, fully convolutional networking (FCNs) and GANs are being used to implement Bayesian theory's deduction of the posterior distribution and probability to the posterior probability. Secondly, the cross-entropy loss inside the FCN is used as a priori to steer the GAN's training process, overcoming the risk of mode collapse. Thirdly, the GAN's generator is employed as a programmable spatial filter to create the spatial link between the labels. Experiments on two remotely sensed datasets reveal that the suggested method's training is more robust than that of existing GAN-based models. The accuracy rate and maximum intersection (MIoU) of data sets were 0.0465 and 0.0821 points higher than FCN, respectively, and 0.0772 and 0.1708 points higher than FCN [91].

Zhao et al., (2021) suggested that medical image fusion approaches can increase clinical diagnostic accuracy and speed by combining information from many medical pictures. They

present a unique medical image fusion approach based on deep convolution GAN and dense block models. This network design incorporates two modules: a discriminator and a dense block image generator. This study uses the encoder networks to extract image features, fuse them using the Lmax norm and feed them into the decoder to get the final fusion picture. This approach overcomes the flaws of active layer measurements by manual design and processes information of the interlayer using thick blocks to avoid information loss [92].

Li et al., (2021) stated that Medical picture quality is largely dependent on diagnosis and treatment, which has resulted in medical image denoising being a major study area. Due to its superior capabilities for automated feature extraction, background subtraction based upon deep learning approaches has garnered substantial interest. Most existing approaches for medical denoising that are suited to certain forms of noise have difficulty addressing spatially variable noise; in the process, image information is lost and the denoised picture structure changes. About picture context perception and structure preservation, this article first offers a technique for denoising medical images using a conditional generative adversarial network (CGAN) with a bunch of different sounds. The suggested architecture merges the trash image with the matching gradient image as network conditioned information, hence increasing the contrast between both the original signals based on the structural distinctiveness. To investigate visual context, a new generator with remaining dense blocks takes extensive use of the interaction between convolutional layers. Additionally, the reconstructions loss and the WGAN loss are merged as the actual loss function to guarantee that the denoised and genuine images are consistent [93].

Table 2.9 summarizes the GAN techniques used by researchers for image segmentation.

Table 2.9 Summary of GAN based image segmentation

Author & References	Technique	Outcome
Neff et al., (2017)	Adaptation of GAN DCGAN	GANs have the potential to be used for synthesizing training data in this specific application
Tang et al., (2019)	Pix2pix GAN model is used	Robust U-Net model is learned for lymph node segmentation
Rezaei et al., (2020)	RNN-GAN with proposed complementary segmentation mask	show evidence that the proposed framework applies to different types of medical images of varied sizes.

Xiong et al., (2020)	End-to-end Bayesian segmentation network based on GAN (GANs)	two remote sensing datasets and the results demonstrate that the training of the proposed method is more stable than other GAN based models
Zhao et al., (2021)	Novel medical image fusion algorithm based on deep convolutional generative adversarial network and dense block models	Overcome the weaknesses of the active layer measurement by manual design in the traditional methods and can process the information of the intermediate layer
Li et al., (2021)	Image denoising method based on conditional generative adversarial network	Reconstruction loss and WGAN loss are combined as the objective loss function to ensure the consistency of denoised image and real image

Table 2.10 represents the comparative analysis between various GAN utilized by researchers for image segmentation based on four parameters such as accuracy, processing speed, real time and complexity.

Table 2.10 Comparative Analysis of GAN based image segmentation techniques

Frameworks	Accuracy	Processing Speed	Real Time	Complexity	Remarks
Neff et al., (2017)	✓	✓	✗	✗	High complexity
Tang et al., (2019)	✓	✓	✗	✓	Not real time
Rezaei et al., (2020)	✓	✗	✗	✗	High Complexity
Xiong et al., (2020)	✓	✓	✗	✗	High Complexity
Zhao et al., (2021)	✓	✓	✗	✗	High Complexity
Li et al., (2021)	✓	✓	✗	✗	High Complexity

GAN's have proven to be highly suitable for the real time segmentation of medical images as they are more robust. Due to its capability of being unsupervised, they do not require high labelled training datasets. The computation capability of GAN's are proven to be fast and precise when compared to CNN's. Because of these capabilities, it is more useful in real time diagnosis. These reasons have accelerated the research in utilizing different GAN models for medical image segmentation.

2.2.6. Fuzzy Based Medical Image Segmentation

Fuzzy algorithms have proven to detect the intensity inhomogeneities, which occurs a lot in medical images. Fuzzy techniques provide advantages such as automation, invariance to intensity heterogeneity, and excellent accuracy. For different inconsistencies, fuzzy logic has proven to be the state of the art. The below survey indicates the fuzzy algorithm in the segmentation of medical images. It also discusses the different pros and cons of using fuzzy algorithms.

Kannan et al., (2010) discussed a robust clustering for breast and cerebral magnetic resonance image segmentation. The commonly employed conventional fuzzy c-means algorithm for medical image analysis has limitations due to its use of the squared-norm distance metric to compare the centres and data items in medical pictures that are distorted by noisy, outliers, as well as other imaging abnormalities. To solve these constraints, this article proposes a unique objective function based on the conventional optimization problem of fuzzy c-means that combines the resilient hardware abstraction layer distance for clustering damaged mammary and brain medical imaging datasets. While partitioning the given dataset, this paper offers an effective equation for optimal cluster centres and an equation for ideal membership grades by minimising a unique objective function. To address the question of how the initial centres of clusters affect clustering efficiency, this research provides a unique centre initialization strategy for performing the learning algorithm for segmenting medical images. To test the suggested method's performance, experiments are conducted using synthetically generated breast and brain pictures. Additionally, the reliability of the clustering techniques is assessed using the silhouette methods, and the results are compared to those obtained using other recently released fuzzy means. The findings show the effectiveness of the suggested clustering approach [94].

Zhang et al., (2012) stated that with the existence of the occlusion's phenomena, segmentation becomes much more difficult in medical image analysis. However, fuzzy means, as an efficient

technique for dealing with PVE, faces significant efficiency issues. To do this, this research offers an improved Fuzzy C Means FCM technique on the input picture, designated as FCM and separated into two stages. The first step will extract many intervals from which cluster centroids may be computed, and the second phase will execute picture segmentation using an enhanced FCM method. FCM can generate satisfactory segmentation accuracy in much less than 1 sec and can meet the real-time needs of medical image processing, according to experiments on medical pictures [95].

Rastgarpour et al., (2014) discussed an integrated strategy to automate medical picture segmentation that maximizes the benefits of existing approaches while minimizing their drawbacks. Inhomogeneity of intensity is a difficult and unsolved topic throughout this domain, which has gotten less attention because of such an approach. It has a substantial effect on segmentation accuracy. This research presents a new runtime environment fuzzy level set method for resolving this problem using an integrative approach. It can develop directly from the Gauss Kernel-Based Flexible C-Means initial level set GKFCM. Additionally, the GKFCM data are used to examine the parameters driving stage set development. Additionally, the proposed approach comprises locally approved synthesis, which would be based on a picture modelling that accurately depicts the substance of real-world pictures and contains high-intensity variabilities as an image component. These additions simplify level set administration and provide further context assistance when level anisotropy occurs. The suggested technique offers a few advantageous properties, including automation, invariance to intensity heterogeneity, and excellent accuracy. The suggested algorithm's performance was evaluated using medical pictures acquired using various modalities. The results demonstrate its efficacy in segmenting medical images [96].

Gupta et al., (2017) stated that ultrasound is among the most extensively used and least expensive diagnostic techniques in medicine. They provide a hybrid system for segmenting ultrasonic medical images accurately that combines the properties of inner dense clumping with spatial constraints, the threshold contour-based method, and the distance normalized level set (DRLS) algorithm. While flexible classifications are used to create the curves that disperse to define a predicted area or item boundaries, it also aids in forecasting the appropriate parameters that regulate level set evolution. Additionally, the DRLS formulation speeds up processing by removing the requirement to re-initialize clustering functions. The suggested method's performance is assessed through a series of tests using both synthetically generated ultrasound images. The investigational findings indicate that the suggested method enhances segmentation

accuracy and generates superior outcomes by effectively segmenting the object boundaries [97].

Bozhenyuk et al., (2019) suggested that digital images into multiple segments of splitting an image into sections that have some properties that are constant and homogenous. Segmentation of images is a vital step in detecting abnormalities and arranging therapy. Medical pictures are segmented using segmentation algorithms to uncover anatomical components and abnormalities. When conducted by medical experts, fragmentation of Magnetic Resonance (MRI) takes a long period. Recognizing automation is a timely task if the appropriate evaluation is supplied. Indeed, there is no common approach for segmenting medical images; the selection is made based on the imaging modalities, the characteristics of the area of interest, and the application. No one segment model is appropriate to all medical picture modalities, nor are all techniques efficient for each. Segmentation is a tough problem in many practical uses of image processing and computer vision, demanding more research. The Hybridized Ant Fuzz Algorithm (HAFA) is considered in this work for MRI segmentation. The HAFA parameters are investigated for several groupings of MRI pictures. The algorithm was tested using medical photos from the OsiriX collection as well as real patient images. The experimental results demonstrate that the suggested strategy excels and outperforms alternative methods in terms of accuracy and consistency [98].

Bibiloni et al., (2019) stated that Vessel detection is the first step towards automatic detection and in-depth inspection of retinal images to aid ophthalmologists. Their research seeks to develop a real-time system for fragmenting vessels in iris images using imperfect morphological techniques. This framework strikes an advantageous balance between expressive capacity and computing needs because the content in the immediate neighbourhood is processed swiftly using several fast operations. This framework is focused upon that fuzzy black top-hat transformation, which is a straightforward yet extremely powerful technique. On average, the system analyses photos from the DRIVE and STARE datasets in 37 and 57 milliseconds, respectively. Thus, it may be utilised in combination with a physician's examination, incorporated into more complex systems, or as a pre-screening technique for massive volumes of data. It exceeds alternative state-of-the-art techniques concerning real computational efficiency and competitive performance [99].

Table 2.11 shows the summarised table for the literature review conducted based on the fuzzy algorithms and techniques for the medical image segmentation.

Table 2.11 Summary of Fuzzy Based Medical Image Segmentation

Author	Technique	Outcome
Kannan et al., (2010)	Unique fuzzy c-means objective function	Clustering performance is impacted by the initial centres of clusters.
Zhang et al., (2012)	FCM method based on the image's histogram	Using FCM, it is possible to get acceptable results in much less than 0.1 seconds and meet the real-time needs of medical image processing.
Rastgarpour et al., (2014)	Integrative approach to present a novel kernel-based fuzzy level set method.	The suggested technique offers several advantageous properties, including automation, invariance to intensity heterogeneity, and excellent accuracy.
Gupta et al., (2017)	Active contour approach using distance regularized level set (DRLS) function	Helps determine the best settings for regulating the progression of the level set
Bozhenyuk et al., (2019)	The Hybridized Ant Fuzz Algorithm (HAFA) for MRI segmentation	In contrast to analogues, experimental findings reveal that the suggested method performs well and is accurate.
Bibiloni et al., (2019)	Real-time fuzzy morphological method	It can be utilised concurrently with the evaluation of the patient, incorporated into more complex systems, or employed as a pre-screening tool for huge volumes of data.

Table 2.12 shows the comparative analysis of various fuzzy algorithms used by researchers for medical image segmentation based on the four parameters such as accuracy, processing speed, real-time and complexity.

Table 2.12 Comparative Analysis of Fuzzy Based Medical Image Segmentation

Frameworks	Accuracy	Processing Speed	Real Time	Complexity	Remarks
Kannan et al., (2010)	✓	✗	✗	✗	High complexity
Zhang et al., (2012)	✓	✓	✓	✗	High complexity
Rastgarpour et al., (2014)	✓	✗	✗	✗	High complexity
Gupta et al., (2017)	✓	✓	✗	✗	High complexity
Bozhenyuk et al., (2019)	✓	✗	✓	✗	High complexity
Bibiloni et al., (2019)	✓	✓	✗	✗	High complexity

When dealing with different analogs and intensity variations among the medical images, fuzzy logic helps in identifying these variations more accurately and precisely. But the need of large datasets require the usage of this technique by merging with other CNN techniques.

2.3 Deep Learning-Based Brain Tumour Segmentation Algorithms

Automated brain tumor segmentation is the most challenging task because of the intensity inhomogenities between the healthy and unhealthy tissues. For real time automated segmentation, algorithms should hold properties such as highly efficient, fast processing, and less complex architectures. Below literature discusses the deep learning based automated segmentation algorithms.

Zhao et al., (2018) stated that brain tumour segmentation that is accurate and reliable is crucial for diagnosis of cancer, treatment planning, and outcome evaluation. By merging fully convolutional neural networks and Conditional Random Fields CRFs in a unified framework, they suggested a unique method for segmenting brain cancer while maintaining their appearance and structural consistency. On 2D picture patches and image slices, the following processes are utilized to develop a deep learning-based segmentation method: 1) learning FCNNs from input pictures; 2) retraining CRFs as Supervised Learning with FCNN parameters set in image slices; and 3) fine-tuning FCNNs and CRF-RNNs using image slices. They train three distinct algorithms utilizing single two-dimensional patches and slices collected in

diagonal, frontal, and transverse views, which they then combine to fragment malignancies that used a voting-based hybrid approach. Their method segmented neural images segment faster over approaches that rely on image patches. The technique was assessed using imaging data from the Multidisciplinary Brain Tumour Image Classification Challenge 2013, 2015, and 2016. The experimental findings indicate that their technique is capable of building segmentation models using Flair, T1c, and T2 scans that perform as well as those constructed using Flair, Computed tomography, and T1-weighted scanning [100].

Ari et al., (2018) suggested that the method of treating brain cancer is highly dependent on the physician's expertise and understanding. As a result, utilizing an automated tumour detection system is critical in assisting radiologists and clinicians in detecting brain cancers. The suggested technique consists of three stages: pre-processing, tumour classification using ensemble learning machines local receptive fields (ELM-LRF), and tumor region extraction using image processing. To begin, the noise was removed using stochastic techniques and local smoothing techniques. The second stage used ELM-LRF to classify cerebral magnetic resonance (MR) pictures as benign or malignant. The third step involved segmenting the tumours. The experiment's objective was to save the physician's time by utilizing only cranial MR pictures with a mass. The categorization accuracy of cerebral magnetic resonance imaging is 97.18 per cent in experimental tests. The evaluation findings indicated that the suggested strategy outperformed other recent research in the literature. Additionally, experimental results demonstrated that the suggested approach is successful and may be utilized to identify brain tumours using a computer [101].

Thillaikkarasi et al., (2019) depicted that brain tumours are caused by the unregulated growth of melanomas in brain tissue. There are two types of brain tumours: benign or malignant. While benign brain tumours may not damage surrounding normal and healthy tissue, malignant brain tumours can harm adjoining brain tissues, eventually resulting in death. Timely detection of brain tumours may be necessary to ensure a patient's survival. MRI scanning is typically used to detect brain tumours. However, physicians are still unable to segment tumours accurately in MRI scans due to the irregular shape and location of tumours in the brain. Effective brain segment is critical for detecting tumours and giving the correct treatment for a patient. Additionally, it offers guidance for the surgeon doing the procedure. The purpose of this research is to provide a unique deep learning strategy based on kernel-based CNNs and M-SVMs for segmenting tumours automatically and effectively. This study is divided into many parts, including pre-processing, feature extraction, picture classification, and brain tumour

segmentation. The MRI image is smoothed and enhanced using the Wavelet coefficients of Gaussian filtering technique in combination with Contextually Limited Adaptive Data Augmentation, which enables the restoration of the tumour's localization, shape, and surface characteristics in the central nervous. As a result, M-SVM is used to classify the images based on the given attributes. Using a kernel-based Neural technique, the tumour is segregated from the MRI images. The experimental findings demonstrate that the suggested strategy is capable of segmenting brain tumours with an accuracy of about 84 per cent when compared to existing algorithms [102].

Sun et al., (2019) stated that Malignant tumours comprise most initial neurological disorders. For diagnosis, therapy, and risk factor identification, robust and precise tumour delineation and lifetime prediction are critical. The overarching objective of this research is to develop a system based on deep neural networks for malignancy identification and prognostic prognosis in cancer utilizing multimodal MRI data. They achieve consistent tumour segmentation performance by using three distinct three-dimensional network architectures. This method has the potential to significantly eliminate system bias and improve results. To estimate survival, they obtain 4,524 radio mic properties from segmented tumor sites, and then use a prediction system and cross-validation to choose the best predictive features. Finally, a randomized forests classifier was tested to forecast an individual's survival rate. Their technique is ranked second and fifth in the 2018 multifunctional classification of Brain Challenge, out of more than 60 teams, for survival prediction and realized, with a remarkable 61.0 per cent accuracy in identifying short-, intermediate-, and long-survivors [103].

Mlynarski et al., (2019) stated that for many modern tumour detection methods, machine learning is used in conjunction with segmented pictures to identify tumours. This sort of dataset is exceedingly expensive, as characterising tumours by hand necessitates not just time but also scientific knowledge. In contrast, photos labelled "globally" (indicating the presence or lack of a malignancy) were substantially less effective but far less expensive. They seek to build a method for categorization based on deep learning utilizing both fully labelled and lightly annotated training data. The technique is mutually trained for improved semantic segmentation to obtain information from sparse annotations while preventing the network from accumulating irrelevant characteristics for the segmentation task. They evaluate their approach against the Tumour Segment 2018 Challenge's difficult task of segmenting brain tumours in magnetic resonance. They show that as compared to standard deep classification, the suggested technique

dramatically improves segmentation performance. The stated performance is proportional to the ratio of sparsely to annotated training images [104].

Yang et al., (2019) stated that brain tumour segmentation in magnetic resonance imaging (MRI) pictures is critical for early detection, treatment planning, and outcome evaluation. However, due to the great structural variety of gliomas, segmentation accuracy is poor. The objective of this research is to present an autonomous segmentation approach that integrates tiny kernel two-path convolution neural network (SK-TPCNN) with random forests (RF), as well as to demonstrate the SK-feature TPCNN's extraction capabilities and the model's joint optimization capability. The SK-TPCNN structure, by mixing small and big convolutional kernels, may improve nonlinear mapping capability and reduce overfitting; also, the multiformatted information is boosted. The learned features from the SK-TPCNN are then used to accomplish the joint optimization using the RF classifier. The RF classifier successfully combines redundant features and classifies each voxel in an MRI image into healthy brain tissues and various tumour components. The proposed approach is verified and assessed using the 2015 Brain Tumour Segmentation BraTS Training dataset, that it achieves superior performance [105].

Saba et al., (2020) stated that the most dangerous ailment in the world today is a brain tumour. Tumours influence the brain by destroying healthy tissue and escalating intracranial pressure. As a result, the fast proliferation of tumour cells may result in mortality. As a result, early brain tumour diagnosis is a critical undertaking that might potentially save a patient's life. In the suggested research, the Grab cut method has been used to segment accurate lesion symptoms, whereas the Transfer can be done procurement automatic system graphic morphology grouping is perfectly fine to acquire characteristics, which are then concatenated with hand-crafted (colour and size) characteristics using a serial-based method. Entropy is utilized to alter these properties for classification accuracy and speed, and the method was determined vector is delivered to classifiers. The suggested method is verified using therapeutic image processing and computer-assisted intervention techniques datasets from 2015, 2016, and 2017, including the multimodal brain tumour segmentation BraTS database [106].

Rehman et al., (2020) stated that brain tumours are the most lethal type of cancer, with an extremely low life expectancy at their most advanced stage. Brain tumour misdiagnosis results in ineffective medical intervention and reduces patients' chances of survival. Accurate identification of brain tumors is critical for developing an effective treatment plan that can cure and prolong the lives of people with brain tumors conditions. Techniques for digital malignancy

identification and neural networks are two examples of success that have considerably improved the field of machine learning. In comparison to standard previous neural network layers, the deep convnets collect significant and robust characteristics first from the input vector automatically. They undertake three investigations in the framework, utilizing three different convolutional neural network architectures (ImageNet dataset, Vggnet, and Support vector machines (SVM)) to classify brain cancers such as hematoma, glioblastoma, and pituitary. This research subsequently investigates transfer learning strategies, such as fine-tuning and freezing, by utilizing an MRI slice dataset of brain tumour. These data preparation approaches are applied to MRI scans to increase generalizability by expanding the database representative sample and decreasing the possibility of overfitting. The fine-tuned Generative adversarial architecture obtained a massive classification and precision rate of up to 98.69 in the submitted studies [107].

Table 2.13 shows the summarised table for the literature review conducted mainly for the brain tumor segmentation algorithms based on deep learning techniques.

Table 2.13 Summary of Deep Learning-Based Brain Tumour Segmentation Algorithms

Author & References	Technique	Outcome
Zhao et al., (2018)	2D image patching and slices with FCNN variables	The approach could segment brain pictures quicker than image patches. The Multidisciplinary Brain Tumor Imaging Segment Challenge BraTS 2013-2016 assessed their technique.
Ari et al., (2018)	ELM-LRF-based tumour classification and image processing-based tumour region extraction	The reliability of cerebral MR images in terms of categorization is 97.18 per cent.
Thillaikkarasi et al., (2019)	Deep learning (kernel-based CNN) using M-SVM	The given technique is capable of segmenting brain tumors with an accuracy of about 84 percent when compared to existing algorithms.
Sun et al., (2019)	Ensembles of three different types of 3D CNNs	Obtaining a promising 61.0 per cent accuracy in short-survivor, mid-survivor, and long-survivor categorization

Mlynarski et al., (2019)	Voxel-wise and image-level neural networks.	Classifying and segmenting Subnetworks share many network components and are trained collaboratively using both fully and sparsely annotated data.
Yang et al., (2019)	SK-TPCNN with random forests (RF)	The RF classifier successfully incorporates redundancy features and classifies every Multiresolution voxel into normal brain tissues and various tumour components.
Saba et al., (2020)	The Grab cut approach accurately segments true lesion symptoms.	Entropy-optimized features are employed to provide accurate and rapid classification, and a fused vector is delivered to classifiers.
Rehman et al., (2020)	Convolutional neural network architectures Alex Net	The MRI segments are utilized to the generalizability of the results, hence expanding the sample size of the dataset, and reducing the chance of over-fitting.

Table 2.14 discusses the comparative analysis of deep learning based brain tumor segmentation algorithms with respect to four parameters such as accuracy, processing speed, real time and complexity.

Table 2.14 Comparative Analysis of Deep Learning-Based Brain Tumour Segmentation Algorithms

Frameworks	Accuracy	Processing Speed	Real Time	Complexity	Remarks
Zhao et al., (2018)	✓	✓	✗	✗	High complexity
Ari et al., (2018)	✓	✗	✗	✗	High complexity
Thillaikkarasi et al., (2019)	✓	✗	✗	✗	High complexity
Sun et al., (2019)	✓	✗	✗	✗	High complexity
Mlynarski et al., (2019)	✓	✗	✗	✗	High complexity
Yang et al., (2019)	✓	✗	✗	✗	High complexity
Saba et al., (2020)	✓	✓	✗	✗	High complexity

Rehman et al., (2020)	✓	✓	✗	✓	Not Real time
-----------------------	---	---	---	---	---------------

Due to the intensity variations within the brain MRI images, a high-end deep learning algorithm is required for its segmentation. The researchers for accurate and precise segmentation of brain tumors have proposed different deep learning architectures, but the need for real-time diagnosis via deep learning architectures is still a major challenge. Some of the architectures are successfully capable of incorporating redundant features classify every Multiresolution voxel into normal brain tissues and various tumor components. Some architectures are trained collaboratively using both fully and sparsely annotated data. CNN's have proven to reduce the chances of over-fitting from MRI images. However, due to the complex nature and less accuracy and computational speed of these architectures, usage of these in real time is a major challenge.

2.4 Problem statement

Segmentation of brain tumours is amongst the most difficult tasks in medical image processing. Brain tumour segmentation's objective is to provide precise delineations of brain tumour areas. In recent years, deep learning algorithms have shown promising results when applied to several computer vision problems, including image classification, object identification, and semantic segmentation.

Numerous algorithms based on deep learning have been used for brain tumor segmentation with promising results. Given the extraordinary advancements made possible by state-of-the-art technology, utilize this survey to present an in-depth examination of recently established deep learning-based brain tumor segmentation approaches. A recent study has already aided in the enhancement of the human capacity for diagnosing medical pictures. Medical pictures are produced in different of different forms, including CT, MRI, X-RAYS, and ultrasound. Bear in mind that when you examine different modalities, consider the fact that each will have its own set of constraints. Accurate segmentation is a difficult undertaking due to its intricacy. Using MRI images as a test case, this research aims to provide a systematic approach for real-time segmentation of diagnostic imaging CT scans. This research will develop algorithms for real-time volume definition of tissues, organs, and tumors. The purpose of this work is to optimize real-time brain tumor segmentation efficiency.

2.4.1. Gaps in research

The present limitation of brain MRI segmentation techniques is their computing speed and efficiency, which must be addressed to do real-time processing. The next work will focus on enhancing the accuracy and precision of segmentation algorithms, as well as on reducing the amount of user intervention. As fresh picture data become available, it is risky to depend only on the existing model due to biological variety all these problems are solved by the proposed methodology.

The current issue with brain MRI segmentation approaches is that they have poor computational speed and efficiency, which must be addressed for real-time processing.

By focusing on qualitative measurements like accuracy, specificity, sensitivity, and precision while using quantitative factors like the dice score coefficient, peak signal to noise ratio, structural similarity index, efficiency of segmentation algorithms can be increased.

According to the above-mentioned literature review, hierarchical dense CNN architectures have been demonstrated to be the state of the art. Because of the deeper structures, networks with hierarchical structures achieve better tumor localization outcomes [51]. As per the literature review conducted, the following are the benefits of deep learning systems:

- **Robust:** These algorithms separate homogeneous regions such as noise, etc.
- **Speed:** These algorithms work faster in a GPU environment and due to their faster execution it has the capability to diagnose the disease.
- **Featured Engineering:** These networks has the capability to extract features on its own. It can scan features from structured as well as unstructured data as well. It can easily learn features that are more complex.
- **Efficiency:** These models are very efficient as once trained can perform multiple routine tasks without the requirement of labelled dataset. Efficiently used for disease prediction.
- **Performance:** It gives the best performance by attaining high accuracy in short period of time.
- **Real Time:** Deep learning when applied to medical imaging can diagnose and predict diseases in real-time.

The importance of the research is emphasizing the proposed model's requirements. This is done based on the comparative analysis performed on various categories of literature survey conducted in the above sections. The survey suggested that for proposing a model to meet the

real-time segmentation requirements for the brain tumor segmentation, the following properties such as robustness, accuracy, complexity, performance has to be satisfied. The proposed model has attained high accuracy and less complex architectures to be utilized in a real-time environment.

2.5 Summary

In this chapter, the survey of brain tumor detection methods was discussed in detail. A complete study of brain tumor segmentation, K-means and Clustering Algorithm segmentation, deep learning techniques, tumor categorization using deep neural networks, tumor categorization using support vector machine, and edge detection approach for brain tumor identification were covered. Finally, the analysis of the survey was summarized above. It is analyzed that many effective brain tumor segmentation and deep learning algorithms were used in the survey. Based on the literature survey conducted it is concluded that for real-time segmentation of brain tumors, the proposed technique should be more robust, more precise, and accurate, and must have fast processing speed.

Based on these requirements, the proposed model comprises of the transfer learning based hierarchical dense convolutional neural networks and RT-GAN. The proposed model is based on the studied literature survey and it provides solutions for all properties of and comparative analysis of CNN and GAN. GAN's provide high processing speed and do not require large labelled datasets. GAN's have proven to be highly suitable for the real time segmentation of medical images as they are more robust. Due to its capability of being unsupervised, they do not requires high-labelled training datasets. The computation capability of GAN's are proven fast and precise when compared to CNN's. Because of these capabilities, it is more useful in real time diagnosis.

CHAPTER 3

PROPOSED METHODOLOGY

3.1 Overview

Segmentation is a common topic in medical image analysis [108]. This is particularly true for Convolutional Neural Network (CNN) and GAN-based approaches, such as Electron Microscopy (EM) segmentation, brain lesion, skin cancer tissue segmentation, organ, and so on, which have made great progress in medical image segmentation tasks. The use of segmentation in these works assists in the development of diagnostic and treatment strategies. Semantic segmentation is popular for GAN and CNN-based techniques providing a category name to each pixel and outperforming other algorithms in terms of efficiency and accuracy [109]. Medical segmentation tasks face various challenges, including a partial number of instances and a broad diversity of tissue and lesion shapes and sizes. Semantic CNN's attempt to address these issues.

Semantic pictures and context information may be gathered by increasing the amount of convolution operation or by re-creating the inputs from the outcome vectors of the convolution process [110]. These approaches allow the convolution kernel to receive context information from a variety of receptive fields of various sizes. Small or huge reflexes are related to small or large features. For a solitary receptive field, convolution features focus on the focal region of interest while ignoring surrounding information. The methodology is a focused paradigm for science, a consistent and rational approach centered on opinions that direct researchers and other users to choose. It contains theoretical analyses of the community of methods and concepts linked to a branch of expertise, which differs according to their historical creation in the different disciplines. It is a theoretical examination of the Segmentation of Medical Images [111].

3.2 Proposed Method

It is presented the study's contribution to the efficient creation of a Hierarchical clustering-based deep learning algorithm and real-time GAN for autonomous brain tumor segmentation in Magnetic Resonance Imaging (MRI) images.

Figure 3.1 shows the basic and traditional segmentation algorithm followed in various architectures. In this, images are fed only to the CNN architectures and segmented image is shown as the output.

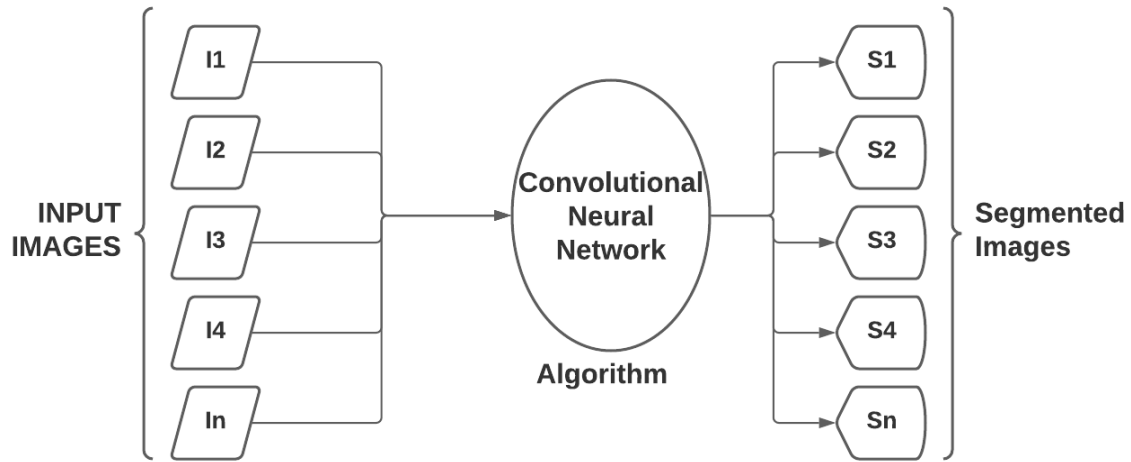


Figure 3.1 Traditional Segmentation Algorithm

The dense hierarchical CNN algorithm is shown in Figure 3.2. In this case, the typical segmentation architecture is altered by adding a transfer-learning layer to the CNN architecture. This will cut down on the number of huge datasets needed to train the new model. Using a pre-trained model in conjunction with a CNN layer will improve segmentation accuracy.

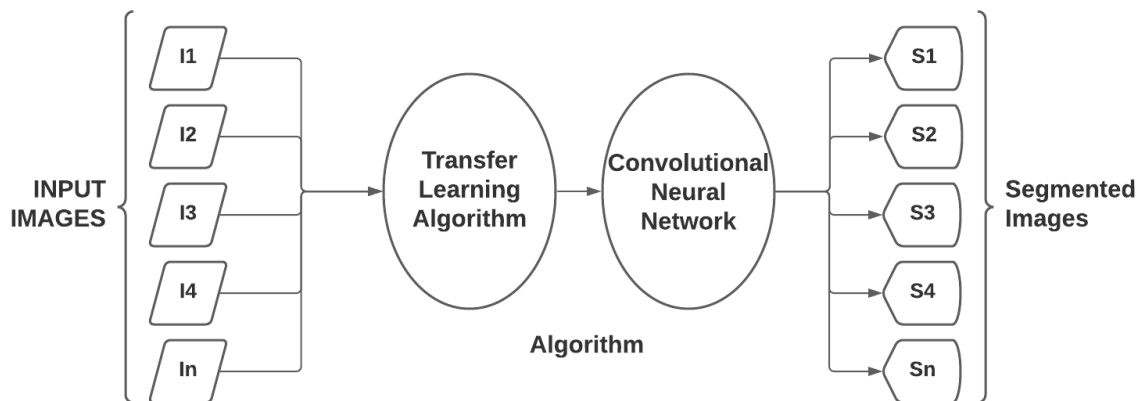


Figure 3.2 Dense Hierarchical CNN algorithm

Figure 3.3 shows the Generative Adversarial Network GAN algorithm. The preliminary goal of this study is to use the Hierarchical Dense CNN technique to segment brain tumors in MRI images. The hierarchical clustering dense CNN model that has been suggested is a two-stage model.

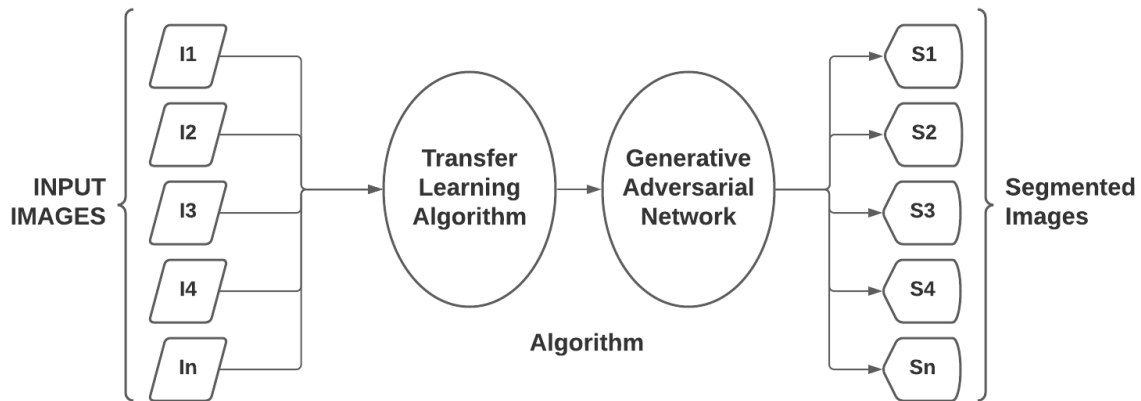


Figure 3.3 Generative Adversarial Network (GAN) algorithm

The initial phase is to create a "transfer-learning network (T-Net)," which is then followed by a "segmentation network (S-Net)." It is qualified to do automatic tumour image segmentation using hierarchical categorization to improve the convolutional system's efficacy and accuracy. The segmentation approach employs a hierarchical clustering method rather than a single-level clustering method. The location and shape of the brain tumour are first determined, and tumours are then classified into various categories of tumorous tissue. The data is supplemented in order to balance the training dataset based on image quality. The proposed methodology is depicted in Figure 3.4.

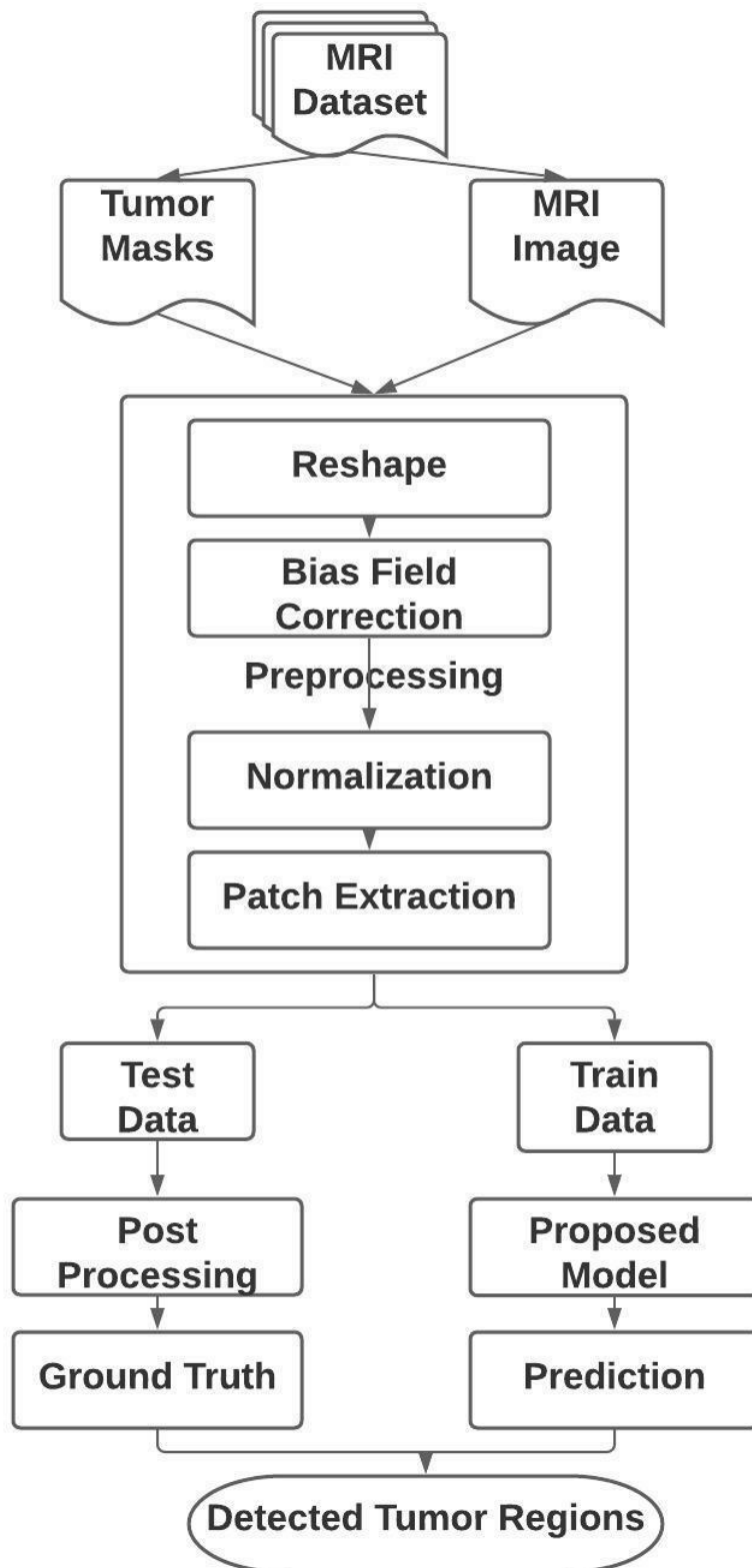


Figure 3.4 Proposed Methodology

The photos acquired as of the dataset are divided into many inter-categories and treating all of them equally has an impact on classification accuracy. This work uses hierarchical clustering segmentation to improve multi-classification segmentation classification accuracy. In this research, hierarchical clustering will be utilized to enhance the effectiveness of the segmentation procedure. This research investigates the effectiveness of the proposed technique utilizing quantitative criteria for instance peak signal to noise ratio, entropy, and mean square error. These quantitative features are paired with qualitative functions such as accuracy, precision, and sensitivity.

Step 1: It is a collection of the raw data. It contains three patients dataset containing 155 scans brain tumor MRI images of each image modality as T1, T2, T1ce and FLAIR. There are divided into two parts tumor masks and MRI images. The dataset also includes complete masks for a brain tumor.

Step 2: After getting the data, pre-processing is applied to the raw data to resize, bias field correction, normalization, and patch extraction.

- **Resize:** MRI images are a wide range of pixels that have a high resolution, and their computation is difficult to manage. There are reduced high-resolution pixels in MRI. Image reduction stores fewer images in a smaller amount from the original data.
- **Bias Field Correction:** It is utilized for pre-visualized images, high pass filtering, and homomorphic filtering. Some flaws and defects in the captivating ground caused by the MRI image, picture assets from an MRI dataset show inhomogeneities of images.
- **Normalization:** The normalization technique is used to provide a constant difference and strength crosswise various affected roles. a collection of power attractions for each structure is determined and utilized to choose the MRI sequence in this manner.
- **Patch Extraction:** Patch Extraction is removed for each pixel's rate. Patches are arranged created on the vitality through a high level of vitality are maintained through the threshold. Patches extracted have been adjusted for intensity, the histogram of each sequence for each structure, and patches are standardized to provide element discrepancy and zero cause.

Step 3: It is test data to transfer learning approach improves the knowledge curvature with transporting information from a test model to a qualified convolutional neural network model.

After that, the post-processing has been informed to show the other medical assessments in subsequent fields. It has provided a ground truth value.

Step 4: The train data are expert to conduct segmentation of tumor pictures utilizing hierarchical categorization to enhance effectiveness and correctness. It is encompassing hierarchical dense CNN such as the t-net and the s-net.

Step 5: MRI scans are utilized to detect both low-quality and high-quality gliomas using an improved brain tumor segmentation approach. It is measuring the mean square error, entropy, and the peak signal-to-noise ratio.

3.2.1 Transfer Learning Algorithm

This section describes the development of a transfer learning system for automatic brain tumor segmentation from MRI images. The transfer learning approach improves the understanding curvature by transmitting data from a training convolutional neural network model to transfer to a test set [112]. It is the same as transferring human knowledge to robots so that they can make decisions, find patterns just like human beings. This understanding aids in the examination of a variety of people of varied ages. The proposed transfer learning model starts with 3 convolutional layers, adds a max-pooling layer and more convolutional layer. The segmentation algorithm receives the result of the transfer learning algorithm in the shape of a vector of volume $128 \times 16 \times 16$. Figure 3.5 shows the transfer learning architecture [113].

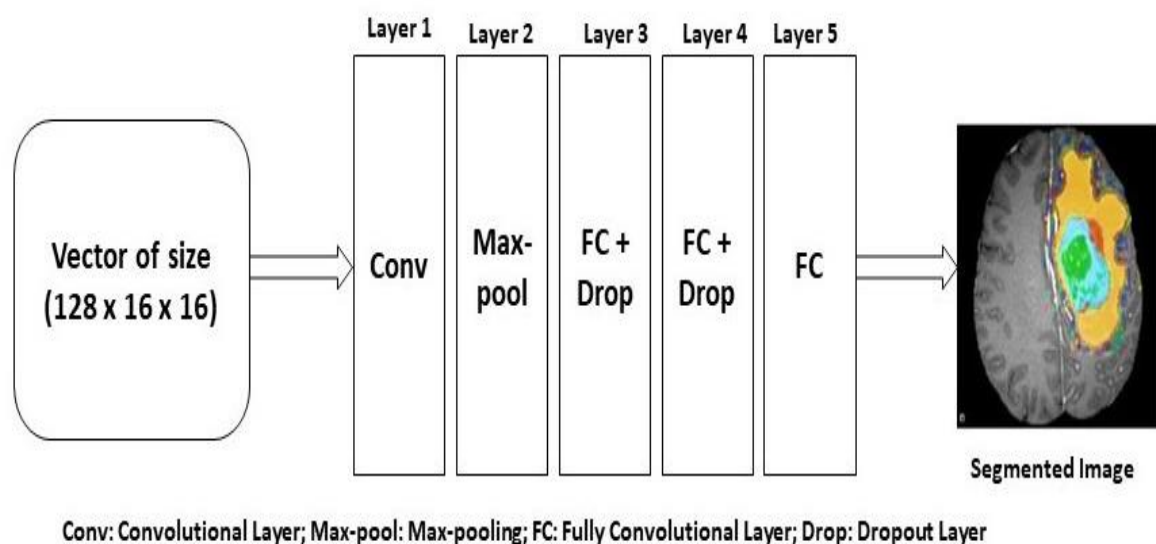


Figure 3.5 Transfer Learning Architecture

Algorithm 1 represents the T-Net algorithm, in which the transfer-learning algorithm is implemented. The image X of 512×512 size are input to this T-net and output is fetched as segmented images of size 240×240 . In this T-net, residual network is used with fine tuning. The images are converted into patches of size 33×33 , which is fed to the modified residual network. The dropout layer helps in removing the unwanted parameters and reduce the size requirement of model, hence making it less complex. These layers are passed through the fully convolutional layer to fetch the segmented output.

Algorithm 1: T-Net Algorithm

Input: X : 512×512

Output: Segmented Image, $X_s \rightarrow 240 \times 240$

Method:

Start

1. X is fed to bias field correction.
2. $X \rightarrow \text{resize}(240 \times 240) \rightarrow X'$
3. $X' \rightarrow$ Intensity Normalization and patch extraction $\rightarrow X_p$.
4. Size(X_p) : 33×33 image.
5. $X_r \rightarrow$ rotate (X_p).
6. Select Fsize ($5 \times 5 \times 3$), slide on X_r .
7. Convolve 3(Fsize) with X_p with $Dr=0.8 \rightarrow X_n$ (generated new image).
8. Max pooling $\rightarrow X_n$.
9. Convolve 2Fsize and image \rightarrow activation map X_a : $128 \times 16 \times 16$.
10. $X_a \rightarrow$ Convolutional layer with Relu $\rightarrow X_r$ (output after convolving).
11. $X_r \rightarrow$ max pooling X_{rp} .
12. $X_{rp} \rightarrow$ fully convolutional layers (with dropout =0.5).

End

X =input image, $X_s \rightarrow$ segmented image, $X_p \rightarrow$ extracted patch, $X_n \rightarrow$ generated new image, $X_a \rightarrow$ activation map, $X_r \rightarrow$ convolved output, $X_{rp} \rightarrow$ Max-pooling output, $Dr \rightarrow$ Dropout

3.2.2 Dense Hierarchical CNN (DH-CNN)

Low-level qualities make up the surface layers of CNN, whereas domain-specific quality makes up the internal layers, and the network's final segments are fine-tuned via shallow fine-tuning. The same attributes aren't required by CNN, but they have an impact on deep-tuned CNN's performance. The final layers are fine-tuned to improve the effectiveness of CNN in brain tumor segmentation. The intensity values in Magnetic Resonance Imaging have no set meaning, and earlier research has shown that these intensity values fluctuate greatly between patients and highly susceptible. Their sensitivity is to the acquiring condition. Normalization of inputs is required for CNN approaches; otherwise, the network is referred to as badly

conditioned. The functionality of CNN is divided into four important categories in this study. The image's pixel values are stored in the input layer. The convolutional layer uses the calculated scalar effect of the size of the input areas and loads the neurons to decide the output neurons in arrangement along with the input areas. The input is downsampled in a pooling layer, which reduces the number of parameters. The completely linked layer will create scores for the different types used in the segmentation process. Figure 3.6 shows the hierarchical clustering process [114].

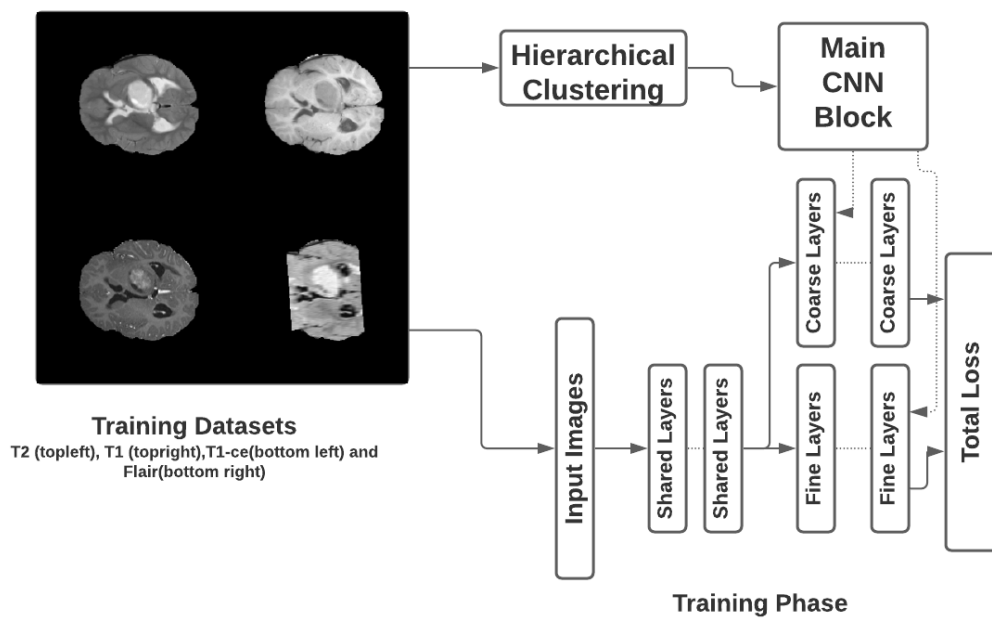
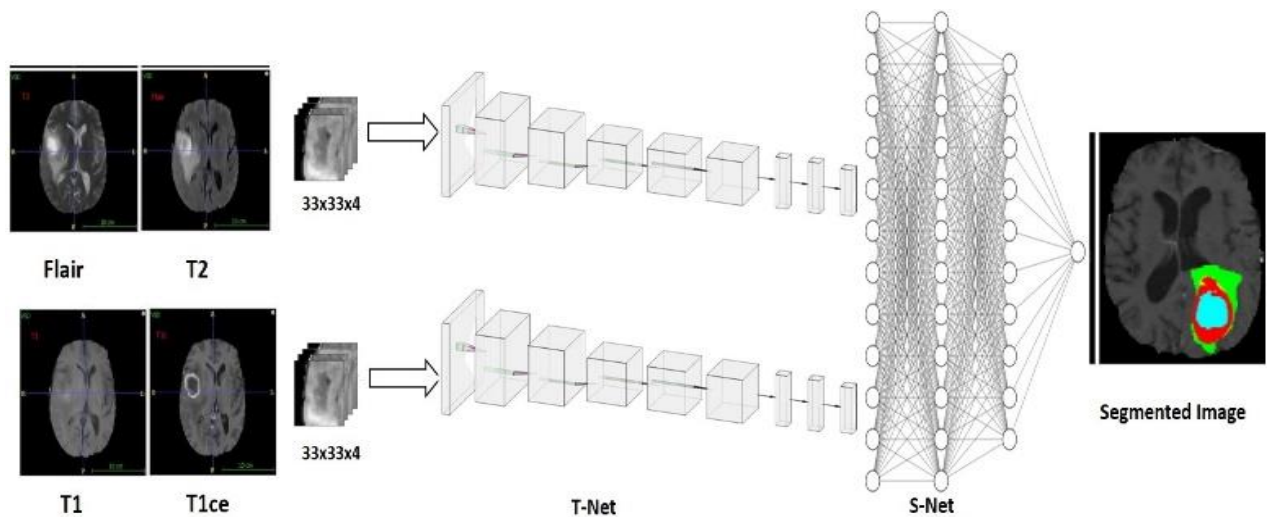


Figure 3.6 Hierarchical clustering process

A cascaded CNN architecture is utilized as a part of a hierarchical clustering technique to assess thick and delicate layers of the image while contemplating the pixel-wise possibility of the beginning loads for each pixel in an image. During the training phase, the CNN utilizes a pre-trained simulation in which a load of complexities is utilized to construct a hierarchy of elements for enhancing loads of training classification photos. Layer-by-layer classification is used to classify various MRI sequences such as T1, T1c, T2, and Fluid-attenuated inversion recovery (FLAIR). The convolution method for 33×36 layers is done in 2 stages: phase 1 and phase 2. Figure 3.7 shows the Hierarchical Dense CNN [115].



T-Net: Transfer Learning Model; S-Net: Segmentation Model

Figure 3.7 Hierarchical Dense CNN

The hierarchical CNN's non-dense architecture is presented in table 3.1, and to anticipate the development of dense design, a 6-layer CNN is used as label four in linear chain topology, with every subsequent layer having twenty-two new kernels.

Table 3.1 Hierarchical Dense CNN of Requirements

Phase	Layers	Features
Convolution	33×36	36
T-Net	$33 \times 108, 33 \times 96$ $33 \times 84, 33 \times 60$ 33×48	108
S-Net	$3^3 \times 180, 3^3 \times 168$ $3^3 \times 156, 3^3 \times 132$ $3^3 \times 144, 3^3 \times 120$	180

Algorithm 2 represents the hierarchical Dense CNN (HD-CNN) Algorithm. In this algorithm the output from the T-net is fed to the HDCNN. In this voxels are fetched, pre-processed and reshaped. Different voxels are pre-processed with reshaping and rescaling. The two stage model is trained as in the first stage represents the T-net in which five layers are present that extract 108 features. Then the output from T-net is passed through the stage 2 i.e HDCNN comprising of six layers where 180 features are extracted. In this all image modalities such as T1, T2, FLAIR and T1ce are used to extract the high grade gliomas and low grade gliomas.

Algorithm 2: Dense Hierarchical CNN Algorithm

Input: X_p -> size 33x 33 are fetched from the X image dataset.

Output: Segmented tumor image- 240 x 240.

Initialisation:

1. X_p -> Batch Normalization -> X_v
2. X_v -> `def vox_preprocess(vox): return np.reshape(vox, vox_shape).`
3. Segmentation loss = Ground truth image – truth image.
4. Reshape(X_v) and Rescale (X_v)
5. Train the dense hierarchical two stage model with the preprocessed images
 - `def train():`
 - Small patch of image x_i is fed to Convolution model of 33 * 36 layers : 36 features are fetched
 - Then the output is fed to the stage 1 comprising 5 layers extracting 108 features.
 - In next step it is fed to the stage 2 comprising 6 layers extraction 180 features
 - Return the segmented tumors.
6. Segmented tumor image of size 240 x 240 is the output from the proposed model.
7. Dice score coefficient's are calculated for the voxels trained with the two stage model.

End

3.2.3 Real Time Generative Adversarial Network (RT-GAN) Algorithm

This is certainly relevant for Convolutional Neural Networks (CNNs), which can learn rotationally invariant features only provided the training data has a significant number of instances at multiple rotations. The objective of this research is to demonstrate how a GAN may be used to recreate the underlying pattern of trained data to sample then augment the regular training data using additional synthetic data. GANs are a kind of neural network model that are trained to generate synthetic samples with the same properties as the distributions of the training set. In the case of images, this means learning to produce images visually comparable to a collection of authentic photographs (through a generator) and hence undetected by an adversary (the discriminator). The original formulation has been expanded to

address concerns such as retrain stability, low resolution, and the absence of a true image reliability gradient descent, and has been applied to image enhancement, sparse data reconstruction, and anomaly detection. Numerous ways for employing GANs to augment training datasets have been developed. The study used adversarial networks to improve the quality of simulated images that were then used for further training. To train a dependent GAN on unlabelled data to generate different versions of a given real image, and, they use a similar GAN to impose attitudes on neutral faces to enhance the representation of underrepresented groups. However, the use of non-conditional Generative algorithms to augment training sets as a pre-processing step without any of the incorporation of additional data has just recently been examined, with promising results in medical image classification challenges [116].

Algorithm 3: RT-GAN Algorithm

Input: MRI images and $k = 1$ as hyperparameter

Output: Generator Loss g and Discriminator Loss d

Start

Step1: Reshaping image $I \Rightarrow 512*512*512 \rightarrow 128*128*128$

Generator:

Step2: I fed to dense layer and leaky Relu and reshaped $\rightarrow \Gamma$ ($16*16*256$).

Step3: Γ is fed to 3 conv2d_transpose and leaky Relu $\rightarrow \Gamma'$ ($128*128*128$).

Step4: Γ' is fed to Conv_2d $\rightarrow I1$ ($128*128*3$).

Discriminator:

Step5: $I1$ is fed to 4 conv_2d and leaky Rely layers $\rightarrow I2$ ($16*16*64$)

Step6: $I2$ is fed to flatten layer $\rightarrow I2'$

Step7: $I2'$ is fed to dropout layer- $I3$

Step8: $I3'$ \rightarrow Final segmented output and compared with generator output.

End

Algorithm 3 represents the RT-GAN algorithm. This algorithm consists of generator and discriminator. The discriminator consists of several layer types such as conv2d, leaky ReLU, flatten, dropout, and dense. The generator consists of several layer types such as Dense, leaky ReLU, reshape Conv2DT, and Conv2D. The network is trained on minibatch stochastic gradient descent. The number of steps to apply to the discriminator, is denoted by k , is a hyperparameter. The proposed model uses $k=1$, the least expensive option, in our experiments to make it less complex. The training MRI images are fed to the generator, which helps in creating the sample input and the tumor masks are fed to the discriminator, where it is compared

to the generated segmented tumor masks. Then the discriminator decides the final segmented tumor image as the output. For training the GAN model, 100 epochs were performed and generator loss and discriminator loss was also fed as the output.

3.3 Implications of Research Problem

The methodology's initial goal is to improve the effectiveness of segmentation algorithms by combining qualitative indicators like Transfer Learning Algorithm, CNN, and GAN in conjunction with quantitative characteristics like to mean square error and peak signal to noise ratio. An enhanced transfer learning algorithm through factor tuning increases the efficiency and computational speed of the brain tumor separation procedure. This study is integrated through a prediction pattern; brain cancers can be diagnosed and treated earlier.

The current issue with brain MRI segmentation approaches is that have poor computational speed and efficiency, which must be addressed for real-time processing. There are focusing on qualitative measurements like accuracy, specificity, sensitivity, and precision while using quantitative factors like peak signal to noise ratio, mean square error, and entropy the efficiency of segmentation algorithms can be increased.

Immense research have been done to decrease class inequality by asymmetric loss functions have been utilized to provide weights for different voxel classes. A range of strategies is utilized to address the problem of class imbalance including selective sampling and adaptive augmentation. These approaches are unsuccessful for excessively unequal datasets. CNN is utilized to solve some of the current 3D (or 2D) image segmentation difficulties. If CNN-based analysis can offer realistic quantities of medical pictures, it might be very beneficial [116].

GAN are neural networks that can create artificial images that look quite like the originals. In GAN the generating and discriminating neural networks are both trained at the same time. GAN's have shown comparatively higher efficiency than the CNN models. This research is therefore included implementing RT-GAN for the brain tumor segmentation making it more efficient for the segmentation. Both DH-CNN and RT-GAN are tested with the help of statistical analysis. RT-GAN has been proved to be comparatively efficient than DH-CNN.

3.4 Summary

Image segmentation is an important and difficult research area around image processing. It has become a hive of activity in the field of picture interpretation. Therefore, 3D reconstruction and other technologies are being utilized to a lesser extent. Image segmentation methods are becoming faster and more accurate. An algorithm that can be used to the kind of image has been developed using new ideas and technology [117]. DH-CNN and RT-GAN are employed in the process of brain tumor segmentation. One of the most common techniques is to utilize a context-based CNN to improve semantic segmentation performance. However, collecting relevant context information from complex and dynamic images is a challenge for medical image segmentation. Transfer learning is used to train CNN and GAN in this study. Transfer learning shortens the learning curve for a new activity by transferring knowledge from similar activities that have previously been taught and learnt using this strategy to the new one [118]. Analyze the information obtained throughout the process of identifying people. This information is utilized to learn and recognize different types of persons at different ages [119]. This procedure is essentially a machine learning process that incorporates extra training data from one or other associated activities while keeping the basic training data in mind. The transfer learning approach improves the knowledge curvature by transmitting information from a trained CNN to a test model [120]. This section compares the traditional and proposed methodology to indicate the changes amongst the two. The proposed methodology discusses the three algorithms (T-net, DH-CNN and RT-GAN) incorporated in the research conducted on brain MRI images.

CHAPTER 4

DATASETS AND EXPERIMENTS

4.1. Overview

Brain tumor detection and diagnosis are hindered by the comparable features of tumor pixels and non-tumor pixels in the brain picture. This chapter discusses a strategy for detecting and segmenting tumor regions in the brain. The current research program's purpose is to produce an effective brain tumor segmentation technology for use in real-world scenarios. To get a greater classification rate, the reference picture is aligned concerning the source brain image using the linear image registration approach. Denoising the registered picture is accomplished using an adaptive median filter. The BRATS dataset (2018) is utilized in this chapter; it comprises 285 brain tumor MRI images that were acquired using four different MRI modalities: T1, T1c, T2, and Flair. The collection is mostly composed of MRI images of low-grade gliomas (LGG) and high-grade gliomas (HGG). MRI scans are utilized to evaluate the proposed brain tumor identification and segmentation system's performance.

4.2. Image processing benchmarks

Benchmarks for evaluating the performance of various learning algorithms on tasks have gained prominence in the field of machine learning. Benchmarking has also acquired prominence in the context of biomedical neuroimaging in recent years. These benchmarks, which are occasionally referred to as "challenges," all have one thing in common: They encourage users to improve their algorithms on a learning dataset provided by the administrators and then deploy them to a shared, impartial test dataset in an organized fashion. It contrasted with numerous literature analyses, inside which one group implements multiple ways to a dataset of their selection, preventing a reasonable analysis so this group may not be equally knowledgeable about every method and may invest more work to developing algorithms than others [121].

Once benchmarks are established, the test dataset typically becomes an emerging business standard for assessing possible improvements within the image analysis task under evaluation. The annotation and assessment processes may also stay consistent when additional

data is introduced (to avoid the danger of over-fitting this single dataset over time) or when relevant benchmarks are begun. Benchmarking requires a web-based application for automatically analyzing segmentations given by specific groups, as this ensures that the test set's labels are never made public. This virtually guarantees that any conclusions produced are not affected by unintentional approach overexertion and are thus representative of the product's classification results in practice. Recent community milestones in image fragmentation and interpretation in medicine include methods for arterial centreline extraction, arterial segmentation and restriction grading, liver segments, scar tissue detection in digital color fundus images, and trachea extraction from CT scans. Quite a few community-wide attempts have been exerted to apply different algorithms to image features a contemporary example is brain excavation ("masking"), even though the majority of the gradually revealed used to evaluate multiple segments and segmentation methods, such as STAPLE, were established used in brain imaging or, more precisely, brain tumor segmentation [121].

4.3. Set-Up of The BraTS Benchmark

The BraTS benchmark was held in connection with both the MICCAI 2012 and 2013 conventions as two remote challenge workshops. Users tend to discuss the challenges' setup, including the teams' participation, the picture data, the subjective annotation process, the validation processes, and the software services used to compare various algorithms.

The BraTS software resources are currently accepting contributions, encouraging different teams to gather testing data for use in creating segmentations that can be compared to all previous submissions. A centralized location for both benchmarks and the most recent BraTS-related activities [122].

4.4. Glioma grading using Machine learning

Glioma grading using machine and supervised learning may be performed using MR data. A popular machine learning pipeline entails morphological operations and ranking using a feature selection technique such as Classifier Feature Elimination, which achieves an accuracy of 95.5 percent in the best situation. They achieve the best results when the SVM features are selected. SVM is also often employed as an understandable classifier, and it produces excellent results, up to 94.8 percent on anatomical imaging.

When just anatomical sequences are given, feature extraction can be employed in a deep learning strategy to discriminate between binary grades. Convolutional neural networks, such as VGG-16, achieve an accuracy of up to 95%, whereas random forests achieve an accuracy of 88.77%. For instance, convolutional neural networks provide promising results for glioma grading but remain computationally intensive and intelligible.

And that's why picked a computational modeling classifier such as SVM since it gives more comprehensible results while requiring fewer computer resources [123]. GAN's have proven to be less complex and contains high computational power as compared to the CNN's. These networks attain high efficiency and accuracy.

4.5. Multimodality Feature Acquisition

Recent years have seen a surge in interest in multi-modal feature learning, view of the fact that multi-modal information can provide extra information for identifying the physical environment. Multi-modality provides skills that have been applied to a range of object tracking applications, including three-dimensional form recognition and retrieval, mortality prediction, RGB-D machine vision, and human re-identification. Although multi-modality assessment models have been used for a range of computer vision issues, it remains a relatively unexplored subfield of medical image interpretation, particularly when it comes to the difficulty of brain tumor segmentation. Towards this purpose, the research offers an early attempt to develop a system for brain tumor segmentation using cross-modality deep feature learning. The cross-modality feature transition (CMFT) and fusion (CMFF) processes suggested were unique in comparison to previous multi-modality feature learning approaches [124].

4.6. Experiments on the BraTS 2018 Benchmark

To test the performance of the proposed model, use the BraTS 2018 datasets. BraTS 2018 focuses on the segmentation of inherently heterogeneous (in appearance, form, and histology) brain tumors, mainly gliomas, using multi-institutional pre-operative MRI images. Furthermore, BraTS'18 focuses on the prediction of patient overall survival using integrative analyses of radiomic characteristics and machine learning techniques to define the clinical value of this segmentation job. The BraTS 2018 dataset comprises 285 training cases, with 210

high-grade gliomas (HGG) cases and 75 low-grade gliomas (LGG) cases, as well as 66 validation instances.

The BraTS dataset is made up of three patients' scans, with 155 scans for each image modality (T1, T2, T1ce, and Flair), as well as segmented tumour masks. T1 restoration, also known as spin-lattice relaxing, includes the transmission of radiation by "high-energy atomic nuclei" to the physical circumstances, which results in the restoration of longitudinal magnetization. T2 decay, also known as spin-spin relaxing, happens when nuclei send and receive radiation from neighbouring nuclei and communicate with one another, resulting in a reduction of transverse magnetization in the direction of SMF. Cerebrospinal fluid appears dark on T1 weighted imaging and brilliant on T2 weighted imaging, as well as by T2 tissue characteristics.

T1-weighted imaging shows CSF to be black, while T2-weighted imaging shows it to be bright. The Fluid Attenuated Inversion Recovery is a third regularly utilised sequence (Flair). The Flair sequence is comparable to a T2-weighted image, but the TE and TR periods are significantly longer. The anomalies remain visible, but the normal CSF fluid is dimmed and darkened. T1ce is created by injecting Gadolinium into the T1 weighted pictures, which modifies the signal intensities. T1ce pictures are beneficial for examining vascular architecture and blood-brain barrier breakdown [e.g., tumours, abscesses, lesions, inflammation].

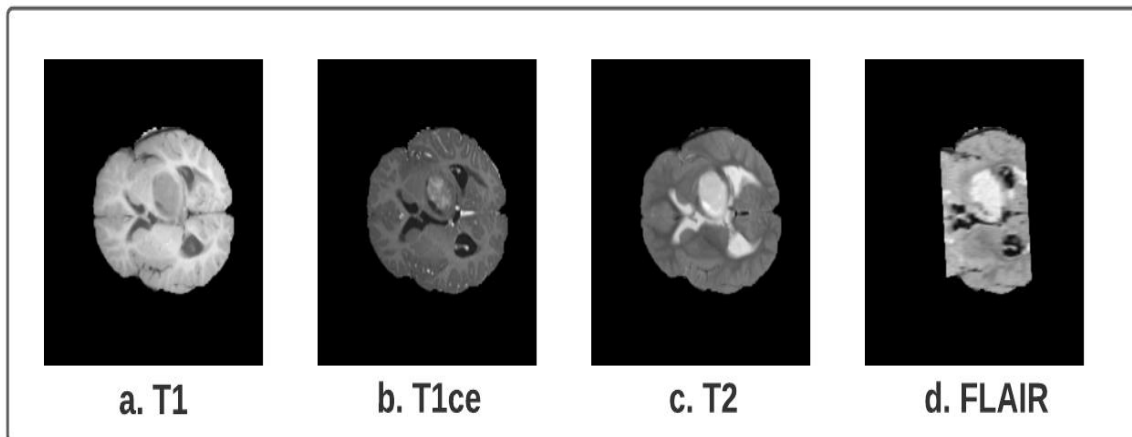


Fig 4.1 Sample from BraTS 2018 datasets (a. T1, b. T1ce, c. T2 and d. FLAIR)

Table 4.1 discusses the dataset description with its division into training, validation and testing sets. The dataset comprises of all the scans of imaging modalities from three patients. The dataset of single patient is divided into five sub dataset folders such as T1, T2, T1ce and Flair.

Each imaging modality comprises of 155 scans. The total number of scans for each patient is 620. The dataset division is performed as 60% of training set, 20 % of testing set and 20% of validation set. The fifth sub-group of dataset is tumored masks or the segmented tumor in ground truth images, which are used by discriminator of the model to perform segmentation tasks with more accuracy.

Table 4.1 Sample Dataset Description with Division into Training, Testing and Validation

Patient Id	Imaging Modality	No. of Scans	Total	Training Set	Validation Set	Testing Set
1.	T1	155	620	372	124	124
	T2	155				
	T1ce	155				
	FLAIR	155				
2.	T1	155	620	372	124	124
	T2	155				
	T1ce	155				
	FLAIR	155				
3.	T1	155	620	372	124	124
	T2	155				
	T1ce	155				
	FLAIR	155				

CHAPTER 5

RESULTS AND DISCUSSION

5.1. Overview

The previous chapters, which deals with research methods, tried to explain the Real time Segmentation of Medical Images. The proposed methodology explains the operation of the BraTS dataset for segmentation of Medical Images. An explanation of the evaluation measures and Qualitative and Quantitative results of the methodology used is shown below with the required tables and figures. The proposed methodology is proved to be comparatively efficient for brain tumor segmentation based on the statistical analysis performed using t-test.

5.2. Evaluation Measures of Brain Tumor Segmentation

In this proposed methodology, various cases have been involved. From the parameters value of datasets, prediction is made and find out the errors for the predicted errors. Numerous Classifier and methods demonstrate the Dice Score Coefficient (DSC), Structured Similarity Index (SSIM), and Mean Squared Error (MSE), Peak Signal to Noise Ratio (PSNR), of models in the below tables and figures.

- **Structured Similarity Index (SSIM)**

SSIM is used to compare the original and upgraded slices in terms of similarity.

$$SSIM(x, y) = \frac{(2\mu_x\mu_y + c_1)(2\sigma_{xy} + c_2)}{(\mu_x^2 + \mu_y^2 + c_1)(\sigma_x^2 + \sigma_y^2 + c_2)} \quad (5.1)$$

Where,

σ = variance

μ = mean and

c = contrast.

- **Dice Score Coefficient (DSC)**

When applied to Boolean data, it may be represented as true positive TP, and false-negative FN, false-positive FP.

$$DSC = \frac{2 TP}{TP + FP + FN} \quad (5.2)$$

- **Mean Squared Error (MSE)**

The MSE is used to determine the cumulative error between both the native and improved slices. MSE values with a lower value are employed to get superior tumor segmentation outcomes.

$$MSE = \frac{1}{mn} \sum_{i=0}^{i-1} \sum_{j=0}^{j-1} [f(x, y) - k(x, y)]^2 \quad (5.3)$$

The rows of the original and final pictures are denoted by (i, x) and the columns by (j, y). f (x, y) and k (x, y) represent the input and enhanced slices, respectively.

- **Peak Signal to Noise Ratio (PSNR)**

PSNR is a technical concept that describes the ratio of a signal's greatest achievable intensity to the ability to corrupt noise to impair the representation's quality. Due to the high dynamic range of many signals, PSNR is frequently stated as a logarithmic number in the decibels system. Noise has a negligible influence because of the high PSNR value.

$$PSNR = 10 \log_{10} \left(\frac{MAX_1^2}{MSE} \right) = 20 \log_{20} \left(\frac{MAX_1^2}{\sqrt{MSE}} \right) = 20 \log_{20}(MAX_1) - 10 \log_{10}(MSE) \quad (5.4)$$

MAX₁ denotes the highest pixel value in MR slices.

5.3. Results of Proposed Methodology

5.3.1 Results of T-Net Algorithm

The below table 5.1 summarizes numerous performance metrics generated while implementing T-Net algorithm from 155 picture datasets, including dice scores, similarity index, and signal to noise ratio. The images with the greatest performance in this dataset are presented in table 5.1.

Table 5.1 Tissue segmentation parameters and performance evaluation(T-Net)

Images	SSIM	PSNR	MSE	DSC
I1	0.8849	55.45 dB	1.857	0.820
I2	0.8990	67.91 dB	0.610	0.860

I3	0.9658	57.12 dB	4.900	0.815
I4	0.8086	59.61 dB	5.090	0.910
I5	0.8920	59.64 dB	1.310	0.780
I6	0.9455	56.25dB	3.620	0.820
I7	0.8090	59.59 dB	5.140	0.890

5.3.2 Results of DHCNN Algorithm:

The below table 5.2 summarizes numerous performance metrics generated while implementing DH-CNN from 150 picture datasets, including dice scores, similarity index, and signal to noise ratio. The images with the greatest performance in this dataset are presented in table 5.2. Image 3 and image 4 has attained higher dice score coefficient values. Structural Similarity index is high for image 6. Image two has attained lower mean square error.

Table 5.2 Tissue segmentation parameters and performance evaluation (DH-CNN)

Images	Structured Similarity Index (SSIM)	Peak Signal to Noise Ratio (PSNR)	Dice Score Coefficient (DSC)	Mean Square Error (MSE)
I1	0.8951	56.45dB	0.85	1.957
I2	0.900	68.91dB	0.87	0.65
I3	0.8168	58.21dB	0.92	5.9
I4	0.8266	60.34dB	0.92	6.01
I5	0.901	60.55dB	0.79	2.23
I6	0.9561	57.61dB	0.80	4.16
I7	0.822	60.60dB	0.91	5.42

The proposed system Dense Hierarchical CNN attained an increased dice score coefficient for necrotic and enhancing tumors when compared to other benchmark models as shown in table

5.3. Hence, the proposed algorithm is more efficient as compared to existing systems and the following objective is achieved.

Table 5.3 Analysis based on Benchmark Models

References	Edema	Necrotic Tumor	Enhancing Tumor
Pereira [125]	0.84	0.72	0.62
Kamnitas [126]	0.90	0.75	0.73
Zhao [127]	0.87	0.83	0.76
DHCNN	0.81	0.83	0.81

Attain the better dice score coefficient by assembling a transfer learning model with a hierarchical dense convolutional neural network for efficient brain tumor segmentation.

5.3.3 Results of RT-GAN Algorithm:

Figure 5.1 depicts a summary of discriminator GAN for several layer types such as conv2d, leaky ReLU, flatten, dropout, and dense, as well as the output forms of variation in param for each layer type.

```
Model: "sequential"
```

Layer (type)	Output Shape	Param #
conv2d (Conv2D)	(None, 128, 128, 64)	1792
leaky_re_lu (LeakyReLU)	(None, 128, 128, 64)	0
conv2d_1 (Conv2D)	(None, 64, 64, 64)	36928
leaky_re_lu_1 (LeakyReLU)	(None, 64, 64, 64)	0
conv2d_2 (Conv2D)	(None, 32, 32, 64)	36928
leaky_re_lu_2 (LeakyReLU)	(None, 32, 32, 64)	0
conv2d_3 (Conv2D)	(None, 16, 16, 64)	36928
leaky_re_lu_3 (LeakyReLU)	(None, 16, 16, 64)	0
flatten (Flatten)	(None, 16384)	0
dropout (Dropout)	(None, 16384)	0
dense (Dense)	(None, 1)	16385

Figure 5.1 Discriminator summary for Tumor segmentation

Figure 5.2 depicts a summary of generator GAN for several layer types such as Dense, leaky ReLU, reshape Conv2DT, and Conv2D, as well as the output shape of variation in param for each layer type.

Layer (type)	Output Shape	Param #
dense_1 (Dense)	(None, 65536)	6619136
leaky_re_lu_4 (LeakyReLU)	(None, 65536)	0
reshape (Reshape)	(None, 16, 16, 256)	0
conv2d_transpose (Conv2DTranspose)	(None, 32, 32, 128)	524416
leaky_re_lu_5 (LeakyReLU)	(None, 32, 32, 128)	0
conv2d_transpose_1 (Conv2DTranspose)	(None, 64, 64, 128)	262272
leaky_re_lu_6 (LeakyReLU)	(None, 64, 64, 128)	0
conv2d_transpose_2 (Conv2DTranspose)	(None, 128, 128, 128)	262272
leaky_re_lu_7 (LeakyReLU)	(None, 128, 128, 128)	0
conv2d_4 (Conv2D)	(None, 128, 128, 3)	18819

Figure 5.2 Generator GAN for several layers

Figure 5.3 depicts a combined summary for the GAN model, with a total parameter count of 7,815,876 as illustrated by this figure. The number of trainable parameters in this GAN model is 7,686,915; the number of non-trainable parameters is 128,961.

```

model_gan.summary()

Model: "sequential_2"

Layer (type)                Output Shape                Param #
-----
sequential_1 (Sequential)    (None, 128, 128, 3)        7686915

sequential (Sequential)      (None, 1)                   128961

=====
Total params: 7,815,876
Trainable params: 7,686,915
Non-trainable params: 128,961

```

Figure 5.3 Combined summary for the GAN model

Figure 5.4 shows the parameter performance for both the discriminator and the generator summary of the GAN model by representing the generator and discriminator loss at every scan of each epoch.

```

1, 1/13, d=0.697, g=0.694
1, 2/13, d=0.673, g=0.693
1, 3/13, d=0.654, g=0.692
1, 4/13, d=0.644, g=0.686
1, 5/13, d=0.611, g=0.670
1, 6/13, d=0.607, g=0.634
1, 7/13, d=0.630, g=0.570
1, 8/13, d=0.689, g=0.513
1, 9/13, d=0.781, g=0.482
1, 10/13, d=0.809, g=0.523
1, 11/13, d=0.766, g=0.707
1, 12/13, d=0.655, g=1.084
1, 13/13, d=0.609, g=1.288
2, 1/13, d=0.627, g=1.121
2, 2/13, d=0.676, g=0.900
2, 3/13, d=0.718, g=0.773
2, 4/13, d=0.677, g=0.722
2, 5/13, d=0.676, g=0.690
2, 6/13, d=0.605, g=0.675
2, 7/13, d=0.618, g=0.655
2, 8/13, d=0.577, g=0.634
2, 9/13, d=0.569, g=0.608

```

Figure 5.4 Parameter performance

Figure 5.5 shows the model Loss. The given figure represents the loss vs epochs graph and the loss decreases as the no. of epochs increases. Therefore, the testing is done for 100 epoch to decrease the loss to 0.012.

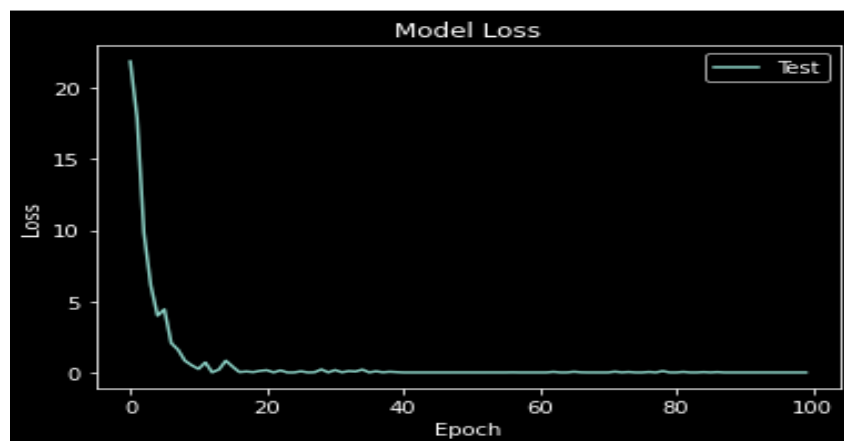


Figure 5.5 Model Loss

Figure 5.6 shows the 97% accuracy of the model. The given figure represents the accuracy vs epochs graphs, and the accuracy increases as the no. of epochs increases. The test accuracy has been increased when the model is tested to 100 epochs.

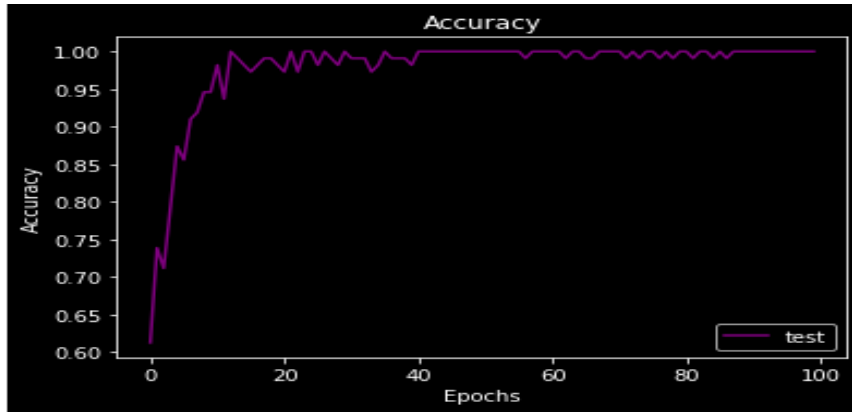


Figure 5.6 Accuracy

Figure 5.7 shows the non-tumor picture. This figure represents the sample output obtained after implementing proposed RT-GAN algorithm, demonstrates and gives 100% confidence that it is not a tumor.

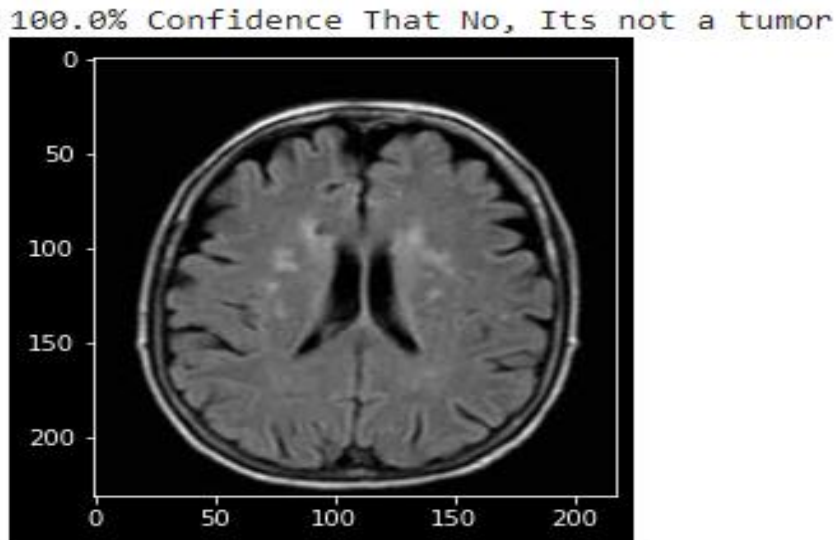


Figure 5.7 Non-Tumor picture

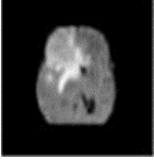
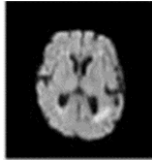
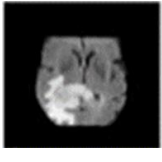
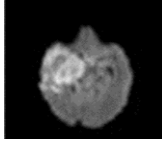
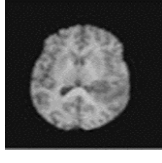
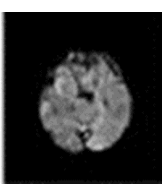
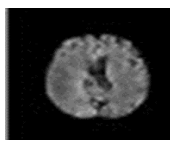
Figure 5.8 shows the actual tumor picture analyzed by the RT-GAN model. RT-GAN model represents the segmented tumor mask along with the complete brain MRI image. The extracted tumor masks attain high precision, which is denoted in the figure.

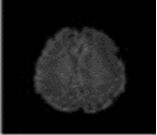
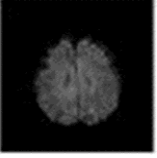


Figure 5.8 Tumor Picture

This section shows the quantitative results using the GAN algorithm. In table 5.4 image 1, the Structured Similarity Index (SSIM) value is 0.9021, Peak Signal to Noise Ratio (PSNR) value is 57.30dB and Dice Score Coefficient (DSC) value is 0.87. Image 2 shows that the Structured Similarity Index (SSIM) value is 0.90110, Peak Signal to Noise Ratio (PSNR) value is 69.01 dB, and Dice Score Coefficient (DSC) value is 0.88. Image 3 shows that the Structured Similarity Index (SSIM) value is 0.8251, Peak Signal to Noise Ratio (PSNR) value is 59.32 dB, and Dice Score Coefficient (DSC) value is 0.93. Image 4 shows the Structured Similarity Index (SSIM) value is 0.8761, Peak Signal to Noise Ratio (PSNR) value is 61.21 dB, and Dice Score Coefficient (DSC) value is 0.93. Image 5 shows the Structured Similarity Index (SSIM) value is 0.9121, Peak Signal to Noise Ratio (PSNR) value is 61.65dB, and Dice Score Coefficient (DSC) value is 0.80. Image 6 shows the Structured Similarity Index (SSIM) value is 0.9561, Peak Signal to Noise Ratio (PSNR) value is 60.23dB, and Dice Score Coefficient (DSC) value is 0.94. Image 7 shows the Structured Similarity Index (SSIM) value is 0.9231, Peak Signal to Noise Ratio (PSNR) value is 62.16dB, and Dice Score Coefficient (DSC) value is 0.90.

Table 5.4 Results using RT-GAN algorithm

Images	Image number	Structured Similarity Index (SSIM)	Peak Signal to Noise Ratio (PSNR)	Dice Score Coefficient (DSC)
	I1	0.9021	57.30dB	0.87
	I2	0.9110	69.01dB	0.88
	I3	0.8251	59.32dB	0.93
	I4	0.8761	61.21dB	0.93
	I5	0.9121	61.65dB	0.80
	I6	0.8366	60.23dB	0.94
	I7	0.9231	62.16dB	0.90
	I8	0.9081	58.52dB	0.89

	I9	0.8845	62.47dB	0.91
	I10	0.9125	68.97dB	0.89

5.4 Qualitative Results

The photos in Figure 5.9 illustrate the disparity between automated segmentation and real ground values. The images represented shows the quality of segmented images for whole tumor, core tumor and active tumor. The core tumor is represented with yellow color, the active tumor is represented with red color and whole tumor is represented by greean color. It discusses the comparison between the actual ground truth and automated segmentation.

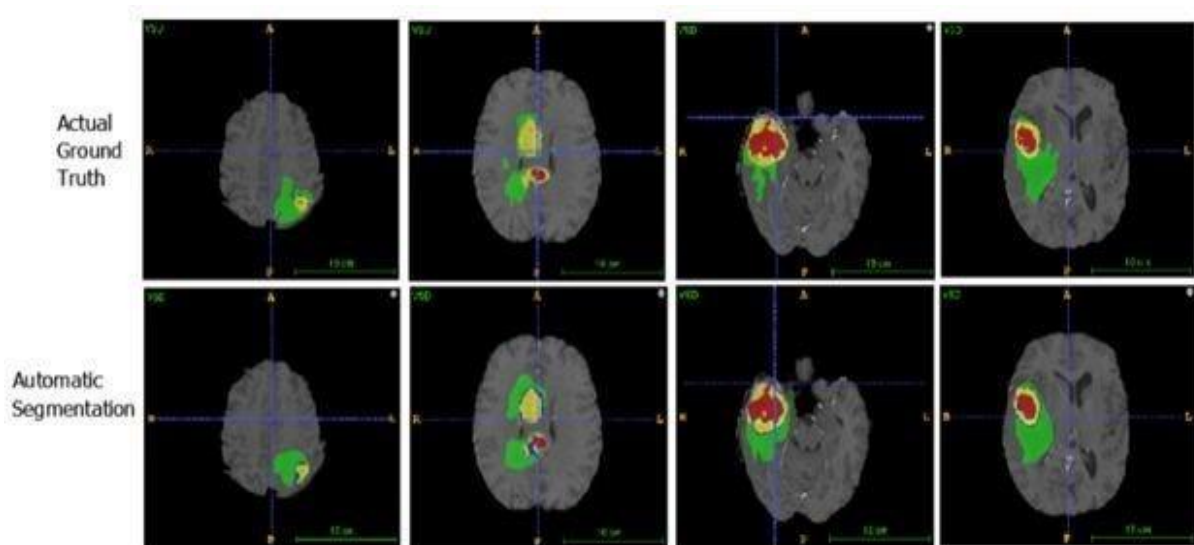


Figure 5.9 Ground Truth vs Automated Segmentation

As illustrated in the photos, the suggested framework for patients properly identifies the position, shape, and size. Figure 5.10 demonstrates the Axial Plane view for T1ce, Pred, and GT. The images represented shows the quality of segmented images for whole tumor, core tumor and active tumor. The core tumor is represented with yellow color, the active tumor is represented with red color and whole tumor is represented by greean color. It discusses the comparison between the actual ground truth and automated segmentation.

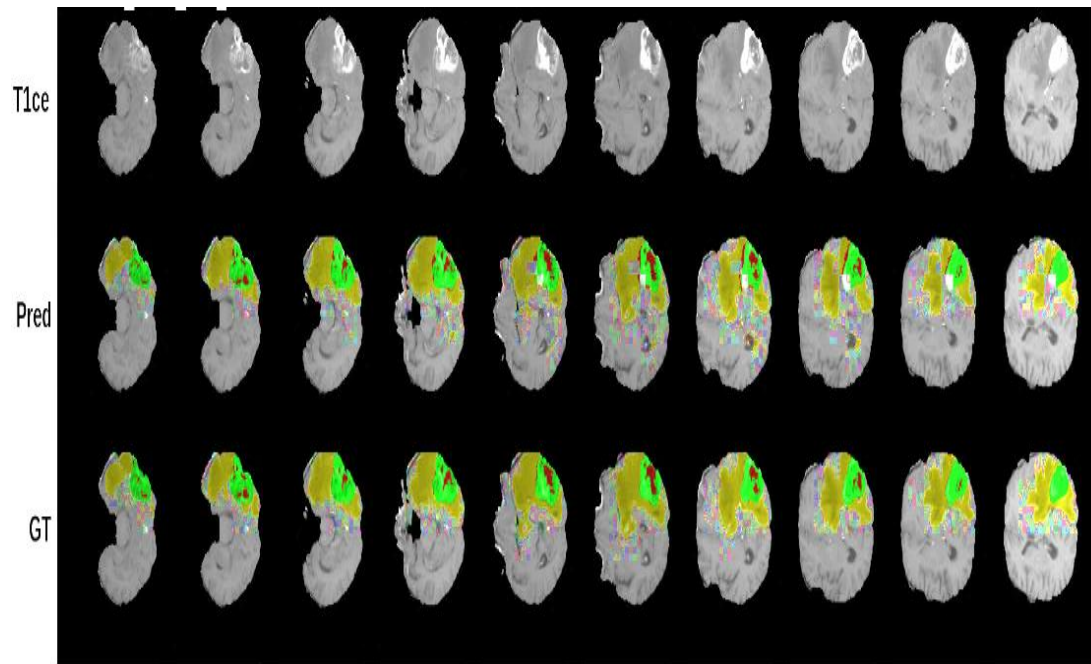


Figure 5.10 Axial Plane View

Figure 5.11 shows the Sagittal Plane View for T1ce, Pred, and GT. The images represented shows the quality of segmented images for whole tumor, core tumor and active tumor. The core tumor is represented with yellow color, the active tumor is represented with red color and whole tumor is represented by green color. It discusses the comparison between the actual ground truth and automated segmentation.

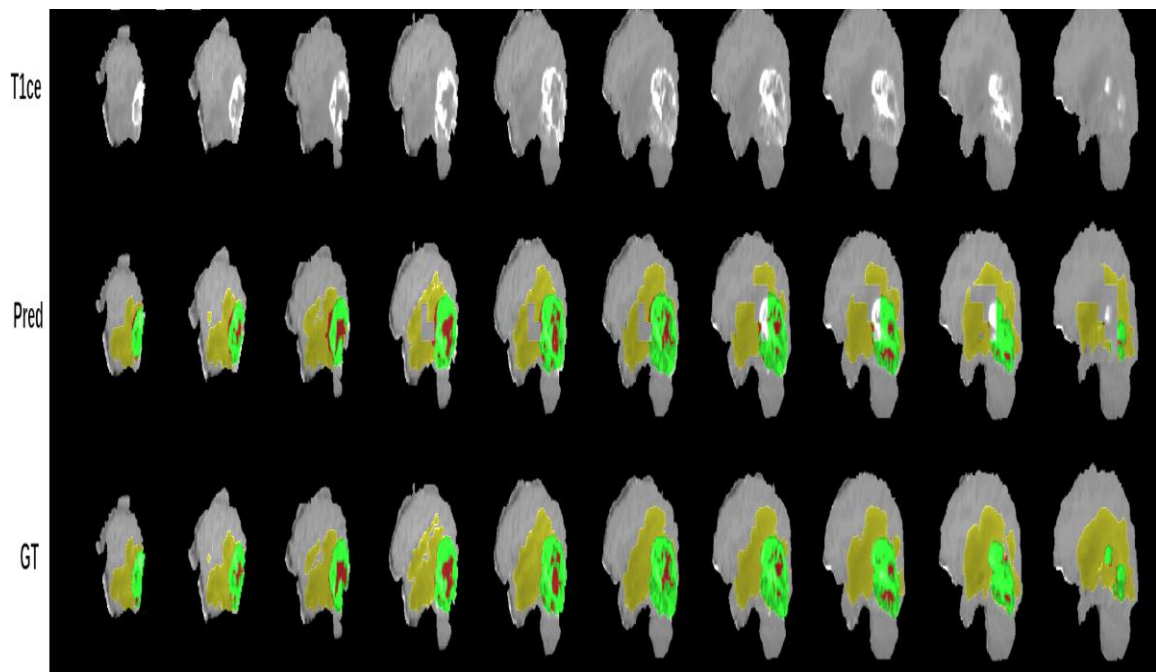


Figure 5.11 Sagittal Plane View

Figure 5.12 shows the Coronal Plane View also shows the Ground truth, Prediction, and T1ce. The images represented shows the quality of segmented images for whole tumor, core tumor and active tumor. The core tumor is represented with yellow color, the active tumor is represented with red color and whole tumor is represented by green color. It discusses the comparison between the actual ground truth and automated segmentation.

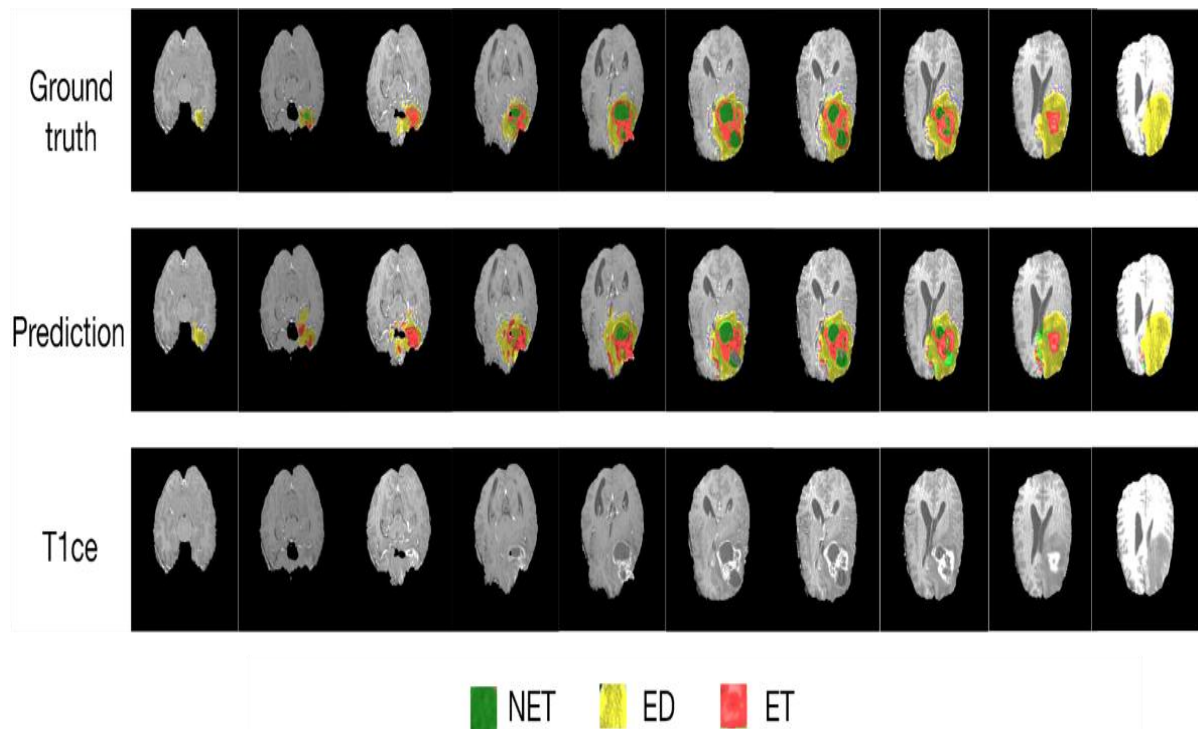


Figure 5.12 Coronal Plane View

5.5 Comparative Analysis

In figure 5.13, the performance of numerous benchmark designs is compared to that of the proposed hybrid model based on the dice score coefficients obtained for segmenting whole tumors. The whole tumors (WT), the core tumor (CT), and the activity tumor (AT) were created using the sub region forecasts.

Figure 5.13 depicts the dice score for the whole tumor evaluated by benchmark models. The dice score value of DH-CNN is less in comparison to benchmark models proposed by Zhao, Kamnitsas and Periera. Therefore there was a need for switching to RT-GAN.

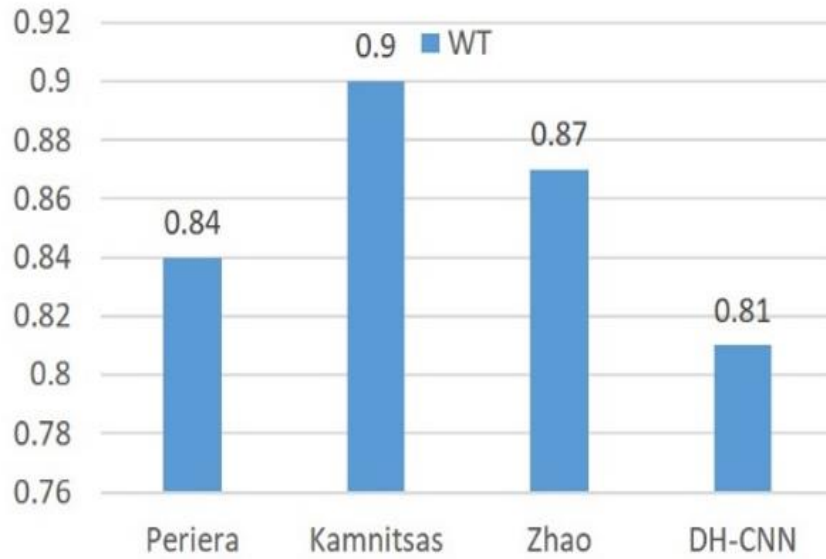


Figure 5.13 Performance of Whole Tumor

Figure 5.3 presents the core tumor segmented from brain MRI images. In the figure below, it is represented that for core tumor, DH-CNN has represented good DSC that are similar to Zhao and comparatively better than Periera and Kamnitsas.

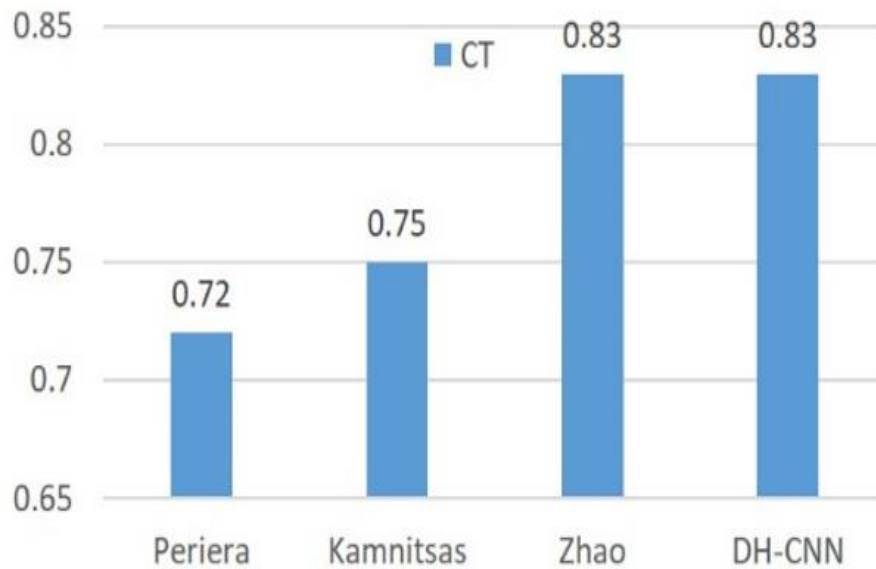


Figure 5.14 Performance of Core Tumor

The dice score for active or enhancing tumor of DH- CNN is comparatively efficient than another benchmark models proposed by Periera, Kamnitsas, and Zhao demonstrates in figure 5.15.

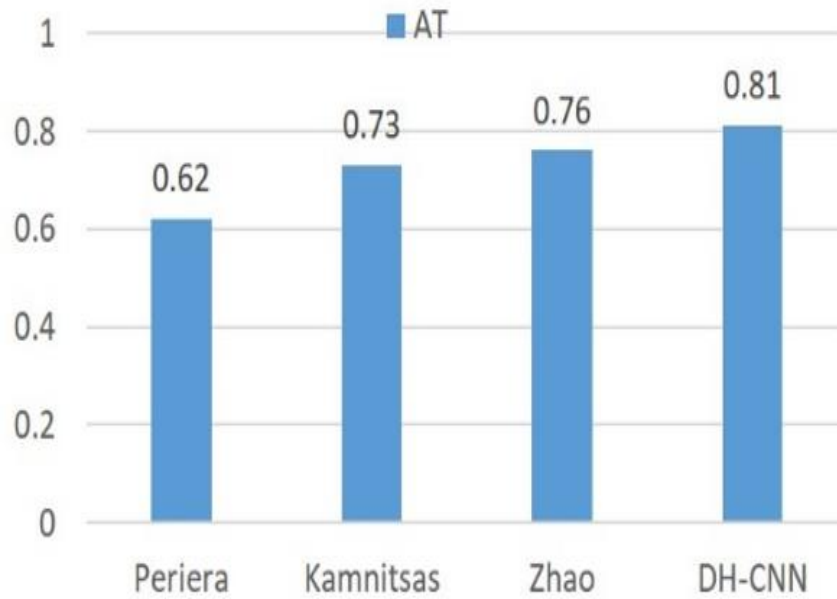


Figure 5.15 Performance of Active Tumor

As seen in figure 5.16, DHCNN when compared to non-dense and non-hierarchical architecture represents a more efficient model for all three categories (whole tumor, active tumor and core tumor). This study adds multi-scale relevant information into the model by making many predictions at various network levels, resulting in a more efficient model. This strategy results in an extremely efficient dice score.

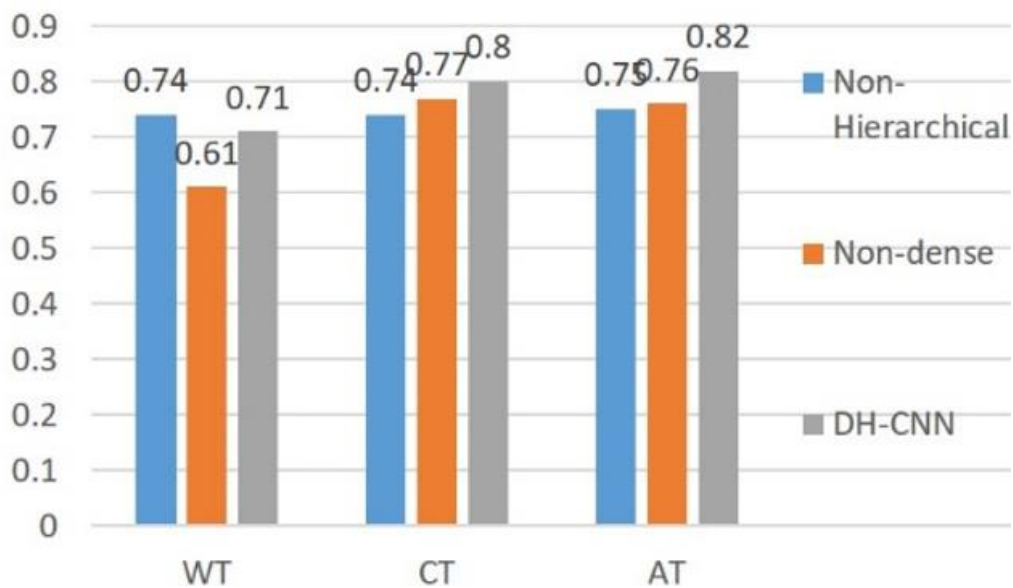


Figure 5.16 Various Network Performance

Table 5.5 shows the comparison table for Structured Similarity Index, Peak Signal to Noise Ratio (PSNR), and Dice Score Coefficient (DSC) based on CNN and GAN algorithm.

Table 5.5 Comparison included with RT-GAN algorithm

Images	Structured Similarity Index (SSIM)		Peak Signal to Noise Ratio (PSNR)		Dice Score Coefficient (DSC)	
	CNN	GAN	CNN	GAN	CNN	GAN
Image1	0.8951	0.9021	56.45dB	57.30dB	0.85	0.87
Image2	0.900	0.9110	68.91dB	69.01dB	0.87	0.88
Image3	0.8168	0.8251	58.21dB	59.32dB	0.92	0.93
Image4	0.8266	0.8761	60.34dB	61.21dB	0.92	0.93
Image5	0.901	0.9121	60.55dB	61.65dB	0.79	0.80
Image6	0.9561	0.8366	57.61dB	60.23dB	0.80	0.94
Image7	0.822	0.9231	60.60dB	62.16dB	0.91	0.90

The average dice score coefficient for CNN is 0.8657, whereas the average dice score coefficient for RT-GAN is 0.8928. This indicates that using a RT-GAN algorithm segments the brain tumor tissues more effectively and efficiently. The RT-GAN model gives an accuracy of 97% and decreases the model loss with respect to the increasing number of epochs.

5.6 Statistical Analysis on Proposed Model

The statistical analysis is performed to verify that the proposed model is comparatively efficient from previously researched models. The T-test has been selected based on the output data such as dice score coefficient, structural similarity index, and peak signal to noise ratio received from the proposed dense hierarchical convolutional neural network and real-time generative adversarial network. In this research work, a T-test was performed for three different parameters to prove the high efficiency of the proposed RT-GAN model.

Table 5.6 represents the difference between the two proposed models on the basis of the T-test performed on the dice score coefficient. This table represents that the standard deviation of discrepancy is better for RT-GAN. The confidence interval when compared is higher for the RT-GAN model. The actual mean is also greater for RT-GAN.

Table 5.6 T-Test on DSC for two proposed models

	DH-CNN	RT-GAN
Actual mean	0.8660	0.8940
Number of values	150	150
t, df	t=208.7, df=149	t=285.2, df=149
P value (two tailed)	<0.0001	<0.0001
Significant (alpha=0.05)?	Yes	Yes
Discrepancy	0.8660	0.8940
SD of discrepancy	0.05082	0.03839
SEM of discrepancy	0.004149	0.003135
95% confidence interval	0.8578 to 0.8742	0.8878 to 0.9002
R squared (partial eta squared)	0.9966	0.9982

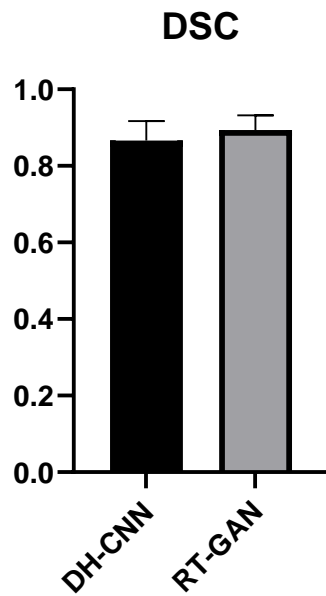


Figure 5.17 T-Test on DSC for two proposed models

Table 5.7 represents the difference between the two proposed models on the basis of T-test performed on structural similarity index. This table represents that standard deviation of discrepancy is better for RT-GAN. The confidence interval when compared is higher for RT-GAN model. The actual mean is also greater for RT-GAN.

Table 5.7 T-Test on SSIM for two proposed models

	DH-CNN	RT-GAN
Actual mean	0.8797	0.8891
Number of values	150	150
t, df	t=207.9, df=149	t=338.4, df=149
P value (two tailed)	<0.0001	<0.0001
Significant (alpha=0.05)?	Yes	Yes
Discrepancy	0.8797	0.8891
SD of discrepancy	0.05181	0.03218
SEM of discrepancy	0.004230	0.002627
95% confidence interval	0.8713 to 0.8880	0.8839 to 0.8943
R squared (partial eta squared)	0.9966	0.9987

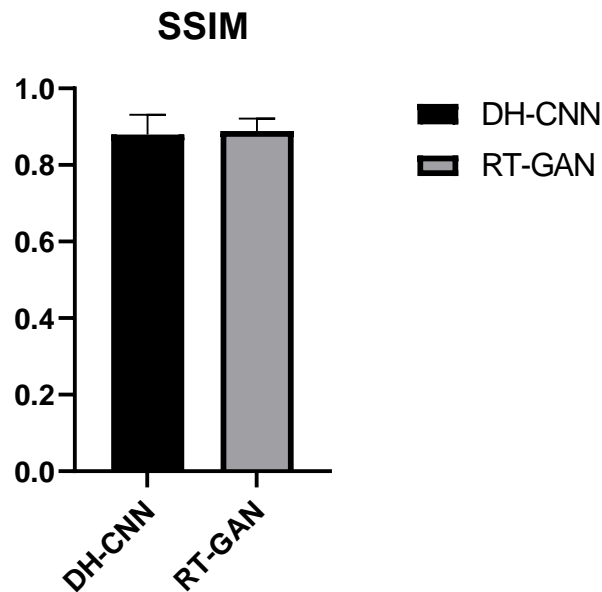


Figure 5.18 T-Test on SSIM for two proposed models

Table 5.8 represents the difference between the two proposed models on the basis of t-test performed on peak signal to noise ratio. This table represents that standard deviation of discrepancy is better for RT-GAN. The confidence interval when compared is higher for RT-GAN model. The actual mean is also greater for RT-GAN.

Table 5.8 T-Test on PSNR for two proposed models

	DH-CNN	RT-GAN
Actual mean	60.40	61.56
Number of values	150	150
t, df	t=192.2, df=149	t=218.3, df=149
P value (two tailed)	<0.0001	<0.0001
Significant (alpha=0.05)?	Yes	Yes
Discrepancy	60.40	61.56
SD of discrepancy	3.849	3.455
SEM of discrepancy	0.3142	0.2821

95% confidence interval	59.78 to 61.02	61.00 to 62.12
R squared (partial eta squared)	0.9960	0.9969

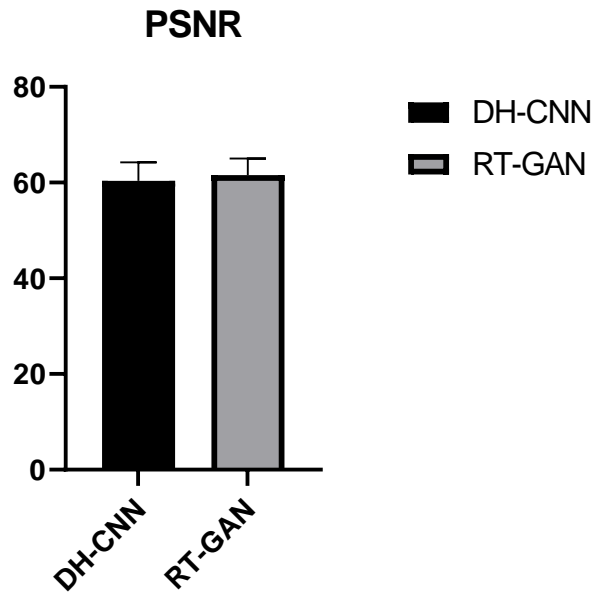


Figure 5.19 T-Test on PSNR for two proposed models

These statistical T-tests conducted on dice score coefficient, structural similarity, and peak signal to noise ratio fetched from both DH-CNN and RT-GAN. The conducted T-test not only extract the t values but also fetch the actual mean, standard deviation and confidence interval values. On analyzing these values separately for three datasets, it has been observed that RT-GAN perform comparatively efficient than DH-CNN. Based on the T-tests performed on dense hierarchical CNN and real time GAN it is observed that RT-GAN model has high efficiency for automated brain tumor segmentation and is attaining good results when compared to the other model.

CHAPTER 6

CONCLUSION AND FUTURE SCOPE

6.1. Overview

This chapter concludes the thesis and summarizes the investigation on “REAL TIME SEGMENTATION OF MEDICAL IMAGES”. It highlights the main outcomes of this thesis along with suggestions for future research directions and ends with the final remarks.

6.2. Conclusion

In brain tumor segmentation, it is necessary to segment the tumorous region and classify it from healthy regions so that it can be clinically utilized. The efficiency of algorithms segmenting brain tumors from magnetic resonance images (MRI) is predicted from the dice score coefficients. A high value of the dice score coefficient represents efficient and accurate brain tumor segmentation from MRI images. This research focuses on providing a more efficient algorithm for brain tumor segmentation that works in real-time scenarios. Following conclusions can be made while conducting the research:

A hierarchical structure dense Convolutional and RT-GAN for brain tumor segmentation is proposed based on MRI data. Pre-processing steps include non-uniformity correction and intensity normalization as part of the strategy being advocated. To train the CNN model, a small dataset and many parameters necessitated an increase in training data patches. The patch is extracted and applied to the Hierarchical Dense CNN after pre-processing. The multilevel dense Classification method is consisting of multiple steps: the transferable learning technique (T-net) and the segmented algorithms S net. Whenever metastatic tumor tissues were segmented, adding a dropout rates level to both the T and S nets enhanced the dice score coefficient. To enable the creation of more complex architectures, the CNN was modeled using discrete 3×3 kernels. Using deep neural networks reduces the alteration in segmentation. A steadier valuation of the tumor volume can be made, yielding a better understanding of tumor evolution.

The methodology's primary goal was to improve segmentation techniques' effectiveness by combining measures including such dice score factor with quantitative characteristics which include MSE as well as peaks signal-to-noise ratio.

Results are obtained by comparing the performance of the recommended methodology with that of other current methods. As compared to the general tumor, the value of active tumor is 0.81 and the value of central tumor is 0.83, the recommended approach was judged to be superior to other methods with a dice score of 0.81.

The obtained findings support the Generative Adversarial Network approach. In terms of structural similarity index SSIM, RT-GAN outperforms DH-CNN as DH-CNN has a value of 0.8951 whereas RT-GAN has a value of 0.9021. The average dice score coefficient for DH-CNN is 0.8657, whereas the average dice score coefficient for RT-GAN is 0.8928. The average peak signal to noise ratio for DH-CNN is 60.38db, whereas the peak signal to noise ratio for RT-GAN is 62.084db. The average mean square error for DH-CNN is 3.761, whereas the average mean square error for RT-GAN is 2.431.

Increasing the efficiency of segmentation algorithms is crucial to keep death rates at a minimum. The segmentation of brain tumors will be faster and more efficient in the future when it comes to an upgraded deep learning approach with parameter adjustment. Brain malignancies can be recognized and treated more quickly if this study is included in a predictive model. Also used RT-GAN algorithm ineffective way to calculate the value of Structured Similarity Index Measure (SSIM), Peak Signal to Noise Ratio (PSNR), and Dice Score Coefficient (DSC) value.

The research is concluded with the help of statistical T- tests performed on both DH-CNN and RT-GAN. The t-tests were performed on data obtained on parameters as DSC, PSNR, and SSIM. The attributes calculated during statistical analysis included the t score, actual mean, standard deviation, and confidence interval. These analyses has also proven that RT-GAN has performed comparatively efficient for brain tumor segmentation conducted for brain MRI images.

6.3. Future Scope

Additional research in the future may be conducted to increase the reliability, precision, and computing speed of segmentation algorithms while decreasing the amount of user input. Accuracy and precision for real-time brain tumor segmentation algorithms may be enhanced by adding past knowledge via implemented RT-GAN and comparing them to DHCNN. Multiscale analysis and parallelizable techniques such as deep learning are interesting options for enhancing computer efficiency. The efficiency of computation will be critical in real-time application domains.

As part of future research, the work intends to integrate the previously established CNN architecture for brain tumor classification with the recently presented RT-GAN design for brain tumor segmentation to accurately segment and localize tumors in real-time during brain surgery. A real-time adaptation of these tiny structures is achievable. Tests on additional medical picture databases and other topics are planned. Future updates will add more photos and suitable segmentation masks to the dataset, improving the shortcomings. Aside from the RT-GAN technique, also examine employing additional classifiers for future work, such as conditional GAN's and conditional random forest.

The future scope of this research indicates that various GAN-based models such as increasing the convolutional layers or instead of leaky Relu using Relu can be implemented for the same datasets. More models of GAN can be merged with transfer learning and then fetch the results obtained from the new model. GAN models with transfer learning approach is an unexplored area, which can be researched upon for real time segmentation of medical images. The researched model if on implementation attain a high accuracy can be integrated with the prediction model so that the diagnosis and detection of disease can be done at an earlier stage. This will help in reducing the mortality rate occurring because of tumors.

References

- [1]. Parascandolo, Patrizia, Lorenzo Cesario, Loris Vosilla, Marios Pitikakis, and Gianni Viano. "Smart brush: a real time segmentation tool for 3D medical images." In *2013 8th International Symposium on Image and Signal Processing and Analysis (ISPA)*, pp. 689-694. IEEE, 2013.
- [2]. Taha, Abdel Aziz, and Allan Hanbury. "Metrics for evaluating 3D medical image segmentation: analysis, selection, and tool." *BMC medical imaging* 15, no. 1 (2015): 1-28.
- [3]. Isa, Iza Sazanita, Siti Noraini Sulaiman, Muzaimi Mustapha, and Noor Khairiah A. Karim. "Automatic contrast enhancement of brain MR images using Average Intensity Replacement based on Adaptive Histogram Equalization (AIR-AHE)." *Biocybernetics and Biomedical Engineering* 37, no. 1 (2017): 24-34.
- [4]. Serag, Ahmed, Alastair G. Wilkinson, Emma J. Telford, Rozalia Pataky, Sarah A. Sparrow, Devasuda Anblagan, Gillian Macnaught, Scott I. Semple, and James P. Boardman. "SEGMA: an automatic segmentation approach for human brain MRI using sliding window and random forests." *Frontiers in neuroinformatics* 11 (2017): 2.
- [5]. Huang, Gao, Guang-Bin Huang, Shiji Song, and Keyou You. "Trends in extreme learning machines: A review." *Neural Networks* 61 (2015): 32-48.
- [6]. Menze, Bjoern H., Andras Jakab, Stefan Bauer, Jayashree Kalpathy-Cramer, Keyvan Farahani, Justin Kirby, Yuliya Burren, et al. "The multimodal brain tumor image segmentation benchmark BraTS." *IEEE transactions on medical imaging* 34, no. 10 (2014): 1993-2024.
- [7]. Demirhan, Ayşe, Mustafa Törü, and Inan Güler. "Segmentation of tumor and edema along with healthy tissues of brain using wavelets and neural networks." *IEEE Journal of biomedical and health informatics* 19, no. 4 (2014): 1451-1458.
- [8]. Havaei, M., A. Davy, D. Warde-Farley, A. Biard, A. Courville, Y. Bengio, C. Pal, P. M. Jodoin, and H. Larochelle. "Brain tumor segmentation with Deep Neural Networks. Medical Image Analysis." (2017): 18-31.
- [9]. Yasmin, Mussarat, Muhammad Sharif, and Sajjad Mohsin. "Neural networks in medical imaging applications: A survey." *World Applied Sciences Journal* 22, no. 1 (2013): 85-96.

- [10]. Pham, Dzung L., and Jerry L. Prince. "Adaptive fuzzy segmentation of magnetic resonance images." *IEEE transactions on medical imaging* 18, no. 9 (1999): 737-752.
- [11]. Prajapati, Dhruvi G., and Kinjal R. Sheth. "Super-Resolution Technique for MRI Images Using Artificial Neural Network." *International Journal on Recent and Innovation Trends in Computing and Communication* 5, no. 4 (2017): 55-58.
- [12]. Zhao, Juntong, Zhaopeng Meng, Leyi Wei, Changming Sun, Quan Zou, and Ran Su. "Supervised brain tumor segmentation based on gradient and context-sensitive features." *Frontiers in neuroscience* 13 (2019): 144.
- [13]. Zhao, Juntong, Zhaopeng Meng, Leyi Wei, Changming Sun, Quan Zou, and Ran Su. "Supervised brain tumor segmentation based on gradient and context-sensitive features." *Frontiers in neuroscience* 13 (2019): 144
- [14]. Kong, Youyong, Yue Deng, and Qionghai Dai. "Discriminative clustering and feature selection for brain MRI segmentation." *IEEE Signal Processing Letters* 22, no. 5 (2014): 573-577.
- [15]. Saudagar, Abdul Khader Jilani. "Minimize the percentage of noise in biomedical images using neural networks." *The Scientific World Journal* 2014 (2014).
- [16]. Mehdy, M. M., P. Y. Ng, E. F. Shair, N. I. Saleh, and Chandima Gomes. "Artificial neural networks in image processing for early detection of breast cancer." *Computational and mathematical methods in medicine* 2017 (2017).
- [17]. Noh, Hyeonwoo, Seunghoon Hong, and Bohyung Han. "Learning deconvolution network for semantic segmentation." In *Proceedings of the IEEE international conference on computer vision*, pp. 1520-1528. 2015.
- [18]. Arel, Itamar, Derek C. Rose, and Thomas P. Karnowski. "Deep machine learning-a new frontier in artificial intelligence research [research frontier]." *IEEE computational intelligence magazine* 5, no. 4 (2010): 13-18.
- [19]. Demirhan, Ayşe, Mustafa Törü, and Inan Güler. "Segmentation of tumor and edema along with healthy tissues of brain using wavelets and neural networks." *IEEE Journal of biomedical and health informatics* 19, no. 4 (2014): 1451-1458.
- [20]. Benson, C. C., and V. L. Lajish. "Morphology based enhancement and skull stripping of MRI brain images." In *2014 International Conference on intelligent computing applications*, pp. 254-257. IEEE, 2014.

- [21]. Benson, C. C., and V. L. Lajish. "Morphology based enhancement and skull stripping of MRI brain images." In *2014 International Conference on intelligent computing applications*, pp. 254-257. IEEE, 2014
- [22]. Schmidhuber, Jürgen. "Deep learning in neural networks: An overview." *Neural networks* 61 (2015): 85-117.
- [23]. Angulakshmi, M., and G. G. Lakshmi Priya. "Automated brain tumor segmentation techniques—a review." *International Journal of Imaging Systems and Technology* 27, no. 1 (2017): 66-77.
- [24]. Nachimuthu, Deepa Subramaniam, and Arunadevi Baladhandapani. "Multidimensional texture characterization: on analysis for brain tumor tissues using MRS and MRI." *Journal of digital imaging* 27, no. 4 (2014): 496-506.
- [25]. Bowman, F. DuBois. "Brain imaging analysis." *Annual review of statistics and its application* 1 (2014): 61-85.
- [26]. A. Lenartowicz, R.A. Poldrack, in *Encyclopedia of Behavioral Neuroscience*, 2010
- [27]. Yassin, Nisreen IR, Shaimaa Omran, Enas MF El Houbby, and Hemat Allam. "Machine learning techniques for breast cancer computer-aided diagnosis using different image modalities: A systematic review." *Computer methods and programs in biomedicine* 156 (2018): 25-45.
- [28]. Wu, Liao, Anjali Jaiprakash, Ajay K. Pandey, Davide Fontanarosa, Yaqub Jonmohamadi, Maria Antico, Mario Strydom et al. "Robotic and image-guided knee arthroscopy." In *Handbook of robotic and image-guided surgery*, pp. 493-514. Elsevier, 2020.
- [29]. Shaw, Ashley S., and Adrian K. Dixon. "Computed tomography." *eLS* (2015).
- [30]. Davies, S. C., A. L. Hill, R. B. Holmes, M. Halliwell, and P. C. Jackson. "Ultrasound quantitation of respiratory organ motion in the upper abdomen." *The British journal of radiology* 67, no. 803 (1994): 1096-1102.
- [31]. Lameka, Katherine, Michael D. Farwell, and Masanori Ichise. "Positron emission tomography." *Handbook of clinical neurology* 135 (2016): 209-227.
- [32]. Okamura, Nobuyuki, and Kazuhiko Yanai. "Applications of tau PET imaging." *Nature Reviews Neurology* 13, no. 4 (2017): 197-198.

- [33]. Shalom, Nathaniel Erez, Gary X. Gong, and Martin Auster. "Fluoroscopy: An essential diagnostic modality in the age of high-resolution cross-sectional imaging." *World Journal of Radiology* 12, no. 10 (2020): 213.
- [34]. Arridge, Simon R., and Jeremy C. Hebden. "Optical imaging in medicine: II. Modelling and reconstruction." *Physics in Medicine & Biology* 42, no. 5 (1997): 841.
- [35]. Zanzonico, Pat. "Principles of nuclear medicine imaging: planar, SPECT, PET, multi-modality, and autoradiography systems." *Radiation research* 177, no. 4 (2012): 349-364.
- [36]. Meglinski, Igor, ed. *Biophotonics for medical applications*. Elsevier, 2015.
- [37]. Fatahi, Mahsa, and Oliver Speck. "Magnetic resonance imaging (MRI): a review of genetic damage investigations." *Mutation Research/Reviews in Mutation Research* 764 (2015): 51-63.
- [38]. Bakas, Spyridon, Hamed Akbari, Aristeidis Sotiras, Michel Bilello, Martin Rozycki, Justin S. Kirby, John B. Freymann, Keyvan Farahani, and Christos Davatzikos. "Advancing the cancer genome atlas glioma MRI collections with expert segmentation labels and radiomic features." *Scientific data* 4, no. 1 (2017): 1-13.
- [39]. Fatahi, Mahsa, and Oliver Speck. "Magnetic resonance imaging (MRI): a review of genetic damage investigations." *Mutation Research/Reviews in Mutation Research* 764 (2015): 51-63.
- [40]. Brown, Robert W., Y-C. Norman Cheng, E. Mark Haacke, Michael R. Thompson, and Ramesh Venkatesan. *Magnetic resonance imaging: physical principles and sequence design*. John Wiley & Sons, 2014.
- [41]. Brown, Robert W., Y-C. Norman Cheng, E. Mark Haacke, Michael R. Thompson, and Ramesh Venkatesan. *Magnetic resonance imaging: physical principles and sequence design*. John Wiley & Sons, 2014.
- [42]. Yi, Xin, Ekta Walia, and Paul Babyn. "Generative adversarial network in medical imaging: A review." *Medical image analysis* 58 (2019): 101552.
- [43]. Garcia-Peraza-Herrera, Luis C., Wenqi Li, Lucas Fidon, Caspar Gruijthuijsen, Alain Devreker, George Attilakos, Jan Deprest et al. "Toolnet: holistically-nested real-time segmentation of robotic surgical tools." In *2017 IEEE/RSJ International Conference on Intelligent Robots and Systems (IROS)*, pp. 5717-5722. IEEE, 2017.

- [44]. Hajabdollahi, Mohsen, Reza Esfandiarpour, Kayvan Najarian, Nader Karimi, Shadrokh Samavi, and S. M. Reza-Soroushmeh. "Low complexity convolutional neural network for vessel segmentation in portable retinal diagnostic devices." In *2018 25th IEEE International Conference on Image Processing (ICIP)*, pp. 2785-2789. IEEE, 2018.
- [45]. Li, Zhuoling, Minghui Dong, Shiping Wen, Xiang Hu, Pan Zhou, and Zhigang Zeng. "CLU-CNNs: Object detection for medical images." *Neurocomputing* 350 (2019): 53-59.
- [46]. Schlemper, Jo, Ozan Oktay, Michiel Schaap, Mattias Heinrich, Bernhard Kainz, Ben Glocker, and Daniel Rueckert. "Attention gated networks: Learning to leverage salient regions in medical images." *Medical image analysis* 53 (2019): 197-207.
- [47]. Zhang, Le, Ryutaro Tanno, Mou-Cheng Xu, Chen Jin, Joseph Jacob, Olga Ciccarelli, Frederik Barkhof, and Daniel C. Alexander. "Disentangling Human Error from the Ground Truth in Segmentation of Medical Images." *arXiv preprint arXiv:2007.15963* (2020).
- [48]. Ahammad, Sk Hasane, V. Rajesh, Md Zia Ur Rahman, and Aimé Lay-Ekuakille. "A hybrid CNN-based segmentation and boosting classifier for real-time sensor spinal cord injury data." *IEEE Sensors Journal* 20, no. 17 (2020): 10092-10101.
- [49]. Hao, Jinglong, Xiaoxi Li, and Yanxia Hou. "Magnetic resonance image segmentation based on multi-scale convolutional neural network." *IEEE Access* 8 (2020): 65758-65768.
- [50]. Qin, Xi, Yu Chen, Bohan Wang, David Boegner, Brandon Gaitan, Yingning Zheng, and Xian Du. "Indoor localization of hand-held OCT probe using visual odometry and real-time segmentation using deep learning." *IEEE Transactions on Biomedical Engineering* (2021).
- [51]. Cunningham, Ryan J., Peter J. Harding, and Ian D. Loram. "Real-time ultrasound segmentation, analysis and visualization of deep cervical muscle structure." *IEEE transactions on medical imaging* 36, no. 2 (2016): 653-665.
- [52]. Malviya, Neha, Naveen Choudhary, and Kalpana Jain. "Content-based medical image retrieval and clustering-based segmentation to diagnose lung cancer." *Advances in Computational Sciences and Technology* 10, no. 6 (2017): 1577-1594.
- [53]. Kalshetti, Pratik, Manas Bunde, Parag Rahangdale, Dinesh Jangra, Chiranjoy Chattopadhyay, Gaurav Harit, and Abhay Elhence. "An interactive medical image

- segmentation framework using iterative refinement." *Computers in biology and medicine* 83 (2017): 22-33.
- [54]. Iqbal, Talha, and Hazrat Ali. "Generative adversarial network for medical images (MI-GAN)." *Journal of medical systems* 42, no. 11 (2018): 1-11.
- [55]. Anas, Emran Mohammad Abu, Parvin Mousavi, and Purang Abolmaesumi. "A deep learning approach for real-time prostate segmentation in freehand ultrasound-guided biopsy." *Medical image analysis* 48 (2018): 107-116.
- [56]. Siam, Mennatullah, Sara Eikerdawy, Mostafa Gamal, Moemen Abdel-Razek, Martin Jagersand, and Hong Zhang. "Real-time segmentation with appearance, motion, and geometry." In *2018 IEEE/RSJ International Conference on Intelligent Robots and Systems (IROS)*, pp. 5793-5800. IEEE, 2018.
- [57]. Robinson, Robert, Ozan Oktay, Wenjia Bai, Vanya V. Valindria, Mihir M. Sanghvi, Nay Aung, José M. Paiva et al. "Real-time prediction of segmentation quality." In *International Conference on Medical Image Computing and Computer-Assisted Intervention*, pp. 578-585. Springer, Cham, 2018.
- [58]. Stefaniga, Sebastian-Aurelian, and Mihail Gaiianu. "An approach of segmentation method using deep learning for CT medical images." In *2019 21st International Symposium on Symbolic and Numeric Algorithms for Scientific Computing (SYNASC)*, pp. 273-279. IEEE, 2019.
- [59]. Nguyen, Ngoc-Quang, and Sang-Woong Lee. "Robust boundary segmentation in medical images using a consecutive deep encoder-decoder network." *Ieee Access* 7 (2019): 33795-33808.
- [60]. Girum, Kibrom Berihu, Alain Lalande, Raabid Hussain, and Gilles Créhange. "A deep learning method for real-time intraoperative US image segmentation in prostate brachytherapy." *International Journal of Computer Assisted Radiology and Surgery* 15, no. 9 (2020): 1467-1476.
- [61]. Park, Ikjong, Hong Kyun Kim, Wan Kyun Chung, and Keehoon Kim. "Deep learning-based real-time oct image segmentation and correction for robotic needle insertion systems." *IEEE Robotics and Automation Letters* 5, no. 3 (2020): 4517-4524.
- [62]. Jha, Debesh, Sharib Ali, Nikhil Kumar Tomar, Håvard D. Johansen, Dag Johansen, Jens Rittscher, Michael A. Riegler, and Pål Halvorsen. "Real-time polyp detection,

- localization and segmentation in colonoscopy using deep learning." *Ieee Access* 9 (2021): 40496-40510.
- [63]. Ouahabi, Abdeldjalil, and Abdelmalik Taleb-Ahmed. "Deep learning for real-time semantic segmentation: Application in ultrasound imaging." *Pattern Recognition Letters* 144 (2021): 27-34.
- [64]. Egger, Jan, Tobias Lüddemann, Robert Schwarzenberg, Bernd Freisleben, and Christopher Nimsky. "Interactive-cut: Real-time feedback segmentation for translational research." *Computerized Medical Imaging and Graphics* 38, no. 4 (2014): 285-295.
- [65]. Chitiboi, Teodora, Anja Hennemuth, Lennart Tautz, Markus Hüllebrand, Jens Frahm, Lars Linsen, and H. Hahn. "Context-based segmentation and analysis of multi-cycle real-time cardiac MRI." In *2014 IEEE 11th International Symposium on Biomedical Imaging (ISBI)*, pp. 943-946. IEEE, 2014.
- [66]. Kurzendorfer, Tanja, Peter Fischer, Negar Mirshahzadeh, Thomas Pohl, Alexander Brost, Stefan Steidl, and Andreas Maier. "Rapid interactive and intuitive segmentation of 3D medical images using radial basis function interpolation." *Journal of Imaging* 3, no. 4 (2017): 56.
- [67]. Wei, Min-Song, Fei Xing, and Zheng You. "A real-time detection and positioning method for small and weak targets using a 1D morphology-based approach in 2D images." *Light: Science & Applications* 7, no. 5 (2018): 18006-18006.
- [68]. Zhai, Xiaojun, Mohammad Eslami, Ealaf Sayed Hussein, Maroua Salem Filali, Salma Tarek Shalaby, Abbas Amira, Faycal Bensaali et al. "Real-time automated image segmentation technique for cerebral aneurysm on reconfigurable system-on-chip." *Journal of computational science* 27 (2018): 35-45.
- [69]. Wang, Tianchen, Jinjun Xiong, Xiaowei Xu, Meng Jiang, Haiyun Yuan, Meiping Huang, Jian Zhuang, and Yiyu Shi. "MSU-Net: Multiscale statistical U-net for real-time 3D cardiac MRI video segmentation." In *International Conference on Medical Image Computing and Computer-Assisted Intervention*, pp. 614-622. Springer, Cham, 2019.
- [70]. Zeng, Dewen, Weiwen Jiang, Tianchen Wang, Xiaowei Xu, Haiyun Yuan, Meiping Huang, Jian Zhuang, Jingtong Hu, and Yiyu Shi. "Towards cardiac intervention assistance: hardware-aware neural architecture exploration for real-time 3D cardiac cine

- MRI segmentation." In *Proceedings of the 39th International Conference on Computer-Aided Design*, pp. 1-8. 2020.
- [71]. AlZu'bi, Shadi, Mohammed Shehab, Mahmoud Al-Ayyoub, Yaser Jararweh, and Brij Gupta. "Parallel implementation for 3d medical volume fuzzy segmentation." *Pattern Recognition Letters* 130 (2020): 312-318.
- [72]. Kashyap, Ramgopal, and Pratima Gautam. "Modified region-based segmentation of medical images." In *2015 International Conference on Communication Networks (ICCN)*, pp. 209-216. IEEE, 2015.
- [73]. Nelakuditi, Usha Rani, T. Sri Rama Bharadwaja, and Narayana Bhagiradh. "Novel VLSI architecture for real-time medical image segmentation." In *2015 2nd International Conference on Electronics and Communication Systems (ICECS)*, pp. 1084-1088. IEEE, 2015.
- [74]. Hamdaoui, Fayçal, Anis Sakly, and Abdellatif Mtibaa. "Real-time synchronous hardware architecture for MRI images segmentation based on PSO." In *2015 4th International Conference on Systems and Control (ICSC)*, pp. 498-503. IEEE, 2015.
- [75]. Dergachyova, Olga, David Bouget, Arnaud Huaultmé, Xavier Morandi, and Pierre Jannin. "Automatic data-driven real-time segmentation and recognition of surgical workflow." *International journal of computer-assisted radiology and surgery* 11, no. 6 (2016): 1081-1089.
- [76]. Kashyap, Ramgopal, and Pratima Gautam. "Fast level set method for segmentation of medical images." In *Proceedings of the International Conference on Informatics and Analytics*, pp. 1-7. 2016.
- [77]. Sharma, Rajesh, and Akey Sungeetha. "Segmentation and classification techniques of medical images using innovated hybridized techniques—a study." In *2017 11th International Conference on Intelligent Systems and Control (ISCO)*, pp. 192-196. IEEE, 2017.
- [78]. Gueziri, Housseem-Eddine, Michael J. McGuffin, and Catherine Laporte. "Latency management in scribble-based interactive segmentation of medical images." *IEEE Transactions on Biomedical Engineering* 65, no. 5 (2017): 1140-1150.
- [79]. Labrunie, Mathieu, Pierre Badin, Dirk Voit, Arun A. Joseph, Jens Frahm, Laurent Lamalle, Coriandre Vilain, and Louis-Jean Boë. "Automatic segmentation of speech

- articulators from real-time midsagittal MRI based on supervised learning." *Speech Communication* 99 (2018): 27-46.
- [80]. Mahmood, Faisal, Richard Chen, and Nicholas J. Durr. "Unsupervised reverse domain adaptation for synthetic medical images via adversarial training." *IEEE transactions on medical imaging* 37, no. 12 (2018): 2572-2581.
- [81]. Liu, Chunxiao, Michael Kwok-Po Ng, and Tiejong Zeng. "Weighted variational model for selective image segmentation with application to medical images." *Pattern Recognition* 76 (2018): 367-379.
- [82]. Yu, Haiping, Fazhi He, and Yiteng Pan. "A novel segmentation model for medical images with intensity inhomogeneity based on adaptive perturbation." *Multimedia Tools and Applications* 78, no. 9 (2019): 11779-11798.
- [83]. Choi, Wooram, and Young-Jin Cha. "SDDNet: Real-time crack segmentation." *IEEE Transactions on Industrial Electronics* 67, no. 9 (2019): 8016-8025.
- [84]. Chen, Yating, Gaoxiang Chen, Yu Wang, Nilanjan Dey, R. Simon Sherratt, and Fuqian Shi. "A distance regularized level-set evolution model-based MRI dataset segmentation of brain's caudate nucleus." *IEEE Access* 7 (2019): 124128-124140.
- [85]. Feng, Ruiwei, Biwen Lei, Wenzhe Wang, Tingting Chen, Jintai Chen, Danny Z. Chen, and Jian Wu. "SSN: A stair-shape network for real-time polyp segmentation in colonoscopy images." In *2020 IEEE 17th International Symposium on Biomedical Imaging (ISBI)*, pp. 225-229. IEEE, 2020.
- [86]. Guo, Qiang, Gao-Yang Li, and Yong Wang. "Segmentation Technology of Medical Images Based on Regional Growth." *Journal of Computers* 31, no. 3 (2020): 115-125.
- [87]. Memon, Asif Aziz, Shafiullah Soomro, Muhammad Tanseef Shahid, Asad Munir, Asim Niaz, and Kwang Nam Choi. "Segmentation of Intensity-Corrupted Medical Images Using Adaptive Weight-Based Hybrid Active Contours." *Computational and Mathematical Methods in Medicine* 2020 (2020).
- [88]. Neff, Thomas, Christian Payer, Darko Stern, and Martin Urschler. "Generative adversarial network-based synthesis for supervised medical image segmentation." In *Proc. OAGM and ARW Joint Workshop*, vol. 3, p. 4. 2017
- [89]. Tang, You-Bao, Sooyoun Oh, Yu-Xing Tang, Jing Xiao, and Ronald M. Summers. "CT-realistic data augmentation using generative adversarial network for robust lymph node

- segmentation." In *Medical Imaging 2019: Computer-Aided Diagnosis*, vol. 10950, p. 109503V. International Society for Optics and Photonics, 2019.
- [90]. Rezaei, Mina, Haojin Yang, and Christoph Meinel. "Recurrent generative adversarial network for learning imbalanced medical image semantic segmentation." *Multimedia Tools and Applications* 79, no. 21 (2020): 15329-15348.
- [91]. Xiong, Dehui, Chu He, Xinlong Liu, and Mingsheng Liao. "An End-To-End Bayesian Segmentation Network Based on a Generative Adversarial Network for Remote Sensing Images." *Remote Sensing* 12, no. 2 (2020): 216.
- [92]. Zhao, Cheng, Tianfu Wang, and Baiying Lei. "Medical image fusion method based on dense block and deep convolutional generative adversarial network." *Neural Computing and Applications* 33, no. 12 (2021): 6595-6610
- [93]. Li, Yuqin, Ke Zhang, Weili Shi, Yu Miao, and Zhengang Jiang. "A Novel Medical Image Denoising Method Based on Conditional Generative Adversarial Network." *Computational and Mathematical Methods in Medicine* 2021 (2021).
- [94]. Bibiloni, Pedro, Manuel González-Hidalgo, and Sebastia Massanet. "A real-time fuzzy morphological algorithm for retinal vessel segmentation." *Journal of Real-Time Image Processing* 16, no. 6 (2019): 2337-2350.
- [95]. Bozhenyuk, Alexander, Samer El-Khatib, Janusz Kacprzyk, Margarita Knyazeva, and Sergey Rodzin. "Hybrid Ant Fuzzy Algorithm for MRI Images Segmentation." In *International Conference on Artificial Intelligence and Soft Computing*, pp. 127-137. Springer, Cham, 2019.
- [96]. Gupta, Deep, and R. S. Anand. "A hybrid edge-based segmentation approach for ultrasound medical images." *Biomedical Signal Processing and Control* 31 (2017): 116-126.
- [97]. Rastgarpour, Maryam, and Jamshid Shanbehzadeh. "A new kernel-based fuzzy level set method for automated segmentation of medical images in the presence of intensity inhomogeneity." *Computational and mathematical methods in medicine* 2014 (2014).
- [98]. Zhang, XiaoFeng, CaiMing Zhang, WenJing Tang, and ZhenWen Wei. "Medical image segmentation using improved FCM." *Science China Information Sciences* 55, no. 5 (2012): 1052-1061.

- [99]. Kannan, S. R., S. Ramathilagam, A. Sathya, and R. Pandiyarajan. "Effective fuzzy c-means based kernel function in segmenting medical images." *computers in biology and medicine* 40, no. 6 (2010): 572-579.
- [100]. Zhao, Xiaomei, Yihong Wu, Guidong Song, Zhenye Li, Yazhuo Zhang, and Yong Fan. "A deep learning model integrating FCNNs and CRFs for brain tumor segmentation." *Medical image analysis* 43 (2018): 98-111.
- [101]. Ari, Ali, and Davut Hanbay. "Deep learning-based brain tumor classification and detection system." *Turkish Journal of Electrical Engineering & Computer Sciences* 26, no. 5 (2018): 2275-2286.
- [102]. Thillaikkarasi, R., and S. Saravanan. "An enhancement of deep learning algorithm for brain tumor segmentation using kernel-based CNN with M-SVM." *Journal of medical systems* 43, no. 4 (2019): 1-7.
- [103]. Sun, Li, Songtao Zhang, Hang Chen, and Lin Luo. "Brain tumor segmentation and survival prediction using multimodal MRI scan with deep learning." *Frontiers in neuroscience* 13 (2019): 810.
- [104]. Mlynarski, Pawel, Hervé Delingette, Antonio Criminisi, and Nicholas Ayache. "Deep learning with mixed supervision for brain tumor segmentation." *Journal of Medical Imaging* 6, no. 3 (2019): 034002.
- [105]. Yang, Tiejun, Jikun Song, and Lei Li. "A deep learning model integrating SK-TPCNN and random forests for brain tumor segmentation in MRI." *Biocybernetics and Biomedical Engineering* 39, no. 3 (2019): 613-623.
- [106]. Saba, Tanzila, Ahmed Sameh Mohamed, Mohammad El-Affendi, Javeria Amin, and Muhammad Sharif. "Brain tumor detection using fusion of handcrafted and deep learning features." *Cognitive Systems Research* 59 (2020): 221-230.
- [107]. Rehman, Arshia, Saeeda Naz, Muhammad Imran Razzak, Faiza Akram, and Muhammad Imran. "A deep learning-based framework for automatic brain tumors classification using transfer learning." *Circuits, Systems, and Signal Processing* 39, no. 2 (2020): 757-775.
- [108]. Yu, Ying, Min Li, Liangliang Liu, Yaohang Li, and Jianxin Wang. "Clinical big data and deep learning: Applications, challenges, and future outlooks". *Big Data Mining and Analytics* 2, no. 4 (2019): 288-305.

- [109]. Li, Xiaomeng, Hao Chen, Xiaojuan Qi, Qi Dou, Chi-Wing Fu, and Pheng-Ann Heng. "H-DenseUNet: hybrid densely connected UNet for liver and tumor segmentation from CT volumes". *IEEE transactions on medical imaging* 37, no. 12 (2018): 2663-2674.
- [110]. LaLonde, Rodney, and Ulas Bagci. "Capsules for object segmentation". *arXiv preprint arXiv:1804.04241* (2018).
- [111]. Liu, Liangliang, Fang-Xiang Wu, and Jianxin Wang. "Efficient multi-kernel DCNN with pixel dropout for stroke MRI segmentation". *Neurocomputing* 350 (2019): 117-127.
- [112]. Yang, Jianchao, Zhaowen Wang, Zhe Lin, Scott Cohen, and Thomas Huang. "Coupled dictionary training for image super-resolution". *IEEE transactions on image processing* 21, no. 8 (2012): 3467-3478.
- [113]. Hu, Wei, Yangyu Huang, Li Wei, Fan Zhang, and Hengchao Li. "Deep convolutional neural networks for hyperspectral image classification". *Journal of Sensors 2015* (2015).
- [114]. Shah, Mohak, Yiming Xiao, Nagesh Subbanna, Simon Francis, Douglas L. Arnold, D. Louis Collins, and Tal Arbel. "Evaluating intensity normalization on MRIs of the human brain with multiple sclerosis". *Medical image analysis* 15, no. 2 (2011): 267-282.
- [115]. Hu, Wei, Yangyu Huang, Li Wei, Fan Zhang, and Hengchao Li. "Deep convolutional neural networks for hyperspectral image classification". *Journal of Sensors 2015* (2015).
- [116]. Hashemi, Seyed Raein, Seyed Sadegh Mohseni Salehi, Deniz Erdogmus, Sanjay P. Prabhu, Simon K. Warfield, and Ali Gholipour. "Asymmetric loss functions and deep densely-connected networks for highly-imbalanced medical image segmentation: Application to multiple sclerosis lesion detection". *IEEE Access* 7 (2018): 1721-1735.
- [117]. Lateef, Fahad, and Yassine Ruichek. "Survey on semantic segmentation using deep learning techniques". *Neurocomputing* 338 (2019): 321-348.
- [118]. Nachimuthu, Deepa Subramaniam, and Arunadevi Baladhandapani. "Multidimensional texture characterization: on analysis for brain tumor tissues using MRS and MRI". *Journal of digital imaging* 27, no. 4 (2014): 496-506.
- [119]. Zhou, Chenhong, Changxing Ding, Xinchao Wang, Zhentai Lu, and Dacheng Tao. "One-pass multi-task networks with cross-task guided attention for brain tumor segmentation". *IEEE Transactions on Image Processing* 29 (2020): 4516-4529.

- [120]. Liu, Liangliang, Fang-Xiang Wu, Yu-Ping Wang, and Jianxin Wang. "Multi-receptive-field CNN for semantic segmentation of medical images". *IEEE Journal of Biomedical and Health Informatics* 24, no. 11 (2020): 3215-3225.
- [121]. Menze, Bjoern H., Andras Jakab, Stefan Bauer, Jayashree Kalpathy-Cramer, Keyvan Farahani, Justin Kirby, Yuliya Burren et al. "The multimodal brain tumor image segmentation benchmark BraTS." *IEEE transactions on medical imaging* 34, no. 10 (2014): 1993-2024.
- [122]. Usman, Khalid, and Kashif Rajpoot. "Brain tumor classification from multi-modality MRI using wavelets and machine learning." *Pattern Analysis and Applications* 20, no. 3 (2017): 871-881.
- [123]. Bhatele, Kirti Raj, and Sarita Singh Bhadauria. "Machine learning application in Glioma classification: review and comparison analysis." *Archives of Computational Methods in Engineering* (2021): 1-28.
- [124]. Zhang, Dingwen, Guohai Huang, Qiang Zhang, Jungong Han, Junwei Han, and Yizhou Yu. "Cross-modality deep feature learning for brain tumor segmentation." *Pattern Recognition* 110 (2021): 107562.
- [125]. Yan, Zhicheng, Hao Zhang, Robinson Piramuthu, Vignesh Jagadeesh, Dennis DeCoste, Wei Di, and Yizhou Yu. "HD-CNN: hierarchical deep convolutional neural networks for large scale visual recognition." In *Proceedings of the IEEE international conference on computer vision*, pp. 2740-2748. 2015.
- [126]. Kamnitsas, Konstantinos, Christian Ledig, Virginia FJ Newcombe, Joanna P. Simpson, Andrew D. Kane, David K. Menon, Daniel Rueckert, and Ben Glocker. "Efficient multi-scale 3D CNN with fully connected CRF for accurate brain lesion segmentation." *Medical image analysis* 36 (2017): 61-78.
- [127]. Zhao, Tianyi, Qiuyu Chen, Zhenzhong Kuang, Jun Yu, Wei Zhang, and Jianping Fan. "Deep mixture of diverse experts for large-scale visual recognition." *IEEE transactions on pattern analysis and machine intelligence* 41, no. 5 (2018): 1072-1087.

Thesis

ORIGINALITY REPORT

9%	6%	7%	0%
SIMILARITY INDEX	INTERNET SOURCES	PUBLICATIONS	STUDENT PAPERS

PRIMARY SOURCES

1	link.springer.com Internet Source	1%
2	"Brainlesion: Glioma, Multiple Sclerosis, Stroke and Traumatic Brain Injuries", Springer Science and Business Media LLC, 2021 Publication	<1%
3	"Medical Image Understanding and Analysis", Springer Science and Business Media LLC, 2017 Publication	<1%
4	www.hindawi.com Internet Source	<1%
5	doaj.org Internet Source	<1%
6	dokumen.pub Internet Source	<1%
7	"Medical Image Computing and Computer Assisted Intervention – MICCAI 2019", Springer Science and Business Media LLC, 2019	<1%